



University of Kentucky
UKnowledge

Theses and Dissertations--Kinesiology and Health
Promotion

Kinesiology and Health Promotion

2012

THE EFFECTS OF SEAT POST ANGLE IN CYCLING PERFORMANCE

Saori Hanaki-Martin
University of Kentucky, saorihanaki@gmail.com

Recommended Citation

Hanaki-Martin, Saori, "THE EFFECTS OF SEAT POST ANGLE IN CYCLING PERFORMANCE" (2012). *Theses and Dissertations-Kinesiology and Health Promotion*. Paper 1.
http://uknowledge.uky.edu/khp_etds/1

This Doctoral Dissertation is brought to you for free and open access by the Kinesiology and Health Promotion at UKnowledge. It has been accepted for inclusion in Theses and Dissertations--Kinesiology and Health Promotion by an authorized administrator of UKnowledge. For more information, please contact UKnowledge@lsv.uky.edu.

STUDENT AGREEMENT:

I represent that my thesis or dissertation and abstract are my original work. Proper attribution has been given to all outside sources. I understand that I am solely responsible for obtaining any needed copyright permissions. I have obtained and attached hereto needed written permission statements(s) from the owner(s) of each third-party copyrighted matter to be included in my work, allowing electronic distribution (if such use is not permitted by the fair use doctrine).

I hereby grant to The University of Kentucky and its agents the non-exclusive license to archive and make accessible my work in whole or in part in all forms of media, now or hereafter known. I agree that the document mentioned above may be made available immediately for worldwide access unless a preapproved embargo applies.

I retain all other ownership rights to the copyright of my work. I also retain the right to use in future works (such as articles or books) all or part of my work. I understand that I am free to register the copyright to my work.

REVIEW, APPROVAL AND ACCEPTANCE

The document mentioned above has been reviewed and accepted by the student's advisor, on behalf of the advisory committee, and by the Director of Graduate Studies (DGS), on behalf of the program; we verify that this is the final, approved version of the student's dissertation including all changes required by the advisory committee. The undersigned agree to abide by the statements above.

Saori Hanaki-Martin, Student

Dr. Robert Shapiro, Major Professor

Dr. Richard Riggs, Director of Graduate Studies

THE EFFECTS OF SEAT POST ANGLE IN CYCLING PERFORMANCE

ABSTRACT OF DISSERTATION

A dissertation submitted in partial fulfillment of the requirements
for the degree of Doctor of Philosophy in Exercise Science
in the College of Education
at the University of Kentucky

By
Saori Hanaki-Martin
Lexington, Kentucky

Director: Dr. Robert Shapiro, Professor of Kinesiology and Health Promotion
Lexington, Kentucky
2012
Copyright © Saori Hanaki-Martin 2012

ABSTRACT OF DISSERTATION

THE EFFECTS OF SEAT POST ANGLE IN CYCLING PERFORMANCE

Triathlon involves three different modes of endurance events, swim, bike and run, consecutively. Transitions between events are critical to be successful in the sport; however, many triathletes report impaired running performance due to adverse residual effects from cycling. One of the strategies that triathletes use to manage the adverse effects is to use a bicycle with a more vertical seat post angle. There is limited evidence that support the effectiveness of such bicycle geometry, but many of these studies lacks ecological validity.

Twelve triathletes and cyclists completed a 20-km simulated course with instrumentations for 3D motion, kinetic, and electromyographic analyses under two different seat post angle settings: shallow (ROAD) and steep (TRI). Series of paired-t tests were used for statistical analysis.

Results indicated cycling mechanics between two seat post angle conditions were similar; however, the steep condition resulted in time-delay in muscle activation and pedal force application. There was no significant difference in cycling performance. The athletes were able to retain relatively consistent pedaling techniques with modification of seat post angle.

KEYWORDS: triathlon, pedal forces, kinematics, kinetics, EMG

Saori Hanaki-Martin
Student's Signature

1/30/2012
Date

THE EFFECTS OF SEAT POST ANGLE IN CYCLING PERFORMANCE

By

Saori Hanaki-Martin

Robert Shapiro Ph.D.
Director of Dissertation

Richard Riggs, Ph.D.
Director of Graduate Studies

1/30/2012

ACKNOWLEDGEMENTS

In completing this project, I have received supports from many individuals. Dr. Robert Shapiro, my primary advisor not only guided me through my entire doctoral education, he also taught me to appreciate and cherish family. Dr. David Mullineaux worked with me very patiently through methodology and data processing. He also taught me to have a life outside school. My dissertation committee members, Drs. Tim Uhl and J. W. Yates provided me feedback that was invaluable to completion of this project. Dr. Kyoungkyu Jeon, a visiting scholar from South Korea, assisted my data collections. Also, my good friend and a former classmate, Dr. Tracy Spigelman provided me assistance in many ways. Our little adventures in swimming, cycling and all other things kept me sane!

My big ‘thank you’ also goes to my family. My husband, Paul supported me though this long journey with me. Without your understanding, I could not complete this project. My mother, Kazumi, has been the biggest supporter for my entire life. She has been my inspirations to move forward and to continue challenging myself. My father, Osamu, and my brothers, Manabu and Satoru, also supported me through my education and my life in a foreign land. I also would like to express my appreciations to friends in triathlon and cycling communities in Lexington, Kentucky for generously providing their time to participate in my study.

TABLE OF CONTENTS

Acknowledgements.....	iii
List of Tables.....	iv
List of Figures.....	iiiv
Chapter One: Introduction	
Background.....	1
Statement of Problem.....	3
Purpose.....	4
Research Hypotheses.....	4
Significance of Study.....	5
Assumptions.....	7
Limitations.....	7
Delimitations.....	7
Operational Definitions.....	8
Chapter Two: Review of Literature	
Introduction.....	13
Section I: Cycling Mechanics.....	13
Pedaling Phases.....	13
Cycling Kinematics.....	15
Cycling Kinetics.....	16
Muscles.....	25
Section II: Triathlon Cycling.....	29
Effects of Bike Segment.....	29
Riding Position.....	30
Section III: Instruments and Methodology.....	33
3-Dimensional Motion Capture.....	33
Electromyography.....	35
Summary of Chapter.....	37
Chapter Three: Methods	
Study Population.....	39
Apparatus/Instruments.....	39
Bike.....	39
Kinematic Data.....	41
Analog Data: Pedal Forces & Electromyography.....	41

Protocol.....	41
Data Analysis.....	45
Kinematics.....	45
Pedal Forces.....	45
Joint Kinetics.....	46
EMG.....	47
Aerodynamics.....	48
Dependent Variables.....	48
Kinematic Dependent Variables.....	49
Kinetic Dependent Variables.....	51
EMG Dependent Variables.....	52
Aerodynamic Dependent Variables.....	53
Performance Dependent Variables.....	53
Statistical Analysis.....	53
 Chapter Four: Results	
Introduction.....	55
Kinematics.....	55
Sitting Position and Seat Post Angle.....	55
Joint Angles.....	56
Segmental Angles.....	60
Kinetics.....	63
Pedal Forces.....	63
Pedaling Effectiveness.....	66
Joint Moments.....	67
Muscle Activation.....	69
Aerodynamics.....	76
Performance.....	76
Summary of Results.....	78
 Chapter Five: Discussion	
Introduction.....	79
Seat Post Angle Effects.....	79
Kinematics.....	79
Kinetics.....	82
Time Effects.....	86
Muscle Activations.....	87
Aerodynamics.....	90
Performance.....	91
Summary of Chapter.....	91

Chapter Six: Summary, Conclusions, Recommendations	
Summary.....	93
Conclusions.....	94
Recommendations.....	95
Appendices	
Appendix A: The Study Participants' Profile and Training/Competition History.....	97
Appendix B: SENIAM EMG electrodes placements and MIVC testing methods.....	98
Appendix C: The List of Retroreflective Markers for 3D Motion Analysis and Their Placement Locations.....	102
Appendix D: Matlab Code to Convert Raw Pedal Signals to Usable Force Data.....	104
Appendix E: Descriptions of Pedal Signal Calibrations and Conversion.....	109
References.....	112
Vita.....	119

LIST OF TABLES

Table 3-1: Parameters used in kinetic calculations in Visual3D software.....	47
Table 4-1: The average measured sitting position and measured seat post angle resulted from ROAD and from TRI seat conditions.....	55
Table 4-2: Minimal and maximal joint angle and ROM means and standard deviations for the hip, knee, and ankle at 1 km, 5 km, 10 km, 15 km, and 19 km with two different seat post angle conditions.....	59
Table 4-3: Mean activation level of selected leg muscles during 4 sectors of pedal cycle during cycling in ROAD and TRI conditions at 1-km.....	70
Table 4-4: Time shift, coefficient of cross correlation, and linearity of EMG signal of selected leg muscles between two seat positions at 1-km.....	70
Table 4-5: Finish times of a 20-km simulated course using two different seat post angle settings and bike-type preferences of 12 study participants....	77

LIST OF FIGURES

Figure 2-1: Commonly used pedaling phases during a single pedal cycle.....	14
Figure 2-2: Commonly used joint angle definitions.....	15
Figure 2-3: Two different types used to measure pedal kinetic variables.....	17
Figure 2-4: Crank and pedal angles and determination of the pedal forces and crank torque.....	18
Figure 2-5: Normal, tagnetial, and resultant pedal forces during a typical steady state road cycling condition.....	20
Figure 2-6: Clock diagram of pedal orientation and resultant pedal force at selected points of the pedal cycle.....	21
Figure 2-7: 3 commonly used cycling positions.....	22
Figure 2-8: Example of 2-D (sagittal) link segment model used for inverse dynamics of cycling movement.....	23
Figure 2-9: Resultant pedal reaction force alignment relative to the right lower extremity for six different points in the pedaling cycle.....	24
Figure 2-10: Joint moments at the hip, knee, and ankle joints over a single pedal cycle.....	25
Figure 2-11: Muscle activation patterns of 10 leg muscle during cycling in three different upper body orientations.....	27
Figure 2-12: Schematic diagram of major leg muscle that involves in cycling.....	28
Figure 2-13: Typical road bike and triathlon bike.....	31
Figure 3-1: Measurements of the bike.....	41
Figure 3-2: Diagram of the instrumented force pedal.....	41
Figure 3-3 Locations of the retro-reflective markers used for the 3-D motion analys.....	43
Figure 3-4: The experimental set up for the cycling trials.....	44
Figure 3-5: Bike coordinate system used for 3D motion analysis.....	45
Figure 3-7: Definitions of trunk angle and seat post angle.....	48
Figure 3-8: Phases of the pedal cycle.....	49
Figure 3-9a: Definitions of segmental angles.....	51
Figure 3-9b: Definitions of joint angles.....	51
Figure 4-1: Schematic diagram of measrued sitting postion and measured seat post angle with two cycling positions.....	56
Figure 4-2: Average joint angle change across 5 time points during a simulated 20-km cycling session with two different seat post angles.....	58
Figure 4-3 a & b: Segmental angle across 5 time points during a 20-km simulated cycling session with two different seat post angles.....	61

Figure 4-3 c & d: Segmental angle across 5 time points during a 20-km simulated cycling session with two different seat post angles.....	62
Figure 4-4 a – b: Normalized normal and tangential pedal forces across 5 time points during a 20-km cycling session with two different seat post angles.....	64
Figure 4-4 c: Normalized resultant pedal force across 5 time points during a 20-km simulated cycling session with two different seat post angles.....	65
Figure 4-5: Normalized resultant pedal force at 1 km, 5 km, 10 km, 15 km, and 19 km during a simulated 20-km cycling session with ROAD riding position.....	65
Figure 4-6: Normalized effective pedal force across 5 time points during a 20-km simulated cycling session with two different seat post angles.....	66
Figure 4-7a: Normalized hip joint moment across 5 time points during a 20-km simulated cycling session with two different seat post angles.....	67
Figure 4-7b – c: Normalized knee and ankle joint moments across 5 time points during a 20-km simulated cycling session with two different seat post angles.....	68
Figure 4-8a: Normalized EMG linear envelopes of gluteus maximus and biceps femoris at 1-km of a 20-km simulated cycling session with two different seat post angles.....	71
Figure 4-8b: Normalized EMG linear envelopes of rectus femoris and vastus lateralis at 1-km of a 20-km simulated cycling session with two different seat post angles.....	72
Figure 4-8c: Normalized EMG linear envelopes of gastrocnemius and soleus at 1-km of a 20-km simulated cycling session with two different seat post angles.....	73
Figure 4-8d: Normalized EMG linear envelopes of tibialis anterior at 1-km of a 20-km simulated cycling session with two different seat post angles.....	74
Figure 4-9: Cross correlation for the EMG linear envelopes of the two cycling conditions.....	75

Chapter One

Introduction

Background

Triathlon is one of the fastest growing sports. Since its introduction as an Olympic sport in 2000, the number of members belonging to USA Triathlon, the governing body of the sport in the United States, has increased by seven-fold to over 130,000 in 2010 [9]. The sport involves three different modes of endurance events (swimming, cycling, and running) performed consecutively. Due to the nature of the sport, athletes are required to train and perform well in all three disciplines to become successful. Performance in the two longer segments, cycling and running, has been shown to be strongly correlated with the finish time in the Olympic distance triathlon [10], and effective transitions between these disciplines are considered one of the keys for a better performance [11]. Additionally, many injuries to triathletes are related to the cycle-run dynamics [12]. Training specifically targeting the cycle-run transition has been adapted by triathletes; however, they often express that cycling impairs their running performances. Their testimonies are confirmed by some literature that examines the effects of a prolonged cycling on subsequent running. Prior cycling is reported to affect running performance while the effects of swimming on cycling and running performances are considered small. Experiments comparing runs that preceded and followed an exhaustive cycling session reported increased metabolic cost by $2.3 \pm 4.6\%$ [13] and mechanical cost by $7.1 \pm 6.0\%$ [14] during a run following a cycling bout compared to a pre-cycling run among non-elite triathletes. The change in cost demand can potentially be explained by both physiological and biomechanical changes. A prolonged submaximal cycling session resulted in a decrease in the performance level of the respiratory muscles that persisted through a following running session [15], and the residual effects from preceding events on the working muscles appear to be related to the increased cost required to maintain the similar intensity level in the later part of the triathlon event [10]. A physiological investigation found that progressive chemical changes indicating muscle catalysis and dehydration were observed during the post-cycling portion of a triathlon competition [16]. The activation patterns in the leg muscles were altered during the run proceeded by a cycling session [11, 17]. The increased cost during the post-cycling run was also associated with altered leg kinematics [17]. An extended cycling session also affected running stride kinematics [18].

One of the strategies that has been implemented by triathletes to lessen the effects of cycling on their running performance is changing the bike frame geometry. Specifically, triathletes use steep seat post angles that are more vertical (typically near 80°) than that of conventional road-racing bikes (between 70 to 74°, traditionally 72°) [19]. Seat post angle affects the seat's relative position to the crank axis. The more vertical seat post seen in triathlon-specific bike frame places its rider more directly above the crank axis. This riding posture results in a more extended hip position [20] that has been proposed to facilitate pre-stretch of the gluteus maximus muscle that improves the action of the muscle [4, 21]. A few studies that have examined electromyography (EMG) of the leg muscles during cycling in the conventional and steep seat post conditions revealed an altered pattern of leg muscle use. Brown [22] indicated that a more extended hip position enabled cyclists to generate greater hip torque while biceps femoris activation was reduced. This finding is supported by a study that revealed 72° and 82° seat post angles conditions during a Wingate (anaerobic cycling) test resulted in comparable power outputs while significantly less muscle activation was required when cyclists rode on a bike with steeper seat post angle [23]. The biceps femoris serves to bring the hip into extension during the late stance (near toe-off) and to decelerate the forward moving leg at the knee during the terminal swing during moderate speed running (3.51 m/s) [2]. Therefore, preserving biceps femoris during the preceding cycling segment may improve running performance by possibly preventing fatigue in this muscle. A steeper seat post angle was also reported to improve power output during a 15-second all-out cycling bout [20].

Many studies, including some of the aforementioned, investigated the effects of seat post angle during short, high-intensity or maximal effort cycling bouts. However, most triathlon competitions comprise a longer cycling segment, and it has been implicated that techniques used at different cycling intensities are different [24]. Therefore, it is more practically meaningful to examine a longer duration cycling bout at a submaximal intensity to understand the effects of seat post angles during a triathlon. Previous research has quantified work performed by the cyclist using instrumented pedals. The sum of the pedal forces, horizontal and tangential pedal forces, is partitioned into either effective or ineffective force. The summed pedal force or the resultant pedal force was minimally affected, but pedal angles throughout the pedal cycle were influenced by the seat post angles [25]. This change in pedal angle is likely to

alter the angle of the force application on the pedal, and therefore affect how the resultant force is partitioned into effective and ineffective forces. Changes in muscle activation pattern in the leg due to changed body orientation alone, without any changes in the length of the muscle [22], suggests that the effects of the inertial property of the leg on cycling mechanics can result from altered seat post angles.

Pedal forces can also be used to approximate pedaling efficiencies as an index of pedaling effectiveness calculated as the ratio of efficient force (impulse) to resultant force (impulse) [26]. The effective pedal force is the one that generates the pedal torque and results in external work that moves the cyclist forward. The component of the overall pedaling force that is parallel to the crank arm does not contribute in propulsion of the cyclist, so the energy used to cause this portion of the pedal force is ‘wasted.’ Although it is not possible to quantify how much energy is produced by the cyclist that contributes to different portion of pedal forces, the index of effectiveness provides implications of the portions of force produced during a pedal cycle by the cyclist.

Statement of Problem

Triathlon-specific bicycles characterized by steeper seat post angle are becoming more popular among triathletes with the premise of enhancing more efficient cycling techniques and also of minimizing the residual effects of the cycling segment on the running segment. Riding on this type of bike places the lower body in a more vertically aligned position. Some evidence suggests potential benefits associated with riding in this position is accomplished by using a triathlon-specific bike [22, 27]; however, much of the information currently available is limited to short duration cycling or to the tested riding positions that are not realistic to actual athletic situations. In addition to riding on a bicycle with different frame geometry (road bike and triathlon-specific bike), triathletes cycle in the ‘aero-position,’ where the athlete maintains a forward lean position of the trunk to reduce the frontal resistance. Compared with the upright riding position, the forward lean of the trunk associated with the ‘aero-position’ theoretically deepens the amount of the hip flexion and possibly affects the amount of pelvic tilt in the anterior-posterior direction. Changing the trunk orientation alone did not affect the kinematics of the leg and the pedal; however, it is possible that the different vertical alignment of the

body caused by altered seat post angle due to different fore-aft seat positions can influence the kinematics of the leg and the pedal [28].

The fore-aft positioning of the bicycle seat relative to the crank axis related to changed seat post angle has been shown to alter certain characteristics of pedaling techniques [20, 23, 25, 28]; however, there is limited information regarding the riding position effects on pedaling mechanics that are practically applicable to triathlon competition. Therefore, a comprehensive analysis evaluating the effects of the different seat post angles as the result of altered fore-aft seat positioning, specifically, using bicycle seat positions commonly used in actual competitions (road and triathlon-specific bikes) is required.

Purpose

The purpose of this study is examine the biomechanical factors effected by seat post angle represented as road (shallow seat post angle) and triathlon-specific (steeper seat post angle) bikes, and determine which angle, if any provides a performance advantage.

Research Hypotheses

Primary Hypothesis

- 1) The sagittal pedal and joint kinematics will be influenced by seat post angle modification.
 - a. The pedal will be tilted more anteriorly with steeper seat post angle, as indicated in previous literature [25].
 - b. The hip joint flexion angle will be less with more vertically positioned legs relative to the crank axis associated with the steeper seat post angle.
 - c. Ankle dorsiflexion angle will be lesser during the propulsive phase while it will be greater during the recovery phase of the pedal cycle as a result of more vertically positioned legs with steeper seat post angle.

- d. The knee joint kinematics will remain relatively unchanged since the seat post length remains the same.

- 2) Pedal kinetics will be affected by seat post angle modification.
 - a. A greater contribution of the tangential pedal force to the resultant pedal force throughout the pedaling cycle will be present with steeper seat post angle due to more anteriorly tilted pedal.
 - b. The portion of the resultant force used as the effective pedaling force will increase owing to changed contribution of tangential force with steeper seat post angle arrangement.
 - c. The index of pedaling effectiveness will be different for the two seat post angle conditions.
 - d. There will be a time-shift in the timing of pedal force application associated with steeper seat post angle.
- 3) The muscle activation pattern will be different between two seat post angle conditions
 - a. The biceps femoris activation level will decrease with the steep seat post angle.
 - b. There will be a time-shift for the timing of the muscle activation due to the altered pedal with steep seat post angle.
- 4) The performance will improve with the steeper seat post angle condition
 - a. The time to complete the simulated course will be shorter for the steeper seat post angle condition as the results of modifications in the pedaling technique mentioned above.

Significance of Study

The effects of the cycling on running performance commonly reported by triathletes have been supported by previous research in that prolonged cycling affects

the subsequent run both mechanically and physiologically. Widely accepted triathlon-specific bike frame characterized by a more vertical seat post is proposed to reduce the adverse effect of cycling on running as well as to minimize drag force during cycling. Research has found that a steeper seat post angle improved both cycling and successive running performance [27]. At a fixed intensity (70% of cycling maximal oxygen consumption), athletes on average cycled a 40-km over a minute faster ($p > 0.05$) with a steeper (81°) seat post. This improvement was not statistically significant, but it was practically meaningful. They also completed the following 10-km run nearly 5 minutes faster ($p < 0.05$). The performance improvement associated with a steeper seat post angle may be partially explained by changes observed in muscle activation patterns. A steeper seat post (82°) reduced the magnitudes of the EMG signal of the thigh muscles (biceps femoris, significantly) during a 30-second all-out cycling bout. The muscle activation level expressed as the time integral of % MVC for one second (% MVC·s) indicated that steeper seat post angle resulted in 482.9% MVC·s compared to 712.6 %MVC·s, a reduction by 30% of 72° seat post angle condition during cycling at comparable power outputs [23]. The modified leg muscle activity is considered to be necessary to maintain pedaling velocity consistent to compensate for leg movements that are relatively constrained [22]. Muscle activation pattern changes occurring with seat post angle modifications may imply changes in forces applied to the pedals, but such changes with different seat post angles have not been investigated.

Examining pedal forces provides better understanding of external work performed by an athlete than examining power output during cycling. De Grood [25] measured unilateral pedal forces and observed that steeper seat post angle (80°) caused time delay of both normal and tangential force curves during the first 70° to 90° of the crank cycle and less posteriorly tilted pedal orientation throughout the crank cycle. Orientations of the leg, seat post, and the crank were identified as the determinants of pedal force magnitudes and patterns. It is beneficial to re-examine the determinants of pedal force characteristics and to determine pedal efficiency that are obtained using a more practical setup. The finding will potentially assist triathletes and coaches to enhance triathlon performance.

Assumptions

- 1) The pedal force was assumed to be applied at a fixed, single location without any free-moment. However, the foot-pedal interface allowed the foot to internally and externally rotate, that would allow the free-moment to occur.
- 2) Kinematic and kinetic analyses of body segments were performed using traditional inverse-dynamic analysis under the assumptions of rigid body and friction-less joint [29]. In reality, deformations of the body segments and resistance at the joints would influence the kinetics and kinematics of any human body movements.

Limitations

- 1) The mass of the pedal was not accounted for in the kinetic analysis. This additional mass increased the mass of the foot-pedal segment, thus, affected inertial property of the segment. It could affect the kinetic variables. Additionally, there was a distance (moment arm) between the point of pedal force application and the pedal axis, which would cause the torque at the pedal axis.
- 2) For some muscles of some study participants, the maximal voluntary contraction trials were clearly not their maximal contraction; therefore, the EMG signals during the cycling trials were well-over 100% of MVIC.

Delimitations

- 1) Applicability of the results from this study is delimited as it was a simulated condition rather than actual competition. Absence of competitors and riding a fixed cycle ergometer were expected to influence the athletes' motivation and performance. Additionally, the data collections were performed during the 'flat' portion of the simulated cycling course.

- 2) Omitting the swimming portion prior to cycling also likely had an impact on cycling performance. A pre-cycling swim bout affected physiological efficiency [30] and power output retention [31] among well-trained triathletes during cycling. It was possible that biomechanical changes occur concurrently with the physiological changes.
- 3) The subjects included both cyclists and triathletes with previous competition experience and who were training for at least one future event that would take place within 10 month following the testing sessions. All subjects were accustomed to riding a bicycle; however, the competition level of the participants varied from recreational to elite levels. The distance and the proximity of the upcoming event would affect their performance during the experiment. Additionally, cycling techniques preferred by cyclists and triathletes might be different [26, 28, 29].
- 4) The participants used the clip-less pedals that were fixed onto the instrumented (force) pedals. This pedal-shoe interface setup was different from what the athletes were accustomed to, and it could potentially become a source of variability in cycling mechanics.
- 5) The analysis was performed only on the right side. The right pedal kinetic variables could be influenced by the kinetics and the kinematics of the left limb [4]. Additionally, kinematic and kinetic analyses were limited to the sagittal plane.
- 6) In the current study, a fixed electromechanical delay (EMD) value of 40 ms [32] was considered to examine the timing of muscle activation. However, due to the muscle length [33] and the different contraction types [34] during pedaling motion, it is possible that the length of the EMD differed at different phases of the pedaling cycle.

Operational Definitions

Bottom dead center (BDC)

180° of the pedal cycle. At this point, the pedal is at the lowest vertical position and is the transition point between the down phase and the up phase.

Crank axis

The axis about which the crank arms rotate, which is aligned in the mediolateral direction relative to the bike. It is commonly known as the bottom bracket.

Down phase

The first half of the pedal cycle, between 0° (TDC) and 180° (BDC), during which the pedal travels from the highest to the lowest vertical positions. The torque about the crank axis is applied during this phase [4]. It is also referred to as the propulsive phase in some literature [5].

Effective crank/pedal force (F_{EFF})

Portion of the resultant pedal force that is perpendicular to the crank arm that generates crank torque about the crank axis [4]. It is expressed in Newton (N).

Effective pedal force impulse (J_{EFF})

The time integral of the effective pedal force over one pedal cycle (2π), expressed in N·π. It is calculated as following.

$$J_{EFF} = \int_0^{2\pi} F_{EFF} (\theta) d\theta$$

Index of pedaling effectiveness (I_{EFF})

The ratio (%) of the effective pedal force impulse (J_{EFF}) to the resultant pedal force impulse (J_{RES}). A greater index value indicates that a greater portion of the resultant pedal force was utilized to generate crank torque [2].

$$I_{EFF} = \frac{J_{EFF}}{J_{RES}} \times 100 (\%)$$

Normal pedal force (F_y)

Pedal force (N) that is perpendicular to the pedal surface [4].

Power phase

Part of the propulsive phase of the pedal cycle where a large portion of the crank torque is applied to the crank arm. It is between 25° and 160° from the TDC (0°) of the pedal cycle, at which the pedal is at the highest vertical position [3]

Pedal cycle

A single revolution of the crank arm about the crank axis. One pedal cycle consists of 0° to 360°. 0° (TDC) corresponds to the beginning of the pedal cycle where the pedal's position is at the highest vertically, and 360° corresponds to the TDC of the subsequent pedal cycle.

Reach length (RL)

The horizontal length (cm) between the handlebar and the front tip of the seat. This length was held constant between two experimental conditions in this study.

Resultant pedal force (F_{RES})

The vector sum of normal and tangential pedal forces for which the magnitude and direction of this force indicates the sum of forces applied by the cyclist [4]. This is calculated using the Pythagorean Theorem and expressed in Newtons (N), where x and y are normal and tangential pedal forces:

$$F_{RES} \text{ (N)} = \sqrt{F_x^2/F_y^2}$$

Resultant pedal force impulse (J_{RES})

The time-integral of the resultant pedal force (F_{RES}) over a single pedal cycle expressed in N·2π.

$$J_{RES} = \int_0^{2\pi} F_{RES} (\theta) d\theta$$

Road (conventional) bike

A bike with a frame that has a relatively smaller seat post angle that is typically between 70° and 76°, traditionally, 72° [19, 35]. The seat post angle is indirectly regulated by USA Cycling by fore-aft seat positioning of the seat. For road

cycling competitions, the front of the seat needs to be at least 5 cm behind the crank axis [36].

Seat position (SP)

The fore-aft position (cm) of the seat measured between the front tip of the seat and the center of the crank axis. A positive and a negative seat position value represent anteriorly and posteriorly positioned seat relative to the crank axis.

Seat post angle (SPA)

The angle ($^{\circ}$) between the seat post and the horizontal [37]. This angle is the function of the fore-aft seat position and the seat post length. By convention, 0° corresponds to the horizontal behind the seat, and 90° represents the vertically positioned seat post.

Seat post length (SPL)

The length (cm) between the crank axis and the base of the seat at the center of the seat tube. This length was kept unchanged between two experimental conditions in the current study.

Tangential pedal force

Pedal force (N) that is parallel to the pedal surface. As pedal forces are measured two-dimensionally, tangential force is primarily in the anterior-posterior direction [4].

Triathlon-specific bike

A bike with a frame with a seat post angle that is closer to vertical than that of the road bike (about 73°), typically greater than 75° and near 80° . The USA Triathlon regulates seat post angle indirectly by restricting the fore-aft position of the seat. Under this regulation, the front tip of the seat cannot be more than 5 cm in front of and 15 cm behind the crank axis [38]. A triathlon-specific bike is also absence of the drop bars and has aerodynamic handlebars [19, 35].

Up phase

The second half of the pedal cycle – between 180° (BDC) of a pedal cycle and 360° (TDC) of the successive pedal cycle. During this phase, the pedal travels from the lowest vertical position to the highest. It is also referred to as the recovery phase in some sources [5].

Chapter Two

Review of Literature

Introduction

The aim of this study is to assess the effects of the seat post angle to cycling mechanics. It was hypothesized that making the seat post angle closer to vertical will affect pedal and joint kinematics, and as the result of these changes, the pedal kinetics and the muscle activation patterns would be modified. In this chapter, information that facilitates the understanding of cycling, triathlon, and variables investigated in the current study are provided. *Section I* includes general cycling mechanics and methods to determine variables in analyses of cycling mechanics. In *Section II*, differences between triathlon and road cycling are discussed.

Section I: Cycling mechanics

Cycling has become a well-accepted mode of physical activity as transportation, recreation, physical rehabilitation, and competition. According to the 2009 study by the National Sports Goods Association, bicycle riding is the 7th most commonly participated physical activity among people older than 7 year-old, with over 38 million participants in the US [39]. Despite its use for different purposes, cycling possesses a single objective of propelling forward by transferring the energy from the cyclist's body to the bike. Extensive scientific investigations have been done on cycling in attempt to identify factors that could improve the effectiveness of the energy transfer and to understand the mechanisms of repetitive cyclic motion associated with cycling.

Pedaling Phases

Pedaling phases are used in order to explain the mechanics of cycling effectively. Typically, the pedal cycle is described using the angle relative to the crank axis (also referred to as crank axel), the point about which the crank arms rotate (Figure 2-1). Each pedal cycle begins at 0° and ends at 360°. 0° of the pedal cycle represents the crank arm is positioned in the way that the pedal is at the highest position. 360° of the pedal cycle is the beginning (i.e. 0°) of the subsequent pedal cycle. The most commonly accepted phase classification divides the pedal cycling into two halves, the propulsion phase and the recovery phase [4]. The propulsion phase begins when the pedal is at 0 degree of the pedal cycle known as the top dead center (TDC) and ends when the pedal is at 180 degrees, also known as the bottom dead center (BDC). The propulsion phase is also referred to as the power phase (or power period) by some as it is the period where the cyclist applies most work to rotate the crank arm to progress the bicycle forward [4, 32]. However, others use the term, power phase, to describe the portion of the propulsive phase during which the majority of the pedal force or the crank torque is applied,

specifically, between 25° and 160° of the pedal cycle [3]. The recovery phase begins at the BDC and ends at the TDC. During this phase, amount of work that contributes to actual rotation of the crank arm is either absent or negligible [4, 32]. In typical cycling conditions, two crank arms are fixed at opposite from each other; therefore, while one side does through the propulsive phase, the contralateral side goes through the recovery phase. A few researchers portioned the cycling phases differently. For instance, Bohm et al. [40] classified four phases based on the different movement pattern of the pedal including downward phase ($45^\circ - 135^\circ$), backward phase ($135^\circ - 225^\circ$), upward phase ($225^\circ - 315^\circ$), and forward phase ($315^\circ - 45^\circ$ of the subsequent cycle).

There is an assumption made when the cycling data are normalized to 360° and using the pedal cycle as the time domain for the cycling data. Interpolating the data by 360° is only valid if the angular velocity of the crank arm is consistent. A published crank arm velocity data [22] indicated that there was ± 1 rpm excursion from the target cadence of 60 rpm. The 2 rpm excursion is equivalent of $12^\circ/\text{sec} = 0.22 \text{ rad/sec}$. Therefore, cycling with a peak torque of 60 N.m (at 350 W, 60rpm [41]) would result in the maximal possible power difference of 12 W (3.5% difference). This much of the difference does not appear as important, but depending on the aim of the study, the 12-W difference can be significant.

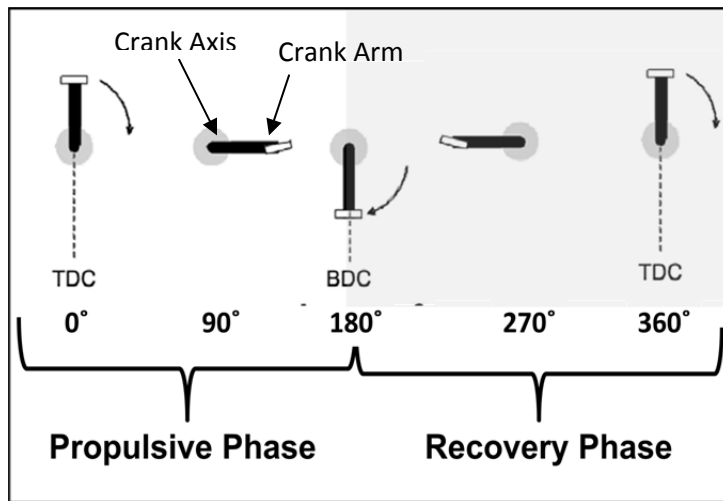


Figure 2-1: Commonly used pedaling phases during a single pedal cycle
 One pedal cycle represent one complete revolution of the crank arm.
 TDC: Top dead center; BDC: bottom dead center.
 Modified from Hug & Dorel, 2009 [1] with permission.

Cycling Kinematics

Bicycling motion primarily occurs in the sagittal plane, and the kinematics of the leg on this plane has been studied most extensively. Collectively, the leg undergoes the extension during the power phase as the pedal is moving downward, and it goes through flexion during the recovery as the pedal moves upward [4, 5]. Most commonly investigated joints are the hip, knee and the ankle. The hip angle defined as the posterior angle between the trunk and the thigh segments represents the amount of the flexion at the joint (Figure 2-2).

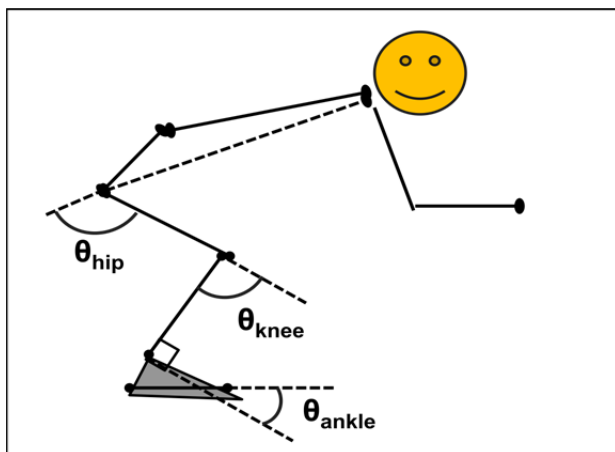


Figure 2-2: Commonly used joint angle definitions

θ_{hip} : Hip joint angle; θ_{knee} : knee joint angle; θ_{ankle} : ankle joint angle

The sagittal joint angles are generally considered fairly consistent due to the mechanically constrained nature of the movement. In a typical cycling, the hip extends from the maximal flexion, typically about 90° at TDC to its minimal flexion angle of about 55° that occurs at BDC [Gregor & Fowler, 1996 cited in [5]]. The hip flexes remaining of the pedal cycle to bring the thigh upward. The knee also undergoes extension during the propulsive phase. Beginning from the maximal flexion of approximately 120°, the knee extends about by 60° to reach its minimal flexion angle at BDC. The ankle goes through plantar flexion movement, but its range of motion (ROM) is considerably smaller (about 20°) than the hip and the knee as the ankle is required to be stiff to transmit the energy generated by the leg muscles to the pedal [5, 42]. The most flexed position (typically in slight plantar flexion) of the ankle occurs at the top of the pedal cycle to let the leg pass forward through TDC [5]. The joint kinematics and coordination in the sagittal plane has been reported relatively consistent among trained cyclists. However, the sagittal joint movement patterns between high-level cyclists and novice have been shown different [43]. The novice cyclists not only cycled with less ankle angle, and their coordination between pedal cycles appeared more variable.

Kinematics in the frontal and the transverse planes has not been investigated as extensively since the magnitude of the movements are smaller and possibly as non-sagittal movements are not considered directly related to cycling performance. However, the movements that occur on these planes have clinical implications. The mediolateral location of the knee relative to the pedal changed with an excursion of 4 – 5 cm through a pedal cycle [McCoy, 1989 cited in [5]]. Particularly medial displacement of the knee occurred through the entire propulsive phase, placing the knee into pseudo-valgus (knocked) knee position. Movements in transverse plane also occur. Although, the actual angle of the rotation was not reported, Wheeler et al. [44] reported moment at the foot-pedal interface was present, which is an indication of axial rotation of the foot on the pedal. The amount of the moment was positively related to the power output, and it depended on the type of the foot-pedal interface. Additionally, the magnitude of the moment was greater among cyclists who had reported chronic knee pain [44].

The segmental angles are other kinematic variables essential in cycling mechanics analysis. In a typical road cycling setting, the pedal angle is mostly anteriorly tilted relative to horizontal; however, during a short period in the mid-portion of the propulsive phase, the pedal is posteriorly tilted. [4]. It is referred to as the “heel-down” pushing position [4]. Some have suggested that this “heel-down” accompanied with ankle dorsiflexion is a strategy to improve the pedaling effectiveness by involving the stretch-shortening cycle of the muscle [42]. The maximal anterior tilt of the pedal (approximately, 30° - 35°) occurs at 270° of the pedal cycle, when the pedal is the most posteriorly located relative to the cyclist. From there, the pedal starts to move toward less posteriorly tilted position. The segmental orientation of the leg segments (thigh and shank/leg) are not often reported as kinematic variables; however, they are measured in the investigations that concerns the inertial effects of these segments [22, 25, 45-47].

Cycling Kinetics

Evaluation of cycling kinetic variables is possible with measured crank arm torque or pedal forces. Of the two major types of the measuring devices commonly used (Figure 2-3), instrumented pedals provide more comprehensive information. A crank arm based power meter (such as SRM power meter, Schoberer Rad Messtechnik, Welldorf, Germany) uses a strain gauge installed between the chain ring and the crank arm to measure the total crank torque as the result of bilateral leg action [48]. Instrumented pedals allow separate measurements of forces applied by individual limbs. Previous research has quantified work performed by the cyclist using these pedals. Some scholars used pedals capable of measuring 3-D pedal forces [44], many studies only considered 2-D pedal forces. A force pedal as one described by Newmiller et al. [6] allows to measure tangential (horizontal to the pedal surface) and normal (vertical relative to the pedal surface) pedal forces.

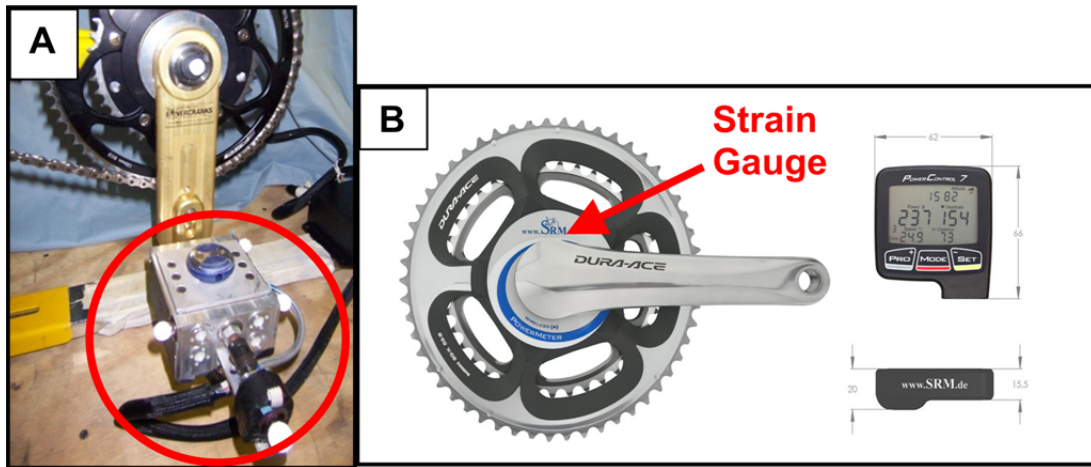


Figure 2-3: Two different types used to measure pedal kinetic variables

- A: 2-D force pedal as described in Newmiller et al. [6]. Deformation of the octagonal strain ring force transducer located in the middle of the pedal causes electrical signals. Normal and tangential forces are measured.
- B: RSM power meter. The torque applied to the crank arm is detected. (www.srm.de with permission)

The vector sum of the tangential (F_T) and the normal (F_N) forces is the total force applied to the pedal referred to as the resultant force (Figure 2-4). To determine the resultant pedal, following equations are used first to determine the horizontal (F_X) and vertical (F_Y) components of the pedal force [2].

$$F_X = F_T \cos(\beta) - F_N \sin(\beta)$$

$$F_Y = F_T \sin(\beta) + F_N \cos(\beta)$$

β is the pedal orientation relative to horizontal.

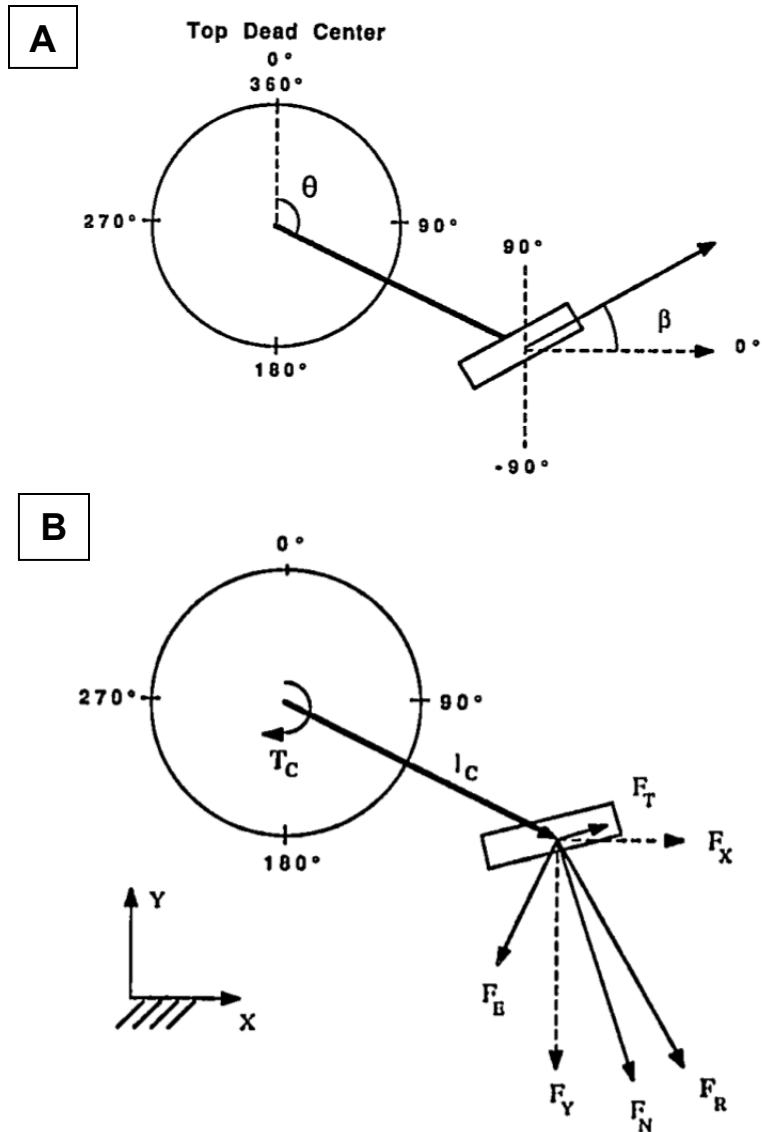


Figure 2-4: Crank and pedal angles and determination of the pedal forces and crank torque

A: The reference angles used in determination of pedal kinetic variables. θ : crank arm angle relative to top dead center; β : pedal orientation relative to horizontal
 B: Definitions of different pedal forces and crank torque. F_N : normal force; F_T : tangential force; F_R : resultant force; F_x : horizontal force; F_y : vertical force; F_E : effective force; T_C : crank torque; l_C : crank length. Coyle et al., 1991 [2] with permission.

The magnitude of the resultant force (F_R), $|F_R|$, then can be calculated using the Pythagorean theorem [2].

$$|F_R| = [(F_X)^2 + (F_Y)^2]^{1/2}$$

The vector product of crank arm vector (l_c), which points along the crank arm from the crank axis to the center of the pedal and the F_R provides crank torque (T_C) in Newton-meter (Nm) [2].

$$T_C = l_c \times F_R$$

Finally, the effective pedal force (F_E) can be determined. The F_E , the portion of the pedal forces that generates the crank torque (T_C) to revolve the crank arm is perpendicular to the crank arm [2, 4, 7]:

$$(|F_E| = |F_R|^2 - [(l_c \cdot F_R)/|l_c|]^2)^{1/2}$$

Where $l_c \cdot F_R$ is the scalar product of the vectors l_c and F_R , and $[(l_c \cdot F_R)/|l_c|]^2$ represents the magnitude of force that is parallel to the crank arm (ineffective pedal force, F_{IE}). This particular method of F_E arbitrarily gives zero when the F_E is not positive [2]. An alternative way of determining the F_E with the direction is to identify the components of the F_N and F_T that are perpendicular to the crank arm with consideration of the polarity of the forces.

Many researchers concern the effectiveness of pedal force application. The ratio of the area under the F_E -pedal cycle angle (θ in rad) curve to the area under the $F_R-\theta$ curve describes how much of the F_R was F_E , the index of pedaling effectiveness (IE) over a pedal cycle (IE_{360}) [2, 49].

$$IE_{360} = \frac{\int_0^{2\pi} F_E(\theta) d\theta}{\int_0^{2\pi} F_R(\theta) d\theta} \times 100 (\%)$$

IE during the propulsive phase is often determined as the majority of the F_E is applied during this phase [2, 4, 22, 40]. And the IE during the propulsive phase is calculated as:

$$IE_{180} = \frac{\int_0^{\pi} F_E(\theta) d\theta}{\int_0^{\pi} F_R(\theta) d\theta} \times 100 (\%)$$

The crank power is a variable that is commonly associated with cycling performance. Crank power has been shown to be associated with cycling performance [2, 50]. The power describes the rate of work performed [51], and the crank power (W) is depended on the angular velocity (ω in rad/s) [4].

$$P_{crank} = \tau_{crank} \times \omega_{crank}$$

The primary pedal force during cycling is the normal force. The plot of typical pedal forces during a pedal cycle is included in Figure 2-5. A clock diagram that shows the resultant force at certain points of the pedal cycle is also included in Figure 2-6. Notably large amount of the normal force is applied during the propulsive phase. In a typical steady state road cycling condition, the magnitude of the normal pedal force found to be approximately 60% of the cyclist's body weight [4, 52], and even with standing pedaling technique used in uphill climbing cycling, cyclists seldom apply the normal pedal force greater than their body weight [53]. During recovery phase, the normal force remains positive. As indicated in the clock diagram, the pedal is moving backward while the pedal is tilted anteriorly. Therefore, at least the part of the positive normal force is the cyclist's attempt to move the pedal backward.

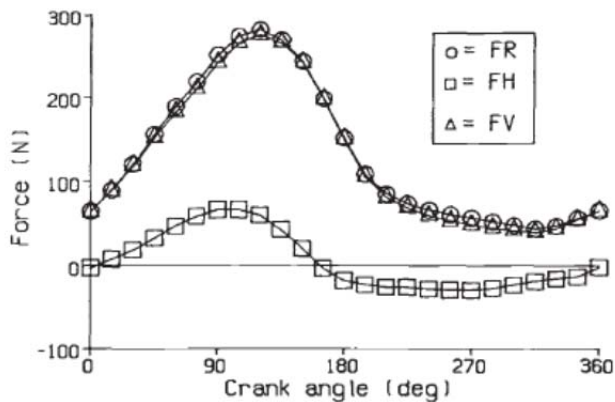


Figure 2-5: Normal, tangential, and resultant pedal forces during a typical steady state road cycling condition

FR: resultant force; FH: tangential force; FV: normal force. For FH, a positive force indicates the anteriorly directed force. The study included 6 healthy recreational cyclists who cycled at 60 rpm with 120W workload. Ericson, 1988 [7] with permission.

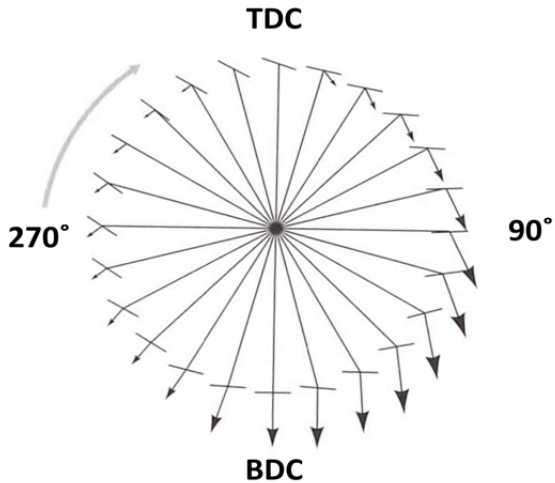


Figure 2-6: Clock diagram of pedal orientation and resultant pedal force at selected points of the pedal cycle

The direction of the resultant pedal reaction force is indicated by the direction of the arrow and the magnitude of the resultant pedal reaction force is indicated by the length of the arrow. The orientation of the pedal is indicated by the tilt of the line representing the pedal. TDC: top dead center (0°), 90° , BDC: bottom dead center (180°), and 270° represent the point of the pedaling cycle. The data is the average of 17 road cyclists who were riding at 90 rpm with power output of 350 W. Broker, 2003 [4] with permission.

The tangential pedal force is significantly smaller in magnitude than the normal force. During the propulsive phase, the anteriorly directed tangential force increases to approximately 100° of the pedal cycle facilitating the forward movement of the pedal. While in the first part of the recovery phase, it is directed posteriorly to progress the pedal backward. As shown in the clock diagram, the resultant force near the TDC and BDC, particularly after 90° to 210° of the pedal cycle, is not positioned near perpendicular to the crank arm. This indicates that even with the large amount of the force is applied during this period, that does not translate to large amount of crank torque produced [4].

The most appropriate pedal force variable that provides better insight to cycling performance is the effective pedal force. It has been documented that individually, cyclists are generally able to exert similar amount of effective pedal force with certain changes in cycling conditions such as shoe-pedal interface [44] and types of crank arms (fixed vs. independent) [54, 55]; however, changing other cycling conditions resulted in modification in effective force. Investigation on different workload (power output), suggest that effective pedal force is positively related to the workload required [41]. Riding position change without leg orientation also affected the effective force. Of three

riding positions tested (upright, drop bar, aerodynamic – Figure 2-7), the effective force was highest with the aerodynamic position [3]. Standing pedaling resulted in significantly higher crank torque than seated pedaling [53]. As consistent crank arm length were used in this particular study, the result indicates that greater amount of effective force was present in standing pedaling position. The magnitude of the effective force is also inversely related to cadence [41]. Kautzs & Hull [46] have suggested that higher cadence may results in more economical with greater effective force and index of pedaling effectiveness due to a greater contribution of the non-muscular component of the pedal forces, which is related to the inertial effect of the leg segments themselves. Lucia et al. [56] suggested lower economy, owing to higher muscle activations associated with lower cadence. On contrary, others supported higher pedaling effectiveness with lower cadence [24, 57]. Cyclists performing at higher levels appear to have a better index of pedaling effectiveness [2, 26]; however, the index was not shown to be positively related to the cycling performance [2]. As the index of pedaling effectiveness is mechanically derived, it may not explain the complete dynamic of cycling movement. As reported by Korff et al., [58] decreased the amount of negative torque (improving pedaling effectiveness) by changing the pedaling techniques (intentionally ‘pulling up’ the leg during the recovery phase) increased the cost of cycling.

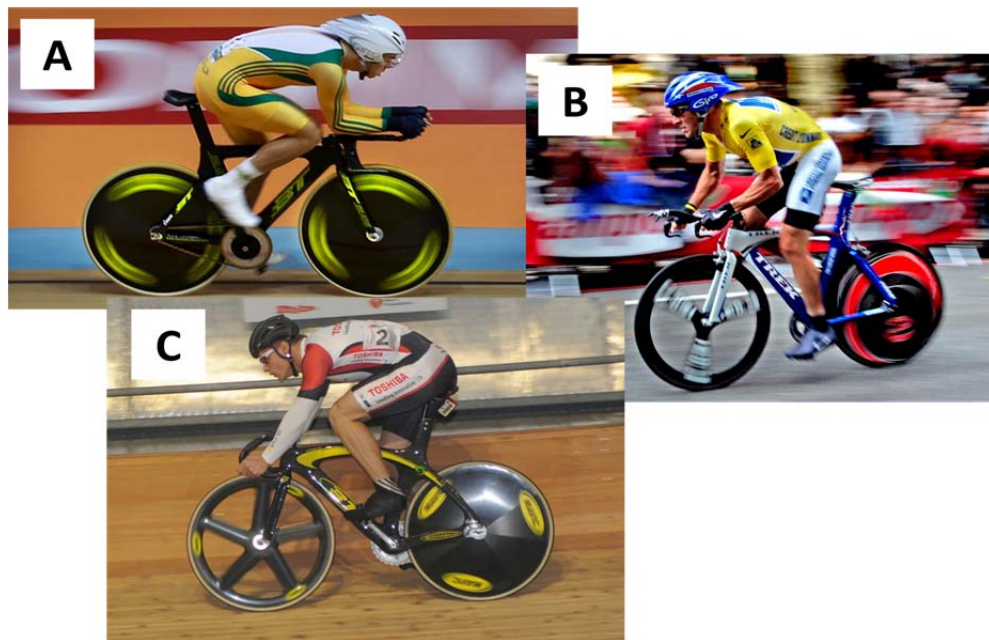


Figure 2-7: 3 commonly used cycling positions
A: aerodynamic position; B: upright position; C: drop position

The determination of joint kinetics variable involves in human movement can be done using the inverse dynamics with measured external forces and kinematics, the

pedal reaction forces. The fundamental inverse dynamics method assumes that rigid body segments with fixed inertial properties and no loss of forces within and between segments [51, 59]. An example of the link segment model and a free-body diagram used for the inverse dynamics are included in Figure 2-8. The joint moments (shown as "M" in Figure 2-8 B) describes the net effects of the structure associated with the joint, including action of all the muscles and less significantly, soft tissues at the joint [4, 51, 59]. Therefore, joint moment values should not be interpreted simply as the action of the muscles.

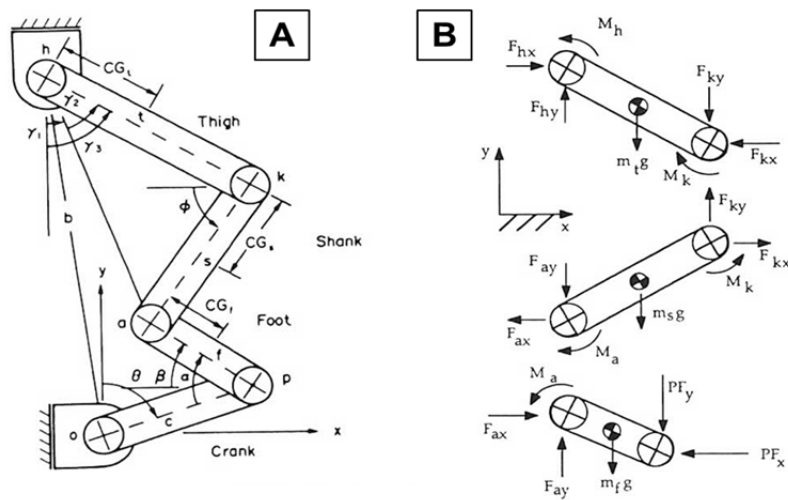


Figure 2-8: Example of 2-D (sagittal) link segment model used for inverse dynamics of cycling movement

A: Bar linkage model of the bicycle-rider system. The segments included are thigh, shank, foot, and crank arm.

B: Free-body diagram of the leg for determination of intersegmental loads. External loads are applied to the foot as horizontal (PF_x) and vertical (PF_y) pedal force.

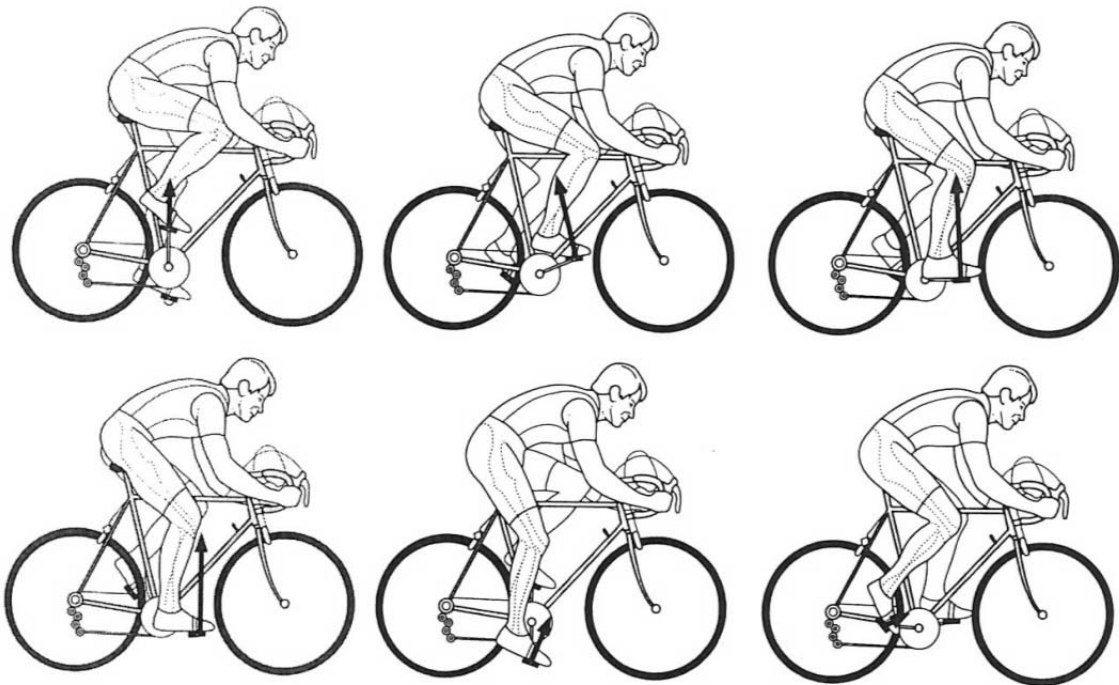


Figure 2-9: Resultant pedal reaction force alignment relative to the right lower extremity for six different points in the pedaling cycle

The direction of the resultant pedal reaction force is indicated by the direction of the arrow and the magnitude of the resultant pedal reaction force is indicated by the length of the arrow. The line of pedal reaction force vector relative to a joint determined the joint moment. From Gregor & Conconi, 2001 [5] with permission.

When the joint kinetics during cycling is concerned, the orientation of the reaction force of the resultant pedal force with respect to the leg segments is critical [5]. As seen in Figure 2-9, the orientation of the resultant pedal force vector determines its effects at the leg joints, as the result, the joint moments and the muscle activation patterns are affected [5].

Typical patterns of joint moment at the hip, knee, and the ankle during cycling are shown in Figure 2-10. During road cycling setting, the knee initially undergo significant amount of extensor moment that occur during the propulsive phase of the pedaling cycle. As the magnitude of the moment corresponds to the environmental demand associated with the joint, and the concurrent displacement is also in extensor direction, it indicates that the knee structures, primarily, the knee extensors are causing the leg to extend against the pedal [4]. The direction of the knee moment, however, switches to flexor moment prior to DBC, where the knee reaches its maximal extension angle [4, 7]. This concurrent knee flexor moment and knee extension movement is not to cause the

force generated, but is related to the different function of the knee muscles at this time [60, 61]. Flexion moment is considered functionally to transition the loading pattern of the pedal force from downward to backward in attempting to improve the effective pedal force [60]. The ankle is entirely in plantar flexion moment through the propulsive phase as it resists against the dorsiflexor moment caused by the pedal reaction force [5]. The hip remains to have extensor moment the entire pedal cycle [4, 7]. During the initial recovery phase, the hip moment is in extensor direction as it acts to direct the backward motion, then becomes flexor moment to bring the leg forward toward the top of the cycle. At this time, the thigh is relatively motionless [4]. In the way, the knee and hip moments act in the opposite direction. The ankle moment changes into dorsiflexion during the last part of the upstroke to clear the foot at the TDC. Roles of muscles are discussed in the following section.

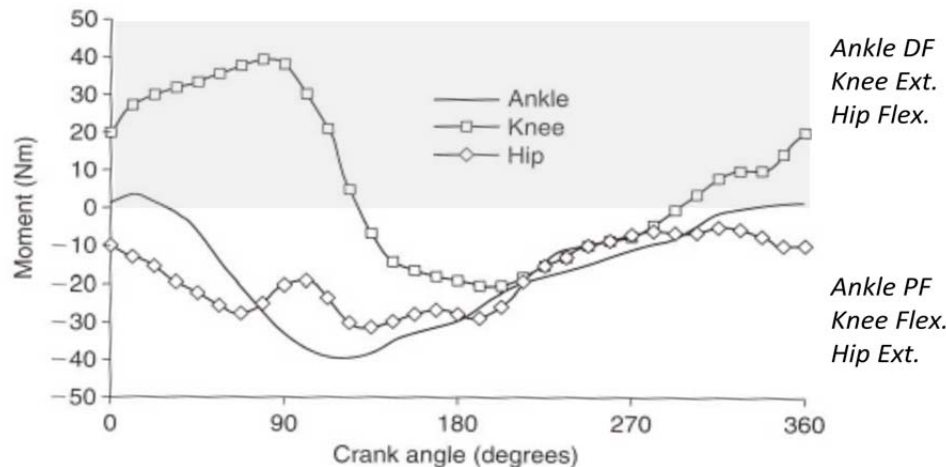


Figure 2-10: Joint moments at the hip, knee, and ankle joints over a single pedal cycle

The shaded area (moment > 0) indicates dorsiflexor moment at the ankle, extensor moment at the knee, and flexor moment at the hip. This data from a cyclist riding at 250 W and 90 rpm. Broker, 2003 [4] with permission.

Muscles

The muscle activation patterns of during cycling have been studied by many researchers. An example of the muscle activation patterns from a recent study is included in Figure 2-11. Note that these EMG graphs have the horizontal axis starting from 180° (bottom dead center) of the pedal cycle instead of 0° (top dead center). Activation patterns of most of the leg muscle are agreed by researchers. During cycling, leg extensors are primarily active to extend the leg during the propulsive phase. The gluteus maximus (GMax) onsets at near TDC and is highly active though the power phase (to 120° to 130°) [3, 62]. The vastii, vastus lateralis (VL) and vastus medialis (VM),

are also highly active through the power phase (90° - 100°), but their onsets are slightly (approximately 20°) earlier than GMax [3, 62]. A biarticular quadriceps muscle, rectus femoris (RF) becomes active earlier than its monoarticular counterparts. It is also highly active through the power phase until approximately 90° [3, 62]. Two types of activation patterns of the hamstring muscles have been reported. The long head of biceps femoris (BF), semimembranosus (SM), and semitendinosus (ST) are active from TDC to BDC. While some cyclists use the hamstring muscles primarily through the propulsion phase, others use them longer, until the mid-recovery phase (about 270°) [62]. The soleus (SOL) becomes active during the power phase (45° - 135°) [62]. The biarticular calf muscles, gastrocnemius lateral (GL) and medial head (GM) become active shortly after the TDC (about 30°) to the half way through the recovery phase, when the tibialis anterior muscle (TA) begins its activation [3, 62]. TA is active through the TDC until GM and GL begins their activations.

Above mentioned muscle onsets and offsets corresponds to the conduction of the electric signal to the muscle. Ryan and Gregor [62] indicated that a 22° -delay on the mechanical response after the onset of the EMG signal due to the electromechanical delay. When cyclists pedaled at 90 rpm and at power output of 250 W, the electromechanical delay was approximately 40 ms. This means that the actual muscle force generation occurs approximately 22 degrees after the onset of the EMG signal.

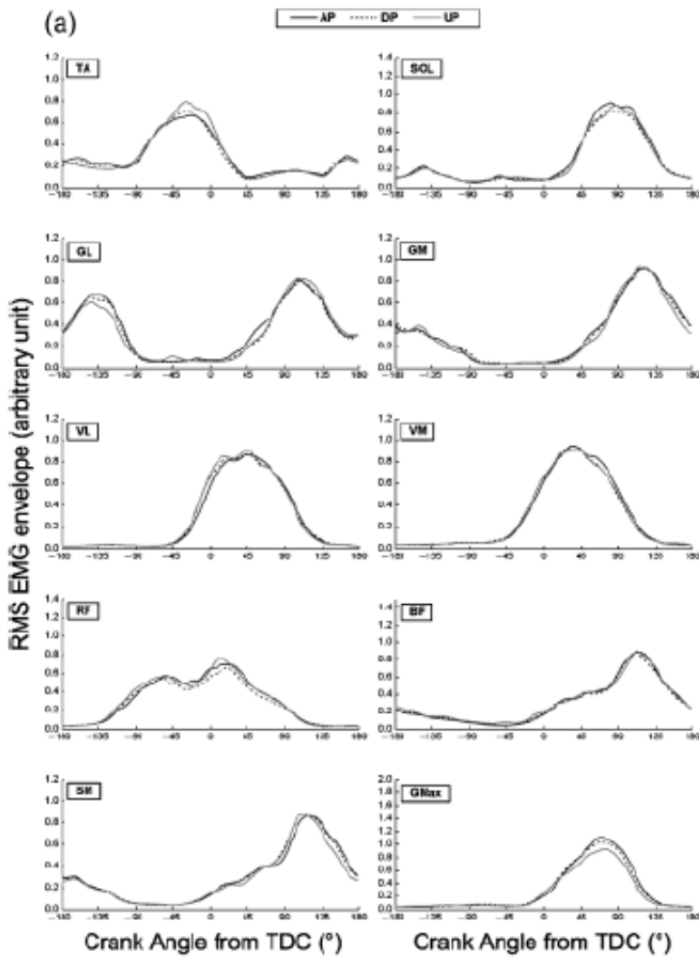


Figure 2-11: Muscle activation patterns of 10 leg muscle during cycling in three different upper body orientations

TA: Tibialis anterior; SOL: solius; GL: gastruocnemius lateral head; GM: gastrocnemius medial head; VL: vastus lateralis; VM: vastus medialis; RF: rectus femoris; BF: biceps femoris; SM: semimembranosus; GMax: gluteus maximus. The data were normalized to the peak magnitude during cycling trials of respective muscles. 3 upper body orientations tested in this study were 1) upright, 2) hands on the drop bars, 3) aerodynamic position. Note that the time (pedal cycle)/horizontal axis is from the bottom dead center (180°) to the subsequent bottom dead center. Dorel et al. (2009) [3] with permission.

Previous studies have identified that the activation of the monoarticular muscles coincided with the joint movement, indicating that these muscles are primarily to generate positive work during pedaling motion [61, 62]. The biarticular muscles, on the other hand, act to allow more effective work transfer between the leg segments and the pedal [61, 63, 64]. A diagram of the muscle links between leg segments (Figure 2-12) illustrate the intersegmental relationship between muscles.

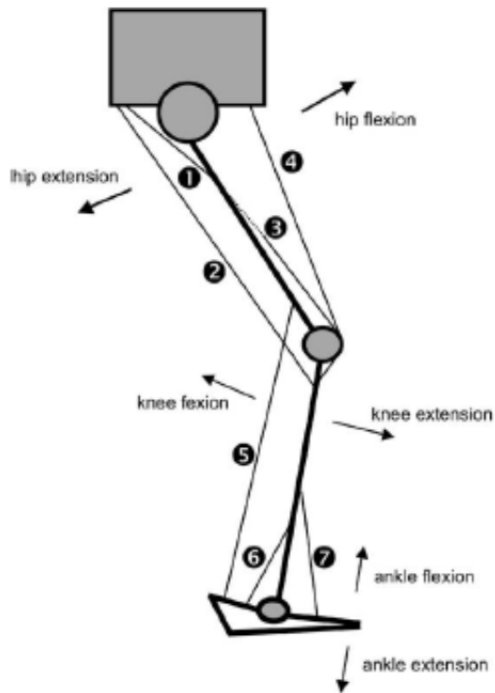


Figure 2-12: Schematic diagram of major leg muscle that involves in cycling

(1) Gluteus maximus (hip extensor); (2) Semimembranosus and Biceps femoris long head (hip extensors/knee flexors); (3) Vastus medialis and Vastus lateralis (knee extensors); (4) Rectus femoris (knee extensor/hip flexor); (5) Gastrocnemius lateralis and Gastrocnemius medialis (knee flexors/ankle extensors); (6) Soleus (ankle extensor/plantarflexor) and (7) Tibialis anterior (ankle flexor/dorsiflexor). Hug & Dorel (2009) [1] with permission.

The biarticular muscles have conflicting roles at the different joints. For example, the hamstring muscles extend the hip and they also flex the knee. During each of the two major phases of the pedaling, the propulsive and recovery phases, however, either extension or flexion of the joints occur concurrently. During the propulsive phase, extension at both hip and the knee joint occur, whereas flexion of these joints occurs during the recovery phase. The similar condition is true for some other leg muscles, such as the rectus femoris and gastrocnemius muscles. Therefore, this ‘shortening’ at one, but ‘lengthening’ at the other joint keeps the length of the muscle somewhat consistent allowing the mechanical energy transfer more efficient to translate the muscle force to the pedaling force [61].

The timing of the biarticular muscles also important in cycling. As discussed earlier, activation of the biarticular muscles, such as gastrocnemius muscle, occurs later than the monoarticular muscle. It acts like a “guide wire” [4] to allow the transfer of the mechanical work more effectively by contracting when the shift in direction of the joint moment happens. The onset of the monoarticular quadriceps muscles occur as the knee moment switches to extensor moment, shortly prior to the TDC to swing the leg forward.

The onset of the rectus femoris (biarticular muscle) is also near the TDC to provide a stable ‘linkage’ between the hip and the knee joints while the vasti (monoarticular) muscles contract to extend the knee. The concurrent flexion at the hip and extension at the knee during the early down phase maintains the length of the rectus femoris relatively consistent to allow to contract more isometric manner [4]. This action of the rectus femoris allows the positive work generated by a large gluteus maximus passed on to the distal segment and to the pedal. Similarly, biarticular, hamstring muscles becomes active when the knee moment switch the direction (from extension to flexion) at the late propulsive phase, facilitate the concurrent movement of the knee and the hip during the direction of action at these joint change. The gluteus maximus, a uniarticular hip extensor, act as a major contributor in producing extension moment during hip extension in the down stroke.

Cycling movement occur in a mechanically constrained environment. Series of kinematic, kinetic, and neuromuscular events occur strategically to apply the force to the pedal more effectively. Understanding of the mechanics of typical road cycling allows recognizing the differences in cycling in triathlon setting.

Section II: Triathlon Cycling

Triathlon is a fast-growing sport that involves three different modes of endurance events, swimming, cycling, and running performed consecutively. Many triathletes report impaired performance on their run after completing the bike segment of the race. As the bike and run segments are the two longer segments in a triathlon race, effective transition between the two disciplines is important. In this section, the effects of the preceding cycling on the run performance are discussed. Then, the effects of riding positions are presented.

Effects of Bike Segment

The cycling is the second leg following the swim leg in a triathlon race. The cycling segment is typically the longest segment in any triathlon distances, and a triathlete can spend anywhere between one-half hour (12 miles for the sprint distance) and 6 hours or longer (112 miles for the Ironman distance) on the saddle. Triathletes often report pain and/or discomfort in the legs that may be accompanied with impaired performance on the following run segment [35]. In order to perform successfully in the sport, the transition needs to be effective [65]. Additionally, some of the overuse injuries associated with triathlon are related to improper techniques, which include transition between bike and run [66].

There have been some disagreements in how the prior cycling would impact the running mechanics and performance. A study reported no kinematic changes were detected during a post-cycling run [67]. A filed study with 2-D motion analysis at the World Cup competition concluded that there was no effects of the preceding 40-km cycling on the running performance among elite triathletes [12]. However, there is more evidence that support that the prior cycling, in fact, affects the running segment. Millet et

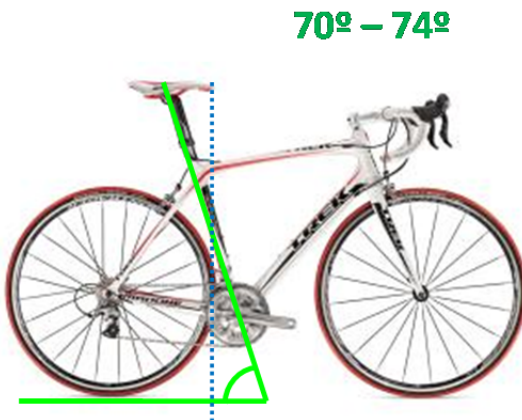
al. found that the run following an exhaustive cycling session was associated with an increased metabolic cost by $2.3 \pm 4.6\%$ [13] and mechanical cost by $7.1 \pm 6.0\%$ [14]. The change in cost demand is sought to be explained by both physiological and biomechanical changes. The respiratory muscle functions were impaired after a prolonged submaximal cycling session that persisted through a following running session [15]. Progressive chemical changes indicating muscle catalysis and dehydration were observed during post-cycling portion of a triathlon competition [16]. Hausswirth et al. reported that decreased running economy after cycling was related to altered kinematic changes including more forward leaned position, altered use of knee flexion during the stance, and increased stride frequency [68]. An extended cycling session also affected stride kinematics [18, 68] and activation patterns in the leg muscles [11, 69] during subsequent run. Even among some of the elite triathletes with years of experience exhibited certain kinematic changes during a run following a cycling session [69]. These triathletes were found to carry the leg muscles' neuromuscular pattern of the preceding cycling. The authors concluded that prior cycling likely affected the motor command during the run.

Some researchers suggested that the residual effects from prior cycling could possibly be an advantage to improve performance. Gottschall and Palmer [70] reported that cycling at higher cadence during bike segment resulted in a higher stride frequency at the beginning of the running leg owing to perseveration associated with the rhythmic activity performed over an extended period of time. In this study, no difference in 2D joint kinematics during cycling and running, but the run speed was faster and the stride frequency was greater during the entire run following cycling at cadence that was 20% higher than the triathletes' preferred cadence. Suriano et al. also reported improved run performance after a 30-minute cycling session [71]. They suggested that variable intensity strategy during the cycling was the factor for the improvement; however, how it affected the run performance was not identified. As the higher economy is linked to successful triathlon performance [10], any strategies to minimize the adverse effects of the cycling and/or improve the running economy in bike-to-run transition is desirable to succeed in the sport.

Riding Position

Various strategies have been implemented by triathletes to enhance their cycling performance levels. One of the most notable differences between triathlon cycling and non-time trial road cycling is the bike geometry. In recent years, increasing number of triathletes has adopted a bike with difference geometry to lessen the effects of cycling on their running performance. Specifically, triathletes use a steep seat post angles that are more vertical (about 80°) than that of conventional road-racing bikes (between 70 to 74°) (Figure 2-13). Seat post angle affects the seat's relative position to the crank axis. More vertical seat post seen in triathlon-specific bike frame places its rider more directly above the crank axis.

Road (shallow)



Triathlon (steep)



Figure 2-13: Typical road bike and triathlon bike

Road bike's seat post angle is traditionally 73° , but typically, between $70^\circ - 74^\circ$. Road bike is characterized by shallower seat post angle and the drop bars to allow more aerodynamic position.

Triathlon bike typically has the seat post angle of greater than 76° , often close to 80° . Triathlon bike is characterized by steeper seat post angle, higher seat position relative to handle bars, and aero-bars in front (no drop bars) to allow more aerodynamic position. Seat post angle is the function of the fore-aft seat position relative to the crank axis and the length of the seat post. Note the position of the triathlon bike's seat is directly above the crank axis. Photos form www.bikepedia.com with permission.

A limited number of published data include the effect of the seat post angle manipulation, and these findings do not agree. A steeper seat post angle as in triathlon bike theoretically reduces the hip flexion angle [5] and rotates the entire body relative to the crank axis that leads to the increase in the anterior tilt of the pedal-foot segment [25, 72, 73]. When tested, however, only minimal effects on kinematics were found. Price and Donne found that changing seat post angle did not have any effects on knee flexion angle, but greater SPA (80°) slightly increased (non-significant) increase in ankle plantar flexion and the amount of hip flexion [73]. Jackson also reported no change in knee angle, but also in hip angles during the last 5 min of 40-min time trial ride (stationary) with seat post angle change (73° and 81°) [74]. DeGrood reported the orientation of the pedal changed with the seat post angle [25]. A greater seat post angle of 80° resulted in more anteriorly tilted pedal orientation compared to the 60° seat post angle. The author suggested that the position and orientation of the body, and seat-to-pedal distance influence joint angles, muscle lengths, and muscle moment arm lengths, and they in turn affect the length-tension relationship and the force-velocity-power relationship of the working muscles resulting in altered effectiveness of force production.

Any kinematic change related to riding position has been proposed to alter the muscle activation pattern on the basis of length-tension relationship of the muscle. In

case of cycling using different seat post angles, it has been suggested that changed hip kinematics facilitates pre-stretch of the gluteus maximus muscle that improves the action of the muscle [21]. Only a few studies examined the effects of the seat post angle on muscle activity. An investigation using electromyography (EMG) of the leg muscles during cycling in the conventional and steep seat post conditions revealed altered pattern of leg muscle use. Brown [22] confirmed that a more extended hip position enabled cyclists to generate greater hip torque while biceps femoris activation was reduced. Richard et al. supports this finding of the changed activation pattern of the biceps femoris muscle. An aerobic all-out testing (Wingate) using two different seat post angle conditions (72° and 82°) revealed that cyclists were capable of maintaining the similar power output while the EMG amplitudes of the quadriceps and hamstring muscles (biceps femoris significantly) were smaller with the 82° condition [23].

Dorel et al. [3] conducted a comprehensive study on the effects of the riding position primarily involving manipulation of the upper body orientation. When muscle activities of 3 different riding positions (upright, hands on the drop bar, and aerodynamic) were compared, aerodynamic position resulted in greater extent of gluteus maximus activation and decreased RF activation. Changing from the upright position to aerodynamic position, it was likely that the hip was brought into more flexed position, rather than extended position as discussed above. Therefore, the position effects to the hip and the thigh muscles are not yet certain. Chapman et al. [28] also investigated the aerodynamic position compared with the upright position. They showed that changing the upper body orientation alone was associated with less relaxation period in leg muscles during pedaling. Leg and pedal kinematics were not affected. It may indicate that it is not the joint kinematics that influences the muscle activation patterns.

Brown et al. [22] examined the effects of the orientation of the entire body. The participants pedaled at several different body tilt positions (increments between prone to 10 degrees posterior tilt from vertical) at a constant workload (60 J) and cadence (60 rpm). The different orientation resulted in systematic change in torque in all hip, knee, and the ankle joint as well as the EMG amplitudes. The muscle activation pattern (onset and offset) were maintained since the controlled joint kinematics at the hip and knee allowed no significant changes in the lengths of the working muscles. The authors concluded that the changes in the joint torques and muscle activation levels were the direct result of the changed effect of the gravity caused by the changed body orientation. The adjustments in the magnitudes of the muscle and the joint torques were as the result of the attempt to maintain the constant cadence in the different pedaling environment.

Regardless of the mechanism of reduction in muscle activation, in triathlon cycling, preserving the muscles that are important in running may be a good strategy. The biceps femoris is an important muscle in running. During the late stance (near toe-off), it brings the hip and knee into extension and during the terminal swing, it decelerates the forward moving leg [2]. Therefore, preserving biceps femoris during the preceding cycling segment may improve running performance by possibly preventing fatigue from using excessively. Candotti et al. [29] found that activation pattern of BF

was different between triathletes and cyclists during cycling. Triathletes used BF less extensively (shorter duration) than cyclists, while the activation pattern for the RF and VL were similar in both groups. Both cyclist and triathlete groups spent about the same amount of time for training, but triathletes trained for 3 different sports whereas the cyclists spent time for cycling exclusively. The authors speculated that specificity of training plays an important role in this difference in muscle activation patterns.

Evidence on seat post angle effects on cycling kinetics is very limited. Power output has been shown to be improved with more vertical seat post angle [20, 75]. Although, the improved power output was hypothesized to be related to the position of the pelvis, but how the hip-pelvic kinematics affect on power generating muscles are unclear. Browning et al. [72] have found that compared to cycling in the regular aerodynamic position (greater hip flexion), cycling in the aerodynamic position with steeper seat post angle (lesser hip flexion angle) reduced the hip extensor moment while increasing the knee extensor moment. Therefore, it is less likely that cycling with steeper seat post angle would increase the activation of the gluteus maximus muscle.

Section III: Instruments and Methodology

Recent movement analysis utilizes different technologies. In this section, details on instruments and methodology commonly used in movement analysis are discussed. First, three-dimensional motion capture system and different methods of determining joint kinematics are described. Details on electromyography are also discussed in this section.

3-Dimensional Motion Capture

Three-dimensional (3-D) analysis has been an important aspect of movement analysis. 3-D movement analysis allows quantification of the movement characteristics; therefore, it makes comparison of different movement patterns easier.

Stereophotogrammetry using retroreflective markers is a common way of capturing the movement of the body. In this method, the instantaneous location of the markers placed on the skin is tracked during the movement. A segmental/local orthogonal frame (also known as technical coordinate system, TCS) defined by a set of markers on a body segment is captured in each data image, and its location and the orientation relative to the global orthogonal frame is determined through the transformation equation [76]. This process provides the segmental kinematics data with assumptions that the relationship between these segmental markers does not change (i.e. no deformations of the segment). Segmental kinematics provides details about the location and the orientation of the segment in space [77]; however, clinical interpretations of this information are difficult. The International Society of Biomechanics (ISB) has developed a standard in reporting joint motion based on the Joint Coordinate System (JCS) [78] to allow the data

expressed in clinically relevant terms. The JCS that was originally proposed by Grood and Suntay [79] allows the description of the relative movement of two adjacent body segments about the joint center (joint kinematics). In order to determine the location of the joint center, the “anatomical markers” on the palpable bony landmarks need to be identified relative to the segmental or local coordinate systems [76]. A typical ‘static’ trial with both anatomical and segmental markers allows the anatomical markers’ position in the segmental coordinate systems, and the location of the anatomical markers, thus, the joint centers are determined using the location of the segmental markers/coordinates. Therefore, it is critical that the location of the anatomical markers determining the joint center is consistent across study participants and/or the testers [80]. The errors in joint kinematics data associated with inconsistent anatomical marker location have been documented previously [81]. Additionally, it has been known that the location of the joint center changes through the joint range of motion [76].

Different methods have been proposed to minimize the errors in joint kinematics that are related to the anatomical marker placement. Schwartz and Rozumalski [82] introduced a methods that does not require anatomical markers. This “functional methods” uses the algorithms to derive the functional joint center of multiple degrees of freedom from two adjacent segments. Authors concluded that this new methods to identify the joint center helped reducing the cross-talk in knee joint angle that is characterized by increased valgus-varus excursion accompanied by reduced flexion-extension excursion. The hip and knee joint kinematics were minimally affected by the markers placed on the segments, thus improved the inter-trial (variability 1 – 3 mm for hip and 3 – 9 mm for knee joint centers and less than 2° for the knee axis) and inter-day (variability approximately 10 mm for hip and knee joint centers and about 4° for the knee axis) repeatability when walking gait was analyzed. Additionally, the authors suggested the setup complexity was reduced by eliminating the needs for application of the anatomical markers. A follow-up study examined the reliability of this functional method in running motion, on contrary, found no significant improvement in reliability of this method [83]. The coefficient of correlation for the hip, knee, and ankle kinematics in all 3 planes (over 0.803) indicated good reliability associated with both traditional method using anatomical markers and the functional methods. However, the authors speculated that running on a treadmill might have reduced the variability present in typical over-ground running.

Another method proposed by Donati et al. [84, 85] utilize a digital model in determining the anatomical frame. This method (“UP-CAST”) does not require anatomical marker, but it estimates the subject-specific bone and anatomical landmarks by determining multiple unlabeled prominences of the bone to match a digital model of the deformable template. The anatomical landmark identification using this method indicated high reliability among examiners who did not have any specific training in bony landmark identification [84]. In the same study, the precision of the landmark identification was affected when the anatomical landmarks on living subjects (the bones covered by the skin and subcutaneous tissues) were estimated compared to when that of bone specimens (no tissues covering the bone). The approximate average of 1.9 –

7.6 mm and 0.8 – 7.0° difference, rather than 0.9 – 4.6 mm and 0.4 – 4.9°, associated with estimation landmarks on living subjects were considered due to the main source of the error associated with the presence of soft tissue [84]. Application of the UP-CAST method to walking resulted in small inter-examiner and inter-trial errors ranging between 0.1° and 0.9° of knee flexion/extension angle, indicating a high repeatability [85]. However, the errors associated with the transverse plane motion were relatively higher, especially between different examiners. This method, as the functional method discussed above, allowed simplifying the methodological set up for the data collection. It appears that these newer methods may be comparable to the conventional method in precision in determining the joint kinematics. These methods without the need for identification specific anatomical landmark may lessen the time and complication of data collections; however, the limitations of these methods should be considered when utilized.

Electromyography

Electromyography (EMG) has been widely used in analysis of different movements including cycling as EMG provides insight to the force produced by the muscles. The functional unit of the neuromuscular system known as the motor unit (MU) includes an α-motor neuron and all muscle fibers that are innervated by the α-motor neuron [86]. The action potential, thereby the activation of a MU occurs when the electrical signal is sent from the α-motor neuron. The EMG signal is composed of the sum of the motor unit potentials (MUPs) that occurred within the data capture volume. The MUPs are directly related to the number of activated MUs, and the number of MUs activated is related to the muscle force. Therefore, the magnitude of EMG signal captured from a muscle provides implications of the force generated by the muscle. The relationship between the EMG signal and muscle force production has been investigated extensively. It is generally agreed that increase in EMG signal magnitude suggests increased force generated by the muscle; however how exactly the EMG is related to the muscle force is somewhat indecisive. Although, some suggested a linear relationship [87], others suggested non-linear relationship between the muscle force and the EMG signal [88]. The difference in this EMG-force relationship is related to the heterogeneity occurs within a muscle. For instance, when the muscle force and EMG are more linearly related when the muscle fiber composition was more uniform [89]. Theoretically, based on the “size principle” [90] , smaller MUs are recruited before larger MUs are recruited, thus, the muscle force should increase at a greater rate than EMG signal would. However, a study suggested that more diverse MU sizes within the muscle were shown to have more linear EMG-force relationship [91]. This disagreement might be due to the methodological limitations associated with the EMG. As typical EMG setup (such as bipolar surface EMG) captures the MUPs from selected area of the muscle, the signal may not be an appropriate representative of the entire muscle [92]. Commonly accepted EMG methods including bipolar method detect and collect the electrical signals from selected MUs; therefore, it may not necessarily represent the activity of the entire

muscle [92]. Additionally, the contraction history of the muscle affects the neural activation at the spinal cord level. While the muscle activation preceded by lengthening of the muscle was reduced, the activation following the shortening of the muscle was increased [93]. Therefore, interpretation of EMG signal should consider the representativeness of the data as well as the nature of the movement analyzed.

Another aspect of EMG signal-force relationship is the timing. In the literature, the muscle activation is typically accompanied by kinematic data as the interpretation of EMG data is more meaningful with movement associated with the muscle activation data. As indicated above, EMG signal represents the MUPs that occur before the actual muscle fiber contraction. There is a time lag between when a MUP occurs and when the force is developed by the motor unit. This time lag known as electromechanical delay (EMD) is defined as the time shift occurred between an EMG signal and the onset of detectable muscle force associated with that EMG signal. This delay occurs not only at the initial onset of the muscle activation, but also during an ongoing contraction. Therefore, it is more appropriate to consider EMD as the time shift that exists in a continuing dynamic activation pattern [92]. The reported EMD values range widely between 5 ms and 150 ms [92], and for cycling, EMD of 40 ms was reported [32]. Differences in EMD are considered to be related to the muscle length. Muraoka et al. (2004) [33] found that the duration of the EMD was related to the amount of slack present in the contracting muscle. The contraction of the gastrocnemius muscle was delayed when the muscle was in lengthened position. Cavanagh and Komi (1979) [34] indicated that EMD was related to time required to stretch the series elastic components such as connective tissues surrounding the muscle contractiles. EMD during concentric contraction was significantly longer (55.4 ms) than during the eccentric contraction (49.4 ms). When analyzing the muscle activation timing is considered, EMD needs to be accounted. Additionally, when the movement task involves different contraction types and/or considerably different muscle length change, EMD of different lengths may need to be taken into account.

Data processing has a significant influence on resulting EMG data. Normalization of EMG signal is necessary to compare the activation levels between different muscles and/or different individuals also to evaluate the EMG data collected under different conditions [88]. Normalization accounts for some anatomical, physiological and technical factors that would influence the EMG signal [94]. Of several different methods of normalization used in research, normalization using the maximal voluntary contraction (MVC) has been widely accepted method as it is recommended by the Journal of Electromyography and Kinesiology and by the SENIAM (Surface ElectroMyoGraphy for the Non-Invasive Assessment of Muscles, a project by a group of European scholars). The benefit of normalization using the MVC is to express the muscle activation level by the percentage of the maximal possible activation capacity (%MVC) [95]. This is beneficial when activation level of different muscles is compared. For instance, expressing muscle activation as %MVC provides an indication of contribution of different muscles during a given task. According to the length-tension relationship, the maximal activation capacity, thus, the greatest muscle force is possible in the mid-range of

motion. It has been shown that the EMG data normalized by isometric MVC at mid-range resulted lower value than data normalized by isometric MVCs collected at other angle through the range of motion (i.e. the greatest isometric MVC occurred at the mid-range) [96]; therefore, when normalized by isometric MVC, the reference MVC value should be collected at the mid-range.

Although, normalization using isometric MVC has been widely accepted, there are some limitations associated with this method, particularly, when the EMG data of dynamic movement task (resulting non-isometric contractions) is normalized by isometric MVC. The isometric EMG signal collected using surface EMG at a given angle not only does not account for the movement that occur underneath the electrodes, but it does not represent the muscle's force producing capability that is affected by the length of the muscle [97]. It has been known that EMG signal during dynamic task exceeds 100 %MVC due to the factors that are not accounted for with isometric reference EMG signal [98]. Additionally, the customization to the isometric MVC testing procedure prior to actual data collection is suggested for data reliability [88]. For these reasons, some researchers consider isometric MVC normalization not as reliable. Some suggest normalizing EMG data during dynamic tasks by a submaximal MVC reference. They indicated more reliable and stable normalization with submaximal MVC [88, 99]. Some research, particularly with pathological subjects, used the mean or the peak EMG of the movement task as the reference for normalization as this method does not require separate set of data for the reference value. Although, this makes the data collection less complicated, using a task-derived reference value is known to reduce the inter-individual variability [95, 99], possibly masking practically meaningful differences. Rouffet and Hautier [100] implemented and examined different submaximal MVC normalization method in cycling to avoid this issue. They determine a reference value from dynamic motion resembling the task (pedaling motion), but with known load (torque-velocity). This new method was found to be as repeatable as isometric MVC, but resulted in higher inter-individual variability, thereby conserving the differences existing among cyclists. The authors also indicated this approach reduce the time and complication of the data collection.

Newer more innovative technology has improved the capability of movement analysis. However, the selection of method should be performed carefully as each method may present both positives and negatives. Researchers also need to consider the limitations in interpretation of the data.

Summary of Chapter

In this chapter, additional details on the background in cycling mechanics were discussed. Additionally, more comprehensive descriptions of the kinematic, kinetic, and EMG variables were provided. The summary of available resources on seat post angle effects on cycling was also included. This section on the seat post angle effects illustrated that there are still unclear areas in the topic. Some of these areas will be

addressed in the current study. Finally, a section discussing technology and methods commonly used in movement analysis are included to facilitate the understanding of the current study.

Chapter Three

Methods

The current study examined the changes occurred in the cycling mechanics with modified riding positions. Specifically, the effects of two different seat post angles that are similar to typical road racing and triathlon bikes were determined. In this chapter, the study methodology including population, instrumentation and protocol are described. The descriptions of data reduction and the statistical analyses and the list of dependent variables are also included.

Study Population

Twelve healthy triathletes and cyclists [7 males: age 28.9 ± 7.6 years; height 1.78 ± 0.05 m; body mass 71.5 ± 7.9 kg and 5 females: age 28.2 ± 2.6 years; height 1.71 ± 0.06 m; body mass 60.4 ± 9.5 kg] volunteered in this study. Prior to conducting the study protocol, written consent approved by the university's institutional review board on human subjects' participation was obtained from each of the participants.

All participants regularly rode their road or triathlon bike with minimum weekly mileage of 30 miles (range 30 – 250 miles/week; average 87.9 ± 74.5 miles/week). At the time of the testing sessions, they were training for an upcoming cycling or triathlon event held within the next 10 months. They also participated in at least one USA Triathlon- or USA Cycling-sanctioned event within a year prior to their participation on this study. All participants did not have any previous or current injuries or other health conditions that would affect their cycling mechanics or that prevented them from their regular training for more than one full day. A questionnaire on their health, cycling/triathlon training, and performance history was completed by each of the participants. The PAR-Q [101] form was also completed to ensure that the participants were healthy enough for the study protocol. A summary of participants' profiles and competition history are included in Appendix A.

Apparatus/Instruments

Bike

A cycling session was performed using a cycle ergometer that controls cycling resistance with an electromagnetic braking system (Velotron Elite ergometer, RacerMate Inc., Seattle, WA). The geometry of the bike frame was adjusted to each participant to match certain geometrical characteristics of the participant's own bike. The seat post length (SPL: the length between the crank axis and the base of the seat), reach length (RL: the horizontal length between the front tip of the seat and the handlebar), handlebar height (HBH: the vertical height difference between the top surface of the seat and the handlebar), and crank arm length (CAL) of the participant's own bike were used to

custom-fit the bike. These measurements are shown in Figure 3-1. The bike included a pair of aerodynamic bars to allow the cyclist to ride in the aerodynamic position. The bike was also equipped with a pair of custom pedals that were capable of measuring 2-dimensional (normal and tangential) forces of the pedal [6]. To simulate a more realistic cycling setup, a clip-less pedal (Model X, SpeedPlay Inc., San Diego, CA), were integrated into the top plate of the instrumented pedal (Figure 3-2).

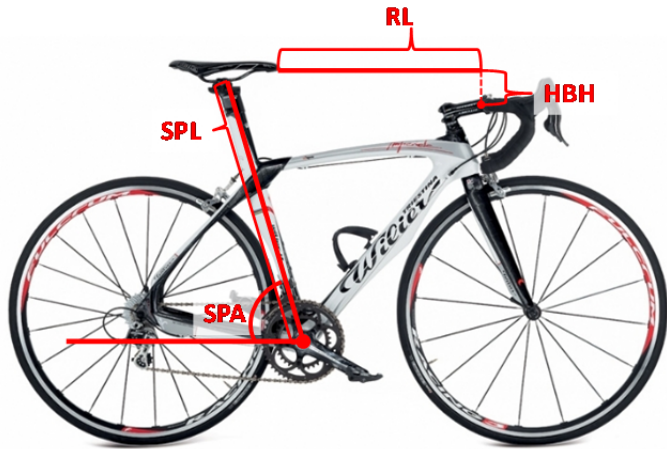


Figure 3-1: Measurements of the bike

SPL: seat post length; RL: reach length; HBH: handlebar height. These three measurements and the crank arm length (CAL, not shown) were recreated in the experimental bike.

SPA (seat post angle) shown in this figure was manipulated as experimental conditions
[Bicycle photo from www.wilier-usa.com with permission]

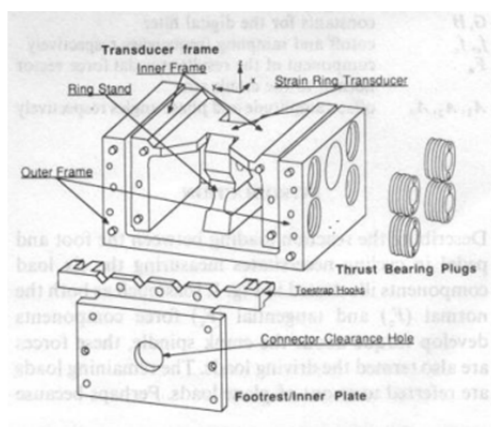


Figure 3-2: Diagram of the instrumented force pedal

The 2-D forces (normal and tangential) were detected from the deformation of the octagonal strain ring force transducer located in the middle of the pedal.

(Newmiller et al., 1988) [6] with permission

Kinematic Data

Using 10 motion capture cameras (Eagle and Eagle 4, Motion Analysis Corp., Santa Rosa, CA), body movement during the cycling session was recorded at a sampling frequency of 100Hz. The calibrated capture volume was 2 m x 2 m x 2 m, and the bike was placed in the center of the volume. The motion analysis software (Cortex v.1.4, Motion Analysis Corp.) identified and tracked the 2 dimensional location of reflective markers placed on the body and the bike in each camera view and then calculated the location of each marker in the three-dimensional volume.

Analog Data (Pedal Forces & Electromyography)

Concurrently with recording of 3-D movement, two-dimensional pedal forces were recorded at 1000 Hz. Additionally, electromyography (EMG) data were recorded using a 12-channel EMG system (MyoSystem 1400, Noraxon USA, Scottsdale, Arizona) including pre-amplifier that is approximately 10 cm away from the electrodes. The EMG system filtered the signal by a 1st order high-pass filter set to a 10 Hz cutoff to improve the signal-to-noise ratio (1 u volts RMS). The unit had the input impedance of 100 MOhm and a common mode rejection ratio of 100 dB. Both pedal force and EMG signals were converted to digital using a 16-bit analog to digital converter (NI-USB-6229, National Instruments, Austin, Texas). The instrumented pedals and the EMG system were synchronized with the motion capture system, and the data were collected simultaneously with the motion data.

Protocol

The experiment was conducted at the Biodynamics Laboratory at the University of Kentucky. At the initial meeting, each participant was familiarized with the instrumental setup including the stationary bike. At that time, the laboratory bike was fitted to the geometry that was similar to the participant's own bike, and a familiarization ride was performed. The participants rode on part of the experimental course (described in a section below) using the custom-fitted experimental bike as long as they felt comfortable with the setup. For the data collection, the participants visited on two separate occasions that were between 7 and 14 days apart. To minimize circadian variations, the testing sessions were performed at the same time of the day. On both testing days, the participant wore the same triathlon/cycling attire used as in a competition. The participant also wore his/her own bike shoes for testing. Two experimental conditions were 1) ROAD: shallow seat post angle resembling the road bike setup, where the seat was positioned 5 cm behind the seat post and 2) TRI: steep seat post angle resembling

the triathlon bike setup with the seat positioned 5 cm in front of the seat post. The order of the experimental conditions was randomized.

Each testing session consisted of completing a simulated 20-km cycling course. Following a warm up on the stationary bike, EMG instrumentation was done on the right limb. After shaving the hair, the skin was cleansed using alcohol. A pair of disposable Ag/AgCl electrodes were placed 2.0 cm apart in a bipolar configuration that is in line with the approximate muscle fiber alignment. The seven muscles instrumented on the right side were: 1) gluteus maximus (Gmax), 2) biceps femoris (BF), 3) rectus femoris (RF), 4) vastus lateralis (VL), 5) lateral gastrocnemius (Gast), 6) soleus (SOL), and 7) tibialis anterior (TA). A reference electrode was placed on the left iliac crest that was contralateral to the side for the EMG data collection. For each muscle, maximal voluntary isometric contraction (MVIC) data were collected. Each of the 6-second MVIC trial included 3 seconds of quiet (no contraction) and 3 seconds of maximal isometric contraction. The electrode locations and MVIC testing were performed in accordance to the SENIAM guideline (Appendix B) [102]. Upon completion of the MVIC sessions, 44 retro-reflective markers were placed on certain body landmarks and the bike for 3-D analysis of cycling session (Figure 3-3). The list of the markers and their locations are included in Appendix C.

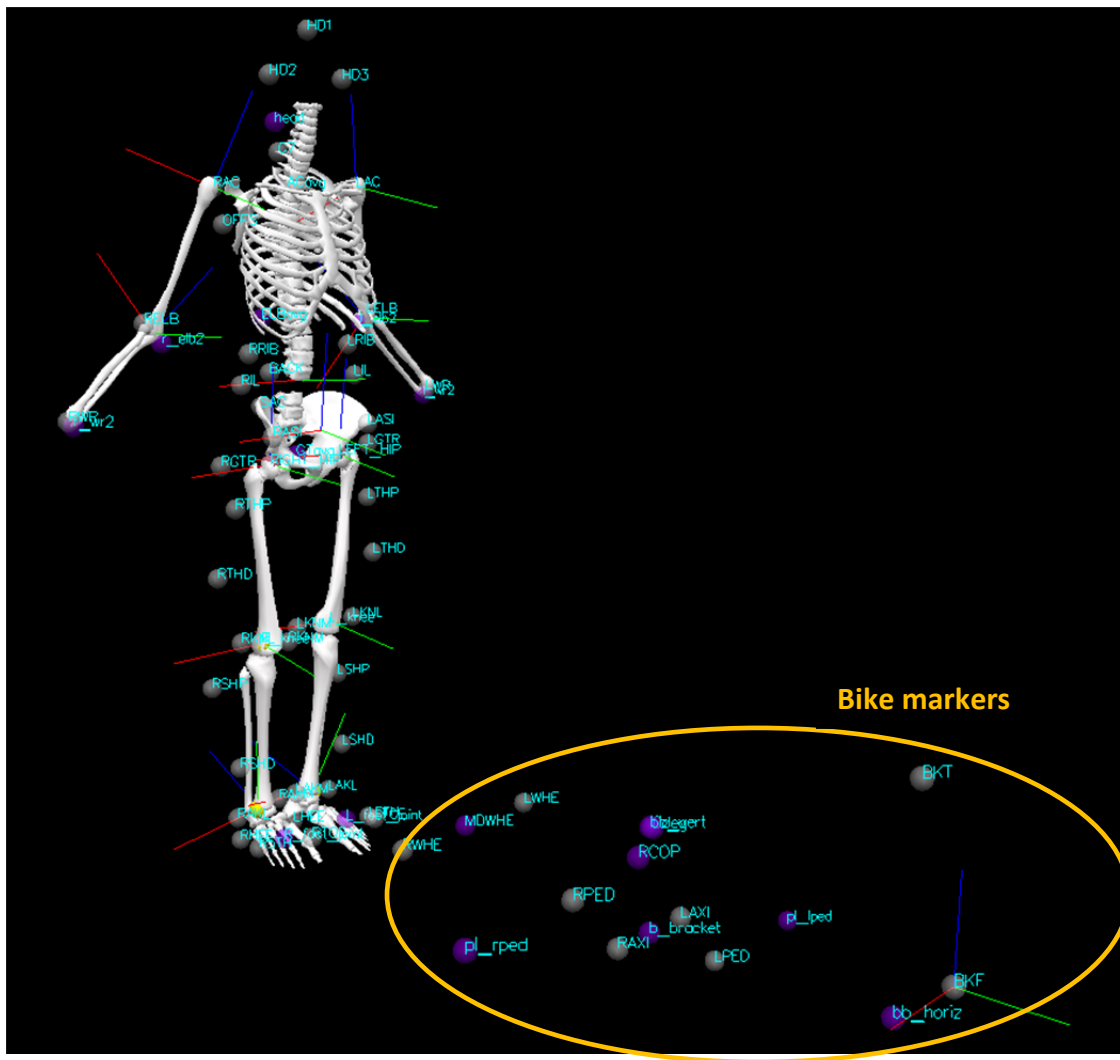


Figure 3-3 Locations of the retro-reflective markers used for the 3-D motion analysis
Total of 44 markers were used to track cycling movement.

An identical simulated cycling course was assigned for all participants and for both seat post conditions. A custom virtual 20-km course was created using Topo Course Creator software (v. 2.0, Racermates Inc., Seattle, WA). The hills in the course were simulated by resistance applied by the electromagnetic unit equipped on the Velotron bike using Velotron 3D software (v.2.0, Racermates Inc., Seattle, WA).The segments on the 20-km course where the data collection was performed were set as 'flat' to prevent the gear and intensity changes. Each participant was asked to complete the course at their race intensity. They were allowed to change gear ratios freely using the virtual gearing system during the ride to maintain constant pedaling cadence. The feedback on the pedaling cadence, cycling distance and speed were provided on the computer screen using the Velotron 3D software, which provides similar feedback that

cyclists typically receive during a race using their own bikes. The virtual competitor was also included on the feedback screen to facilitate more race-like environment. The virtual competitor was set to be within one minute of the participant, so that it would not affect the participant's cycling time. The subject was asked to ride in the aerodynamic position with the elbows and the hands resting on the elbow pads and the aerodynamic bars respectively during the data collection. The data were collected for 30 seconds at 1-km, 5-km, 10-km, 15-km, and 19-km into the ride. The experimental set up is shown in Figure 3-4.

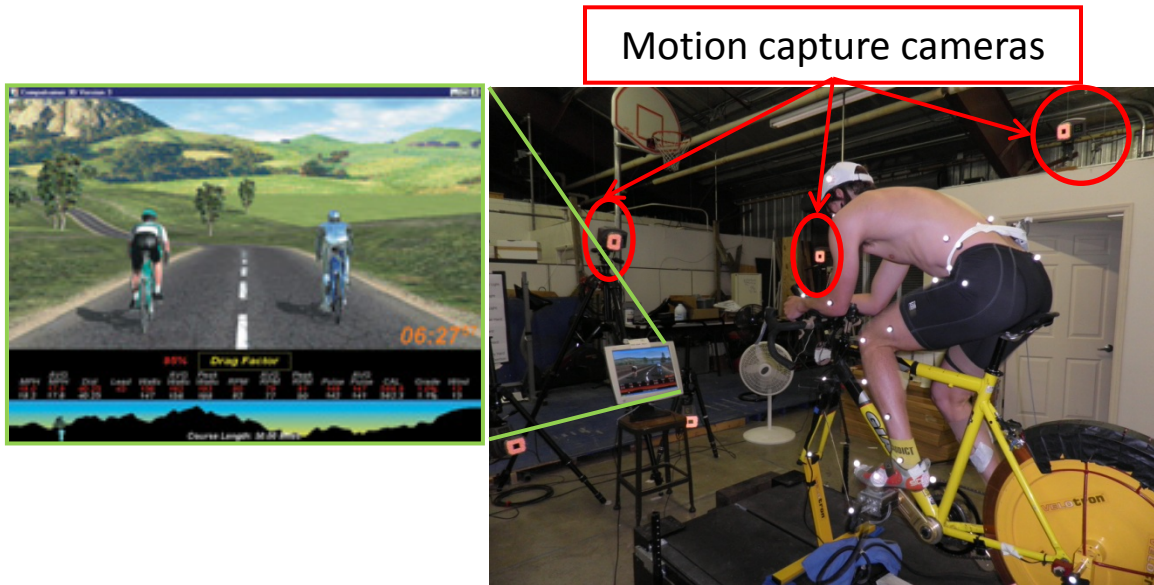


Figure 3-4: The experimental set up for the cycling trials

The cyclist was provided with the feedback on the computer monitor. The feedback displayed on the screen (figure on left) included the pedaling cadence, cycling speed, cycling distance. The virtual competitor and the course profile were also included on the feedback screen.

After each testing session, 3-second zero-load trials of the pedal data were collected at 4 different pedal tilt angles: 0° (horizontal), 90°, 180° (upside down), and 270°. These trials were used to determine the zero-offset values for the dynamic trial pedal force data.

Data Analysis

Kinematics

Recorded 3-D marker data were analyzed using a kinematic model created using Visual3D software (v4.8, C-Motion, Germantown, MD). The 3-D coordinates of the markers were filtered using a fourth order, zero-lag Butterworth filer at cut-off frequencies of 8 Hz (leg markers), 6 Hz (pelvis markers), and 4 Hz (trunk and bike markers) as determined by the residual analysis [51]. The bike coordinate system was established to use as the reference for segmental kinematic variables (Figure 3-5). The local coordinate system of the proximal segment was used as the reference to determine the change of the distal segment to describe the joint kinematics variables (Davis et al, 1991, cited in [59]).

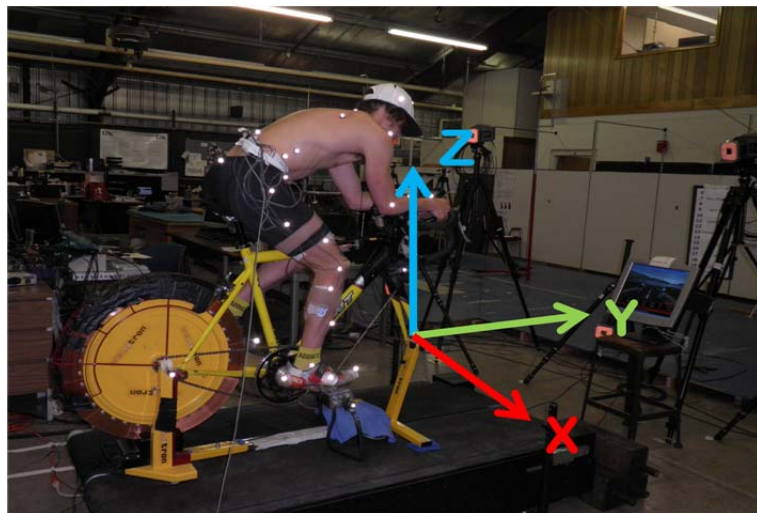


Figure 3-5: Bike coordinate system used for 3D motion analysis

X-axis was directed to the right horizontal, Y-axis was directed anterior, and Z-axis was directed up vertically. The bike coordinate system was used as the reference for the segmental kinematics.

Pedal Forces

A custom code written in MATLAB (R14, The MathWorks Inc., Natick, MA) was used to process the pedal force data (Appendix D). The data, both cycling and zero-offset trial data, were filtered using a forth order, zero-lag Butterworth filter at a cut-off frequency of 20 Hz according to the residual analysis [51]. The middle 1 second of the zero-offset trials was averaged, and for each pedal signal (tangential and normal) the averaged data points were fitted into an equation,

where $Y_{\theta_{ped}}$ was the zero-offset value (in mV) at the pedal angle in radian, θ_{ped} , φ , A , ω were the phase, amplitude, frequency of the fitted curve, respectively. This equation allowed determining the zero-offset values of the instrumented pedal at a given pedal angle. For each data point in the cycling trial, the pedal angle value was entered into the equation to determine the zero-offset value to be subtracted from the raw signal. Additionally, the angle effects of the instrumental pedal were determined using the equations below.

For tangential force signal: $x = a \times \sin(b \times \theta_{ped}) + c$

For normal force signal: $y = a \times \cos(b \times \theta_{ped}) + c$

where x and y were the tangential and normal force signals in mV accounted for the angle effects, and θ_{ped} was the pedal angle. The calibration coefficients, a , b , c were predetermined. The calibration details are included in Appendix E.

Once the pedal force signals were adjusted for the zero-offset and the angle effects, the data were converted to meaningful force data in Newtons by entering into the following linear equation.

For tangent force signal: $Fx = d \times x + e$

For normal force signal: $Fy = d \times y + e$

where Fx and Fy were the tangential and normal pedal force data in Newton, x and y were the tangential and normal data signal in mV that already accounted for the zero-offset and the angle effects, and d and e were the predetermined calibration coefficients.

Joint Kinetics

The converted pedal data were integrated into the kinematics data. The 2-D pedal forces were treated as if they acted at a fixed point, where the foot and the pedal surfaces were connected (i.e. the center of the pedal surface against the foot) during the entire pedal cycle, and with the absence of a free-moment. The integration of the pedal force, kinematic, and kinetic data using the traditional inverse-dynamic method was performed using the model created in Visual3D. In the model, the segmental mass and moment of inertia for the foot, shank (leg), thigh, and the pelvis were determined using Dempster's anthropometric data [103] and Hanavan's estimation model [104] respectively. The parameters used in the calculation of segmental masses and center of mass locations are included in Table 3-1. In Visual3D, the joint moment at the proximal end of a segment was calculated using the following equation:

$$M = \sum_{i=1}^n (C_i + R_i \times A_i) + \sum_{j=1}^q (P_j \times F_q) + \sum_{k=1}^p \tau_k$$

where M was the moment at the proximal end of the segment, $\sum_{i=1}^n(C_i + R_i \times A_i)$ represented the sum of the inertial torques, $\sum_{j=1}^q(P_j \times F_q)$ was the sum of the torques caused due to the external forces, and $\sum_{k=1}^p \tau_k$ was the sum of the external couples [105].

Table 3-1: Parameters used in kinetic calculations in Visual3D software

Segment	Mass	Geometry	Proximal Radius	Distal Radius	Center of Mass
foot	0.0145*mass	cone	0.0380	0.0350	0.4861
shank	0.0465*mass	cone	0.0502	0.0380	0.4544
thigh	0.1*mass	cone	0.0890	0.0598	0.4353
pelvis	0.142*mass	coda pelvis			

The radii are in meters. For the center of mass locations, the ratio of the segmental length represents the distance from the proximal end of the segment.

EMG

The data were first processed by a DC offset based on the zero-offset using the quiet (i.e. not muscle contraction) trial data. Data were then processed using a band-pass (20 – 500 Hz) Butterworth filter. Both the cycling trial and the MVIC trial data were processed using root mean square (RMS) with a window of 20 ms to obtain linear envelopes. The highest of 200-ms moving window of each muscle's MVIC date was used as the reference (i.e. 100 % voluntary effort) to express the cycling trial EMG data. The magnitude of the EMG data for the cycling trial was expressed as the percentage of the MVIC trial (%MVIC). The data were divided into sectors that have been suggested to represent different functions of the muscles during a pedal cycle. For the mechanical data, sectors 1 (330° - 30° of the crank arm angle), 2 (30° - 150°), 3 (150° - 210°), and 4 (210° - 330°) correspond to TDC, propulsive, DBC, and recovery phases of the pedal cycle [106]. In order to account for the electromechanical delay of 40 ms [32], the muscle activities corresponding to the sectors were estimated to occur 17° earlier than that of the pedal forces. Therefore, the sectors 1 – 4 for EMG were 313° - 13° , 13° - 133° , 133° - 193° , and 193° - 313° , respectively. Only the data at the 1-km of the course were analyzed as many EMG signals at later data collections were saturated due to perspiration.

Aerodynamics

Using the trunk tilt angle (Figure 3-7) and prediction equations [8, 107], aerodynamic drag (R_D) was determined for each experimental conditions.

$$A_P = 0.00433 \times (SPA^{0.172}) \times (TA^{0.0965}) \times (m_b^{0.762})$$

A_P , SPA, TA, and m_b represent the projected frontal area of the cyclist and the bicycle, seat post angle, trunk angle, and body mass of the cyclist, respectively. Calculated A_P was entered into the following equation.

$$R_D = 0.5 \times C_D \times \rho \times A_P \times v^2$$

The previously published estimate for the drag coefficients (C_D), [8], the air density at 1 ATM and at 20°C (1.4201 kg/m³, [108]), and the velocity of 30 km/hour (18.75 mph) were used to determine the R_D .

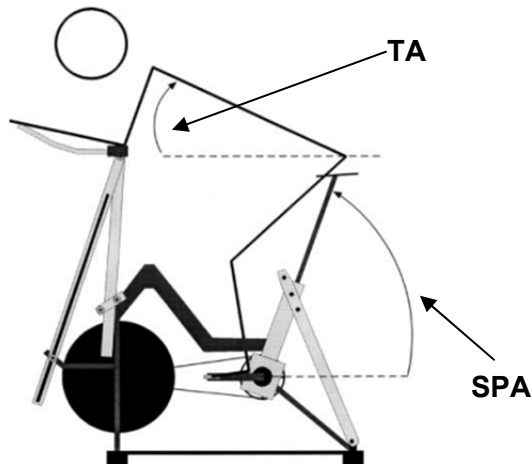


Figure 3-7: Definitions of trunk angle and seat post angle

TA: trunk angle; SPA: seat post angle

(Heil, 2001) [8] with permission

Dependent Variables

A comprehensive analysis of the right leg data, including kinematics, kinetic, and EMG, were performed. All dependent variables, except for the time-integral for the forces, were interpolated into 360 data points to represent series of events occur during a crank arm revolution (0 to 360°; Figure 3-8). To assess the validity of the normalization by the pedal cycle (360°), the crank angle angular velocity and its variance over a pedal

cycle were determined. For the time series of the variables, cross correlation analyses were performed by using methods described in Li and Caldwell [109]. This method was used to determine the amount of the time-shift present between two experimental conditions. The kinetic variables were normalized by the estimated leg mass using estimation coefficients by Zatsiorsky [cited in 110] to account for the effects of the leg mass in the kinetic data. Following equations were used to calculate the leg mass.

$$M_{LE} \text{ (male)} = (14.78 + 4.81 + 1.29) \times BM$$

$$M_{LE} \text{ (female)} = (14.16 + 4.33 + 1.37) \times BM$$

Where M_{LE} and BM are the estimated mass of the leg and the measured body mass respectively. The three numbers in the right side of the equation represent the percentage of the body mass that the thigh, leg and the foot segments accounted for. All kinetic values were expressed as per estimated leg mass.

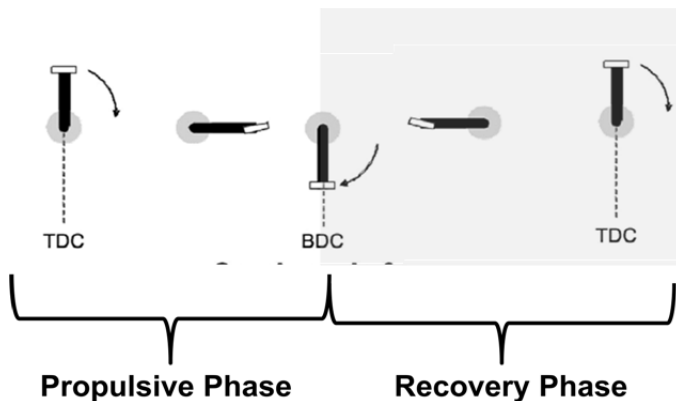


Figure 3-8: Phases of the pedal cycle

TDC: top dead center (0° of the pedal cycle); BDC: bottom dead center (180° of the pedal cycle)

Modified from Hug & Dorel et al. (2009) [1] with permission

Kinematic Dependent Variables (Figure 3-9)

- **Mean trunk lean:** The mean anterior tilt of the trunk relative to up vertical in the sagittal plane over a pedal cycle. 0° represented vertically positioned trunk, and positive angle represents forward lean of the trunk.

- *Mean anterior pelvic tilt*: Anterior tilt of the pelvis relative to up vertical in the sagittal plane over a pedal cycle. 0° represents the vertical positioning of the pelvis, and anteriorly tilted pelvis is described as a positive value.
- *Minimal & Maximal thigh angle*: Segmental angle of the thigh relative to vertical indicating orientation of the thigh relative to the crank axis in the sagittal plane. 0° indicates vertically aligned thigh, and positive angle indicates more horizontally positioned thigh (i.e. distal end/knee side positioned higher toward the trunk, brought into more hip flexion). The mean value was determined for a pedal cycle.
- *Maximal anterior pedal tilt*: The maximal forward tilt of the pedal relative to horizontal in the sagittal plane. The 0° of tilt represents horizontally aligned pedal.
- *Minimal hip angle*: The smallest flexion angle of the thigh relative to the pelvis in the sagittal plane.
- *Minimal knee angle*: The smallest flexion angle of the shank (leg) relative to the thigh in the sagittal plane.
- *Maximal posterior pedal tilt*: The maximal backward tilt of the pedal relative to horizontal in the sagittal plane. The 0° of tilt represents horizontally aligned pedal.
- *Maximal hip angle*: The maximal hip flexion angle of the thigh relative to the pelvis in the sagittal plane.
- *Maximal knee angle*: The maximal flexion angle of the shank (leg) relative to the thigh in the sagittal plane.
- *Minimal & Maximal ankle plantar flexion angle*: The smallest and greatest plantar flexion angle of the foot relative to the shank (leg) in the sagittal plane.
- *Pedal angle cross correlation*: The time shift (degrees of pedal cycle) between pedal angle-time series of ROAD and TRI conditions over a pedal cycle.
- *Hip joint angle cross correlation*: The time shift (degrees of pedal cycle) between hip joint angle-time series of ROAD and TRI conditions over a pedal cycle.
- *Knee joint angle cross correlation*: The time shift (degrees of pedal cycle) between knee joint angle-time series of ROAD and TRI conditions over a pedal cycle.
- *Ankle joint angle cross correlation*: The time shift (degrees of pedal cycle) between ankle joint angle-time series of ROAD and TRI conditions over a pedal cycle.
- *Cross correlation coefficients*: the correlation coefficient between two data series, ROAD and TRI, denoted as r .
- *Linearity*: the linearity between two data series, ROAD and TRI, denoted as R^2 .
- *Measured sitting position*: the horizontal displacement of the intertrochanteric point relative to the crank axis of the bike (in cm). A negative value represents a posterior displacement of the intertrochanteric point.
- *Measured seat post angle*: The angle between the line between the intertrochanteric point and the crank axis relative to the horizontal.

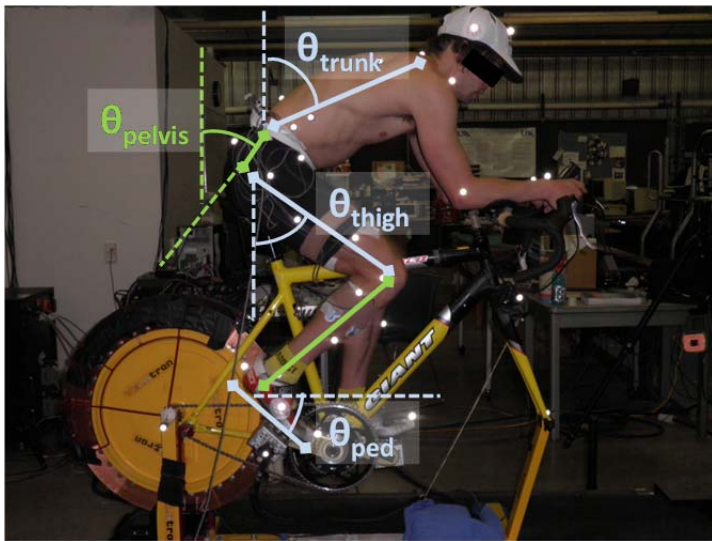


Figure 3-9a: Definitions of segmental angles

θ_{trunk} : trunk lean; θ_{pelvis} : pelvic tilt; θ_{thigh} : thigh angle; θ_{ped} : pedal angle.

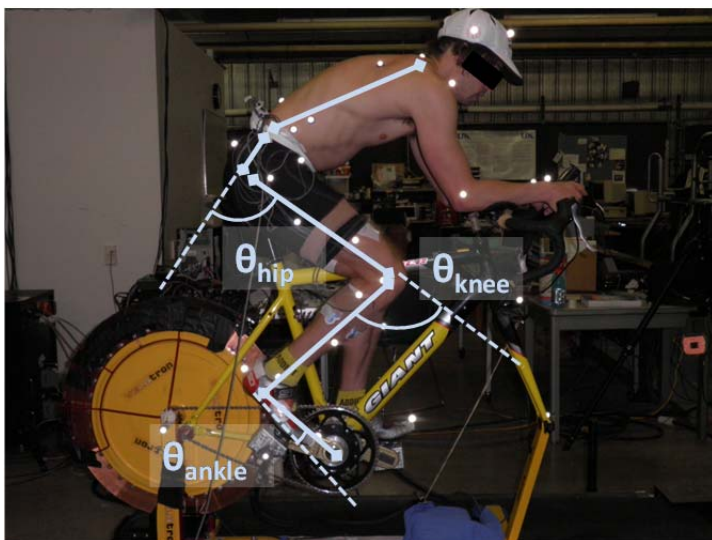


Figure 3-9b: Definitions of joint angles

θ_{hip} : hip angle; θ_{knee} : knee flexion angle; θ_{ankle} : ankle angle.

Kinetic Dependent Variables

- *Minimal & maximal resultant pedal force (F_{RES})*: The minimal and the maximal net pedal force over a pedal cycle.
- *Minimal & maximal effective pedaling force (F_{EFF})*: The portion of pedal force that is effective in generating crank torque; perpendicular relative to the crank arm. The minimal and maximal over a pedal cycle.

- *Mean index of pedaling effectiveness (I_{EFF})*: The ratio of the effective pedal force to the net pedal force. The average for a pedal cycle was determined.
- *Tangential force cross correlation*: The time shift (degrees of pedal cycle) between time series of tangential pedal force for ROAD and TRI conditions over a pedal cycle.
- *Normal force cross correlation*: The time shift (degrees of pedal cycle) between time series of normal pedal force for ROAD and TRI conditions over a pedal cycle.
- *Resultant force cross correlation*: The time shift (degrees of pedal cycle) between time series of resultant pedal force for ROAD and TRI conditions over a pedal cycle.
- *Hip joint moment*: The joint torque at the hip joint relative to the pelvis normalized by the subject's estimated leg mass. Expressed as the time-integral over a pedal cycle.
- *Knee joint moment*: The joint torque at the knee joint relative to the thigh normalized by the subject's estimated leg mass. Expressed as the time-integral over a pedal cycle.
- *Ankle joint moment*: The joint torque at the ankle joint relative to the shank (leg) normalized by the subject's estimated leg mass. Expressed as the time-integral over a pedal cycle.
- *Hip joint moment cross correlation*: The time shift (degrees of pedal cycle) between time series of hip joint moment for ROAD and TRI conditions over a pedal cycle.
- *Knee joint moment cross correlation*: The time shift (degrees of pedal cycle) between time series of knee joint moment for ROAD and TRI conditions over a pedal cycle.
- *Ankle joint moment cross correlation*: The time shift (degrees of pedal cycle) between time series of ankle joint moment for ROAD and TRI conditions over a pedal cycle.

EMG Dependent Variables

- *Minimal & maximal sector 1 muscle activation*: The minimal and the maximal RMS EMG linear envelop normalized by %MVIC over the first sector (313° - 13° of pedal cycle).
- *Minimal & maximal sector 2 muscle activation*: The minimal and the maximal RMS EMG linear envelop normalized by %MVIC over the first sector (13° - 133° of pedal cycle).
- *Minimal & maximal sector 3 muscle activation*: The minimal and the maximal RMS EMG linear envelop normalized by %MVIC over the first sector (133° - 193° of pedal cycle).

- *Minimal & maximal sector 4 muscle activation*: The minimal and the maximal RMS EMG linear envelop normalized by %MVIC over the first sector (193° - 313° of pedal cycle).
- *Cross correlations*: Time-shift (degrees of pedal cycle) of EMG RMS linear envelop data for each muscle between two cycling conditions over a pedal cycle.
- *Cross correlation coefficients*: the correlation coefficient between two data series, ROAD and TRI, denoted as r .
- *Linearity*: the linearity between two data series, ROAD and TRI, denoted as R^2 .

Aerodynamic Variables

- *Mean estimated projected frontal area (A_P)*: Estimated projected frontal projected area (m^2) of a cyclist and the bicycle combined. A mean was determined over a pedal cycle. An equation by Heil [8] was used.
- *Mean estimated aerodynamic drag force (R_D)*: Aerodynamic drag force (N) estimated by using an equation proposed by Pugh [107].
- *Percent difference of aerodynamic drag forces*: the percent difference between mean estimated aerodynamic drag force for ROAD and TRI conditions. Positive value denotes less drag force associated with TRI condition.

Performance Variable

- *Finish time*: The time (minutes and seconds) that was spent for the participant to complete the simulated 20-km course.

Statistical Analysis

For each participant-cycling condition, data for each dependent variable were first averaged across the full revolutions during the middle 10 seconds of the full 30-second trial. On average, there were 44 ± 3 complete revolutions during the 30 seconds for both ROAD and TRI conditions respectively. Therefore, on average, data from 15 complete cycles in the middle of the 30-second trials were averaged and used for analyses. For each variable per cycling condition, the mean and the standard deviation were determined using the averaged data of 12 participants. Except for the EMG data, this process was repeated for 5 time point data. All dependent variables were tested for normality using Shapiro-Wilks tests. To assess the effects of the seat conditions (ROAD and TRI) and the time (1-km, 5-km, 10-km, 15-km, and 19-km) in the kinematic and kinetic variables, two-way repeated-measure ANOVA were performed for normally distributed variables. Sphericity was checked using Mauchly's test. When the sphericity

was violated, Greenhouse-Geisser adjustment was made. When any differences were identified, post hoc pair-wise comparisons were performed with Bonferroni adjustment. When the variables were not normally distributed, Wilcoxon rank tests (test statistics = Z) and Friedman tests (test statistics = Chi-square, χ^2) were performed to assess the effect of the seat condition and the time points respectively. For the EMG data, as the data were not normally distributed, aforementioned non-parametric tests were performed to assess the effect of the seat condition and the 4 different sectors of the pedal cycle. All statistical analyses were performed using SPSS (v.19, SPSS, Inc., Chicago, IL). The α level was set at 0.05.

Chapter Four

Results

Introduction

The purpose of current study was to identify the effects of different riding positions, specifically, different seat post angle resulting from different fore-aft seat positions. It was hypothesized that cycling in a more forward seat position (TRI, steeper seat post angle) would result in changes in cycling kinematics, kinetics, and muscle activation patterns. In this section, results in kinematics, kinetics, EMG, and performance variables are presented.

Kinematics

Sitting Position and Seat Post Angle

Positioning the seat 5 cm behind the crank axis for ROAD condition (solid seat; Figure 4-1) resulted in the measured sitting position of -18 ± 2 cm and the seat post angle of $64\pm2^\circ$. With the seat positioned 5 cm in front of the crank axis (shaded seat; Figure 4-1) resulted in a sitting position of -7 ± 2 cm and seat post angle of $72\pm1^\circ$ (Table 4-1). The participants sat posterior to the crank axis in both seat settings, but with the TRI condition, the participants sat more directly above the crank axis resulting in a greater seat post angle.

Table 4-1: The average measured sitting position and measured seat post angle resulted from ROAD and from TRI seat conditions.

Participants	Sitting Position (cm)		Seat Post Angle (deg)	
	ROAD	TRI	ROAD	TRI
1	-20.7	-8.9	61.9	70.7
2	-20.2	-6.4	61.5	71.9
3	-18.9	-6.6	64.0	72.8
4	-20.3	-8.8	64.1	72.0
5	-19.1	-8.6	63.7	71.6
6	-15.4	-5.1	67.5	74.1
7	-19.6	-12.0	64.9	70.2
8	-16.2	-6.8	64.3	71.5
9	-21.4	-8.3	61.2	71.1
10	-14.4	-4.8	66.6	74.0
11	-19.3	-6.2	63.4	72.9
12	-16.2	-6.0	66.0	72.1
Mean	-18.5	-7.4	64.1	72.1
SD	2.3	2.0	2.0	1.2

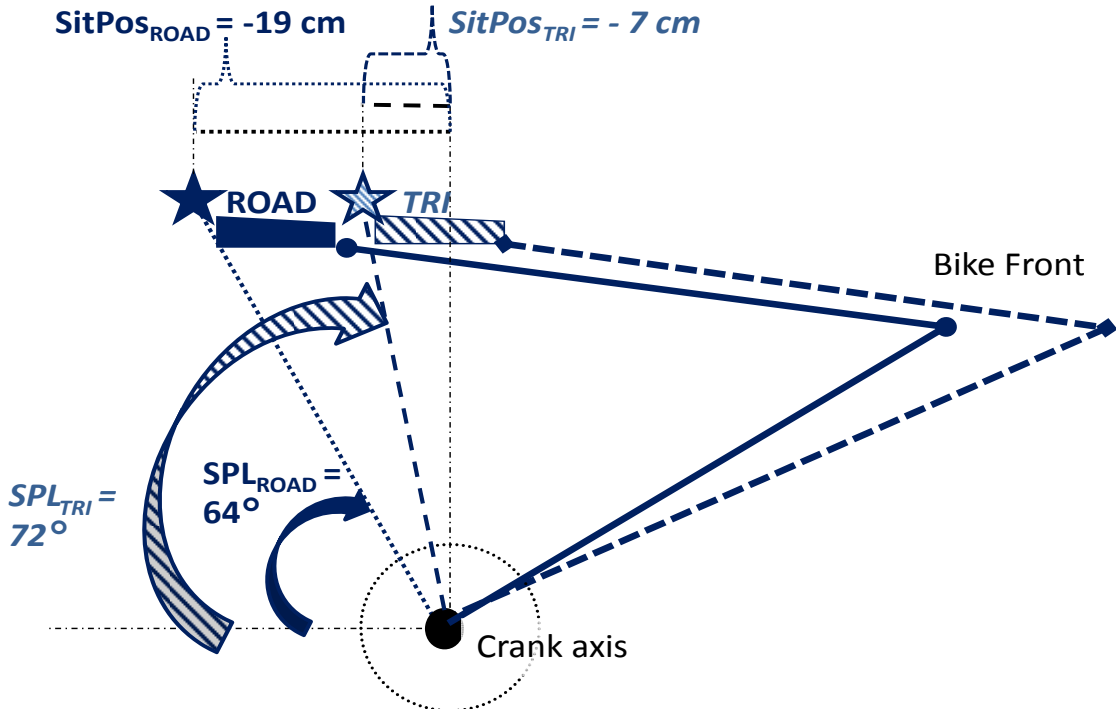


Figure 4-1: Schematic diagram of measured sitting position and measured seat post angle with two cycling positions.

For ROAD condition, the front of the seat was placed 5 cm behind the crank axis horizontally, and for TRI condition, the seat was positioned 5 cm in front of the crank axis. $SitPos_{ROAD}$ and $SitPos_{TRI}$ represent measured fore-aft distance between crank axis and the greater trochanter ('star' in the figure; solid = ROAD and shaded = TRI) for the ROAD and the TRI conditions. SPA_{ROAD} and SPA_{TRI} represent the measured angle at the crank axis between the posterior horizontal and the greater trochanter for the ROAD and the TRI conditions.

Joint Angles

Joint kinematics did not differ significantly between two cycling conditions. Due to the mechanical constraints associated with cycling, joint angles were relatively consistent within the participants. The standard deviation indicated that absolute angles varied across the participants, the patterns were similar across the participants (see Figure 4-2). This trend was particularly noticeable at the hip and the knee that both minimal and maximal joint angles varied (i.e. larger standard deviation) but the variability of the joint ROM were small (Table 4-1). Contrary to the prediction, the minimal and the maximal flexion angles at the hip did not differ between conditions. For one complete pedal cycle, on average, the minimal hip flexion angle was approximately $37 \pm 3^\circ$ for both ROAD and TRI. The maximal hip flexion angle was 84° and 82° for the ROAD and TRI conditions. The ROM at the hip did not differ between ROAD and TRI. Although the hip underwent similar angle excursions between conditions, the timing of the events were different. Cross correlation indicated that hip angle change occurred later in TRI by 8° of pedal cycle.

As anticipated, the knee angle was least affected by the changed cycling position. The knee flexion angles for a pedal cycle were very similar between seat conditions for both minimal and maximal angles (minimal: $\chi^2 = 15.7$, $p > 0.05$, $36\pm2^\circ$ and $38\pm2^\circ$; maximal: $F = 1.3$, $p > 0.05$, $114\pm1^\circ$ and $115\pm1^\circ$ for ROAD and TRI). The timing of knee flexion angle changes was also very similar (no time shift detected by cross correlation) between ROAD and TRI conditions. Angle at the ankle was also similar between the riding conditions ($F = 0.04$, $p > 0.05$; $10\pm2^\circ$ ROAD; $9\pm1^\circ$ TRI for minimal plantar flexion angle; $F = 0.22$, $p > 0.05$; $28\pm2^\circ$ ROAD; $26\pm2^\circ$ TRI for maximal plantar flexion angle). The cross correlation indicated the ankle angle change, on average, occurred later in steep seat post angle condition (15° of pedal cycle delay in TRI).

Across the 5 different time points when the data were captured (at 1-km, 5-km, 10-km, 15-km, and at 19-km) during the 20-km simulated course, joint angles were maintained relatively closely. The minimal hip flexion angle that occurred near BDC ranged between 37° and 38° with the standard error of $2^\circ - 3^\circ$. The hip and knee angles were maintained throughout the entire cycling session (Hip: $36-38\pm9^\circ$ for minimal, $82-84\pm8^\circ$ for maximal; knee: $37\pm2^\circ$ for minimal, $115\pm1^\circ$ for maximal for all 5 time points). The ankle angle appeared to be more variable than the knee angle, but nothing was statistically significant ($F = 0.28$, $p > 0.05$, $9\pm1^\circ - 11\pm2^\circ$ for minimal and $F = 0.72$, $p > 0.05$, $38\pm2^\circ$ for maximal for all 5 time points).

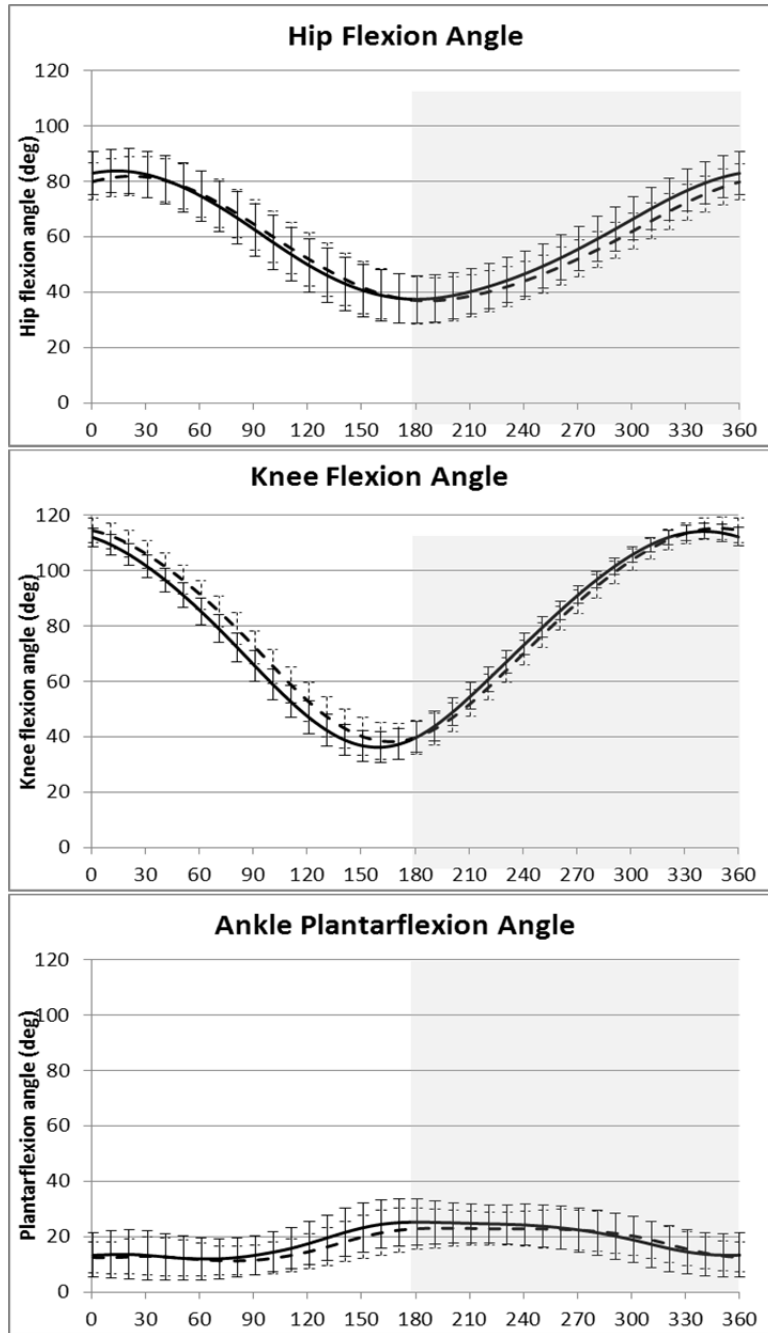


Figure 4-2: Average joint angle change across 5 time points during a simulated 20-km cycling session with two different seat post angles.

The x-axis is degrees of pedal cycle for all graphs (hip, knee, and ankle).

The y-axis represents degrees of flexion for hip and knee graphs. The y-axis represents degrees of plantar flexion; 0 degree represent neutral for ankle graph.

Each graph shows the mean data $\pm 1SD$ (across 12 participants & 5 time points; 1, 5, 10, 15, and 19-km) for the ROAD and TRI. Within each trial for each participant, full pedal revolutions during a 10-second period were averaged. The solid line (—) is ROAD condition and the dotted line (---) is TRI condition.

Table 4-2: Minimal and maximal joint angle and ROM means and standard deviations for the hip, knee, and ankle at 1 km, 5 km, 10 km, 15 km, and 19 km with two different seat post angle conditions. For the hip and knee, the angle and ROM values represent the degree of flexion. For the ankle, the angle and ROM values represent the degree of plantar flexion. The each ROAD and TRI data include average of trials of 12 participants. Each subject's is the mean of the full pedal revolutions during a 10-second period.

		Hip			Knee			Ankle			
		Min Angle	Max Angle	ROM	Min Angle	Max Angle	ROM	Min Angle	Max Angle	ROM	
ROAD	1 km	Mean	38.3	84.1	45.8	36.0	114.1	78.1	10.6	28.6	18.0
		SD	9.1	8.5	2.6	5.9	2.8	2.6	7.2	7.5	6.1
	5 km	Mean	37.2	83.9	46.7	36.3	114.4	78.1	10.3	26.6	16.4
		SD	9.0	8.0	3.0	5.8	2.9	3.0	7.7	8.9	6.0
TRI	10 km	Mean	37.1	84.0	46.9	36.3	114.8	78.5	9.5	27.5	17.9
		SD	9.2	8.0	3.2	6.0	3.0	4.4	6.1	7.6	6.3
	15 km	Mean	37.2	84.3	47.1	35.6	114.3	78.6	10.5	27.5	17.0
		SD	9.6	8.5	3.4	6.0	2.8	4.1	2.8	8.6	6.8
	19 km	Mean	36.2	83.7	47.4	35.2	114.1	78.9	8.5	27.6	19.1
		SD	9.1	7.7	3.5	5.9	2.9	4.0	7.4	8.9	6.6
	1 km	Mean	37.4	82.2	44.8	37.9	115.4	77.5	8.8	26.2	17.4
		SD	8.2	6.7	3.4	7.2	4.7	4.2	5.9	7.9	6.0
	5 km	Mean	36.6	82.2	45.5	38.6	115.5	76.9	10.5	27.0	16.5
		SD	8.1	6.7	3.5	6.8	4.3	4.1	5.2	8.0	5.8
	10 km	Mean	36.4	82.2	45.8	37.8	115.5	77.7	10.2	25.8	15.5
		SD	8.9	7.2	4.1	6.8	3.8	4.7	6.4	7.5	5.5
	15 km	Mean	37.1	83.0	45.9	38.0	115.6	77.6	9.7	26.8	17.1
		SD	9.6	7.5	4.7	6.6	4.3	4.7	4.8	7.1	7.2
	19 km	Mean	35.4	81.1	45.7	37.8	115.1	77.2	7.7	25.4	17.7
		SD	9.5	8.7	4.9	7.4	3.8	6.8	4.1	7.1	6.4

Segmental Angles

Positioning the body more forward relative to the crank axis by increasing the seat post angle affected certain segmental positions. As predicted, the pedal angle was significantly affected (Figure 4-3a). The pedal angle relative to horizontal with TRI setup was $0\pm 5^\circ$ for the minimal and $44\pm 6^\circ$ for the maximal, $6 - 7^\circ$ greater than with ROAD setup ($-6\pm 5^\circ$ minimal, $F = 133.0$, $p < 0.05$; $37\pm 6^\circ$ maximal, Wilcoxon $Z = -2.9 - -3.0$, $p < 0.001$). The least anterior tilt (minimal pedal angle) occurred approximately between $100^\circ - 120^\circ$, during the power phase, and the most anterior tilt (maximal angle) of the pedal occurred close to 300° of the pedaling cycle. During pedaling, the pedal was mostly anteriorly tilted in both conditions, but the tilt was significantly greater in TRI condition. The pedal ROM was not significantly affected by the seat conditions ($F = 4.2$, $p > 0.05$; ROAD $44\pm 1^\circ$ v. TRI $46\pm 2^\circ$). Cross coefficient analysis suggested that there was a time lag of 7° when the seat post was steeper ($r = 0.99$). The trunk forward tilt angle did not differ between ROAD and TRI conditions ($73\pm 1^\circ$ vs. $75\pm 1^\circ$, $F = 2.73$, $p > 0.05$ for minimal anterior tilt; $72\pm 1^\circ$ vs. $74\pm 1^\circ$, $F = 2.7$, $p > 0.05$ for maximal anterior tilt). Riding with a steeper seat post angle increased the amount of anterior pelvic tilt ($F = 16.9$, $p < 0.005$). With TRI position, participants on average tilted 7° greater anteriorly ($11\pm 2^\circ$ ROAD vs. $17\pm 2^\circ$ TRI) (Figure 4-3b). The timing of the pelvic tilt angle change was similar between conditions (1° time shift). The orientation of the thigh was also affected by the riding position change. The minimal and the maximal thigh angles were lesser with TRI condition (minimal angle: $25\pm 1^\circ$ ROAD vs. $18\pm 1^\circ$, $F = 95.1$, $p < 0.05$; maximal angle: $73\pm 1^\circ$ ROAD vs. $61\pm 1^\circ$, $F = 415.0$, $p < 0.05$), indicating that participants did not pick up their thighs (knees) as high when riding with a steeper seat post angle (Figure 4-3c). The timing of thigh angle change was also indicated by cross correlation. The angle change occurred later in TRI condition by 7° of the pedal cycle ($r = 0.99$). Different riding positions resulted in different orientation of the shank segment (Figure 4-3d). The shank was positioned more horizontal with TRI condition (minimal $8\pm 1^\circ$ vs. $17\pm 1^\circ$, $F = 240.1$, $p < 0.05$; maximal $50\pm 1^\circ$ vs. $58\pm 1^\circ$, $F = 216.1$, $p < 0.05$, for ROAD and TRI). Shortly before TDC, the heel was brought higher upward with TRI riding condition. There was no time shift in shank angle change between conditions ($r = 0.99$).

Certain segmental orientations showed statistical differences across different time points during the cycling session. The maximal anterior pelvic tilt at 1-km differed from that at 5-km, 10-km, and at 19-km by 1° ($F = 2.88$, $p < 0.05$). Thigh minimal and maximal angles were also statistically different among the time points ($F = 3.7$, $p < 0.05$ for minimal, $F = 486.9$, $p < 0.05$ for maximal); however, the differences did not appear to have the same pattern as seen in the maximal pelvic tilt angle. The interaction between the seat condition and the time point was present in the maximal thigh angle ($F = 394.6$, $p < 0.05$).

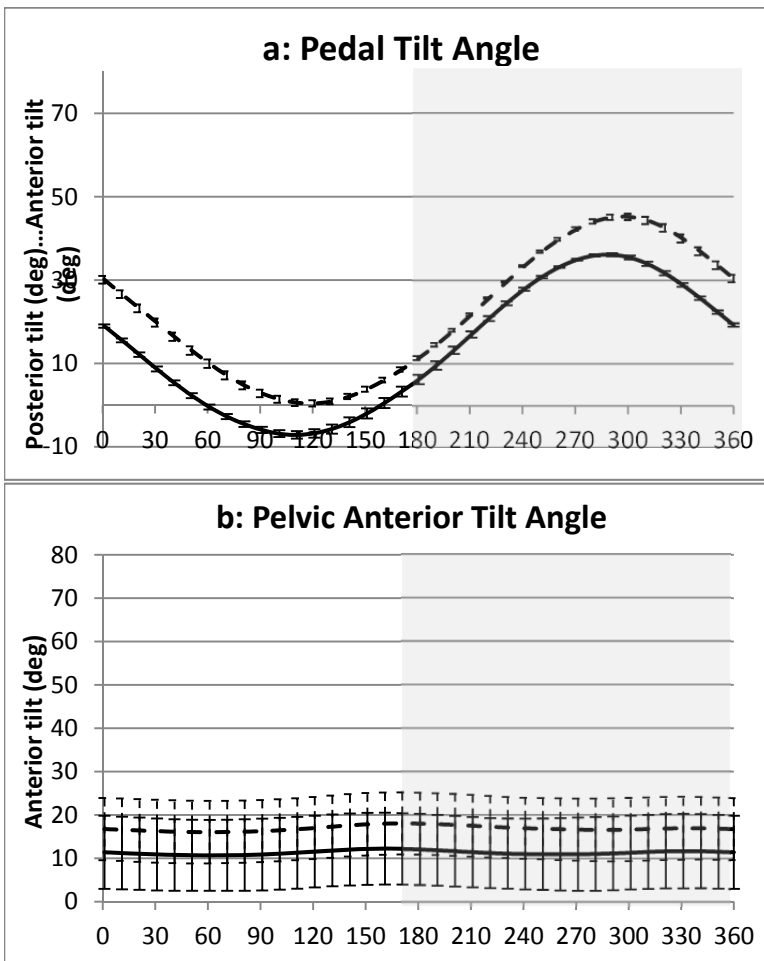


Figure 4-3 a & b: Segmental angle across 5 time points during a 20-km simulated cycling session with two different seat post angles.

a) Pedal Tilt Angle: 0 degree represents horizontal, positive angles are anterior tilt, and negative angles are posterior tilt of the pedals. b) Pelvic Anterior Tilt Angle: 0 degree represents that the pelvis is positioned vertical. Greater angle means greater anterior tilt. The horizontal axis is the pedal cycle (deg), 0° - 360°. The each ROAD and TRI data include average of trials of 12 participants over 5 time points (1 km, 5 km, 10 km, 15 km, and 19 km). Each participant's data are the mean of the full pedal revolutions during a 10 second period. The solid line (—) is ROAD condition and the dotted line (---) is TRI condition. The error bars represents $\pm 1\text{SD}$.

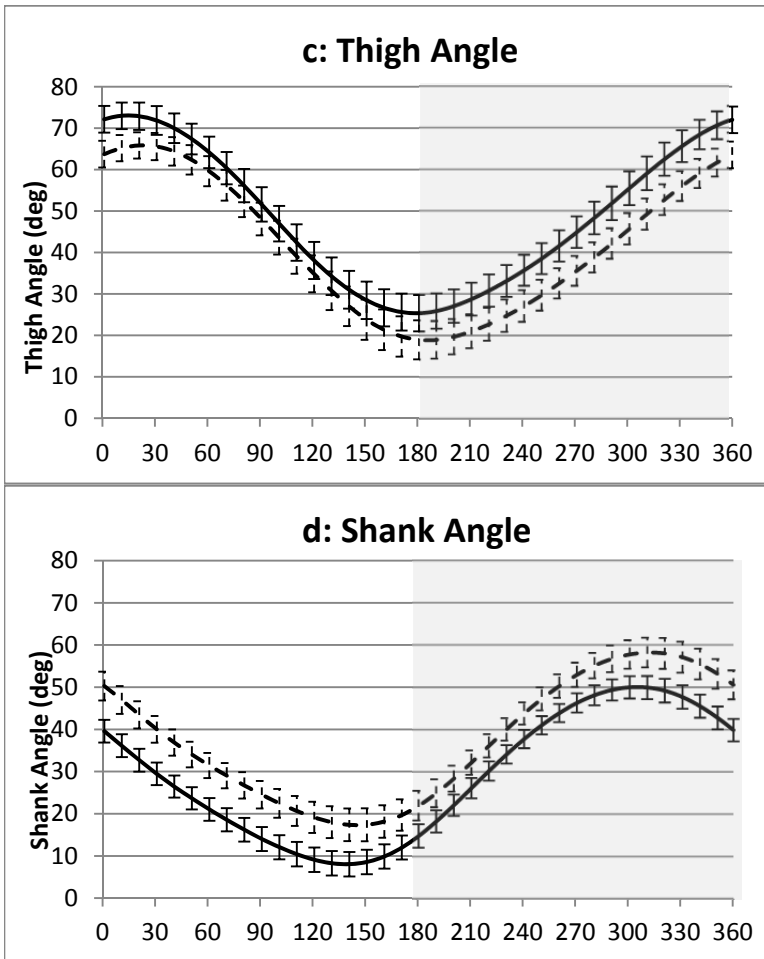


Figure 4-3 c & d: Segmental angle across 5 time points during a 20-km simulated cycling session with two different seat post angles.

a) Thigh Angle: 0 degree represents vertical, positive angles are upward lift of the distal thigh anteriorly (i.e. into hip flexion). d) Shank Angle: 0 degree represents that the shank is positioned vertical. Greater angle means greater anterior tilt (i.e. the distal end picked up posteriorly into knee flexion). The horizontal axis is the pedal cycle (deg), 0° - 360°. The each ROAD and TRI data include average of trials of 12 participants over 5 time points (1 km, 5 km, 10 km, 15 km, and 19 km). Each participant's data are the mean of the full pedal revolutions during a 10 second period. The solid line (—) is ROAD condition and the dotted line (---) is TRI condition. The error bars represents $\pm 1\text{SD}$.

Kinetics

Pedal Forces

Modified cycling position did not result in significant change in pedal forces. The integral of the each component pedal forces (normal and tangential forces) over a pedal cycle did not differ (normal: ROAD 59 ± 17 N·s/kg; TRI 57 ± 14 N·s/kg and tangential: ROAD 2 ± 2 N·s/kg; TRI 2 ± 2 N·s/kg). Graphic representation of the pedal force data is included in Figure 4-4. The largest amount (nearly 23 N/kg) of normal force was applied approximately at the 100° of the pedal cycle, whereas the tangential force peaked with much less amount of about 2 N/kg prior to the normal force's peak. During the recovery (up) phase of the pedal cycle, the normal force was positive values (2 – 20 N/kg), indicating that the force was still applied onto the pedal. The resultant pedal force, however, was different between cycling conditions at all time points except for at 1-km (5-km: 55 ± 16 N·s vs. 44 ± 16 N·s, Wilcoxon Z = -2.1; 10-km: 59 ± 18 N·s vs. 42 ± 17 N·s, Wilcoxon Z = -2.4; 15-km: 59 ± 18 N·s vs. 44 ± 16 N·s, Wilcoxon Z = -2.5; 19-km: 61 ± 19 N·s vs. 43 ± 17 N·s, Wilcoxon Z = -2.6 for ROAD and TRI respectively). Except for the initial phase, the athlete applied greater amount of net pedal force when riding in ROAD position. The difference appeared to be due to less force applied during the recovery phase with TRI condition. In both conditions, the peak resultant force coincided with the peak of the normal pedal force approximately at 100°, indicating that majority of the normal force contributed to the resultant force. The contribution of the tangential force to the resultant force remained unchanged with seat post angle modification (Wilcoxon Z = -1.4, Wilcoxon Z = -1.2, Wilcoxon Z = -1.2, Wilcoxon Z = -1.3, Wilcoxon Z = -0.6, for 5 time points. All p > 0.05).

When the effect of the time points during the cycling session was assessed, there was no difference in the normal and tangential pedal force integrals. However, the resultant forces were different at different time points when the participants rode in ROAD condition ($\chi^2 = 20.5$, p < 0.05) (Figure 4-5). The participants increased the amount of net pedal force applied as the cycling section progressed (50 ± 17 N·s at 1-km, 55 ± 16 N·s at 5-km, 59 ± 18 N·s at 10-km and 15-km, 61 ± 19 N·s at 19-km). When the participants rode in TRI position, there was no change in the resultant pedal force over the time points ($\chi^2 = 5.2$, p > 0.05). The contribution of the tangential force did not differ across different time points of the cycling session neither.

The cross correlation analysis confirmed that modification of cycling position resulted in a time shift in the force application by 9° of the pedal cycle ($r = 0.99$ for both normal and tangential pedal forces). The onset of the force increase in both normal and tangential directions were earlier with ROAD condition than with TRI conditions. Due to the change in timing of pedal force application in both normal and tangential directions, the timing of the resultant force application was also affected by the cycling position change. Riding in more vertical position (TRI) resulted in delayed force application by 12° of the pedal cycle ($r = 0.99$).

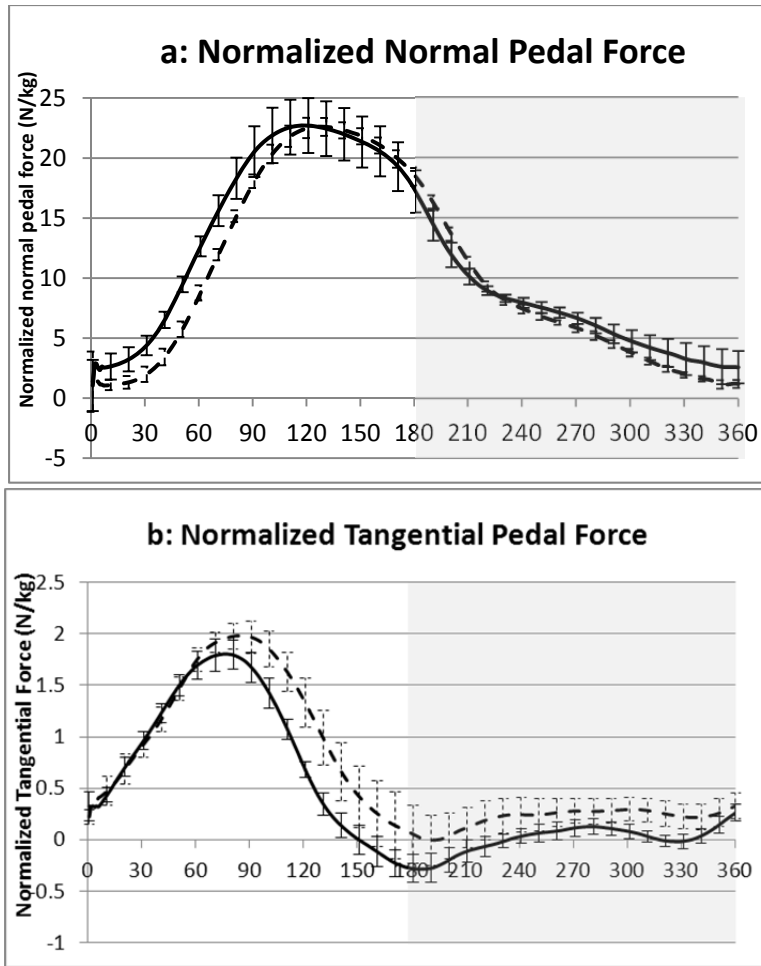


Figure 4-4 a – b: Normalized normal and tangential pedal forces across 5 time points during a 20-km cycling session with two different seat post angles.

The vertical axis is the force magnitude normalized by the estimated leg mass (N/kg); the horizontal axis is the pedal cycle (deg), 0° - 360°. The forces are normalized to estimated leg mass. The each ROAD and TRI data include average of trials of 12 participants over 5 time points (1 km, 5 km, 10 km, 15 km, and 19 km). Each participant's data are the mean of the full pedal revolutions during a 10 second period. The solid line (—) is ROAD condition and the dotted line (---) is TRI condition. The error bars represents $\pm 1\text{SD}$.

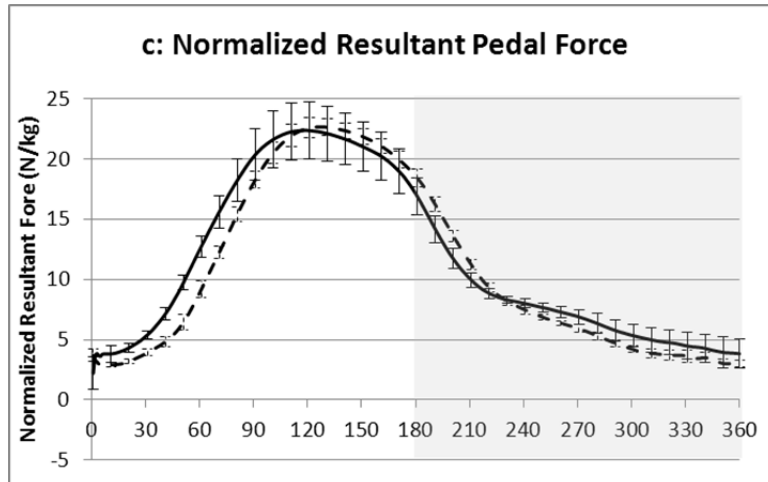


Figure 4-4 c: Normalized resultant pedal force across 5 time points during a 20-km simulated cycling session with two different seat post angles.

The vertical axis is the force magnitude normalized by the estimated leg mass (N/kg); the horizontal axis is the pedal cycle (deg), 0° - 360° . The forces are normalized to estimated leg mass. The each ROAD and TRI data include average of trials of 12 participants over 5 time points (1 km, 5 km, 10 km, 15 km, and 19 km). Each participant's data are the mean of the full pedal revolutions during a 10 second period. The solid line (—) is ROAD condition and the dotted line (- - -) is TRI condition. The error bars represents $\pm 1\text{SD}$.

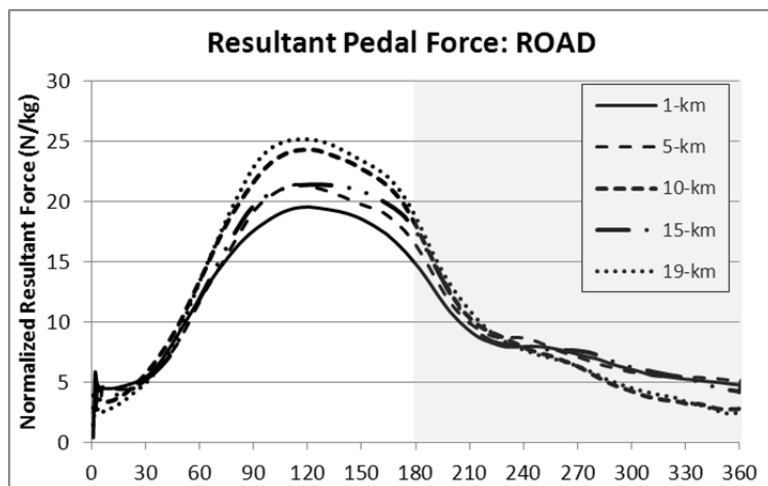


Figure 4-5: Normalized resultant pedal force at 1 km, 5 km, 10 km, 15 km, and 19 km during a simulated 20-km cycling session with ROAD riding position

The vertical axis is the force magnitude normalized by the estimated leg mass (N/kg); the horizontal axis is the pedal cycle (deg), 0° - 360° . The forces are normalized to estimated leg mass. Each time point data include average of trials of 12 participants at the given time point. Each participant's data are the mean of the full pedal revolutions during a 10 second period.

Pedaling Effectiveness

The portion of the pedal force used to drive the crank arm was quantified as the effective pedal force. Different cycling positions did not affect the net effective pedal force. A graphic representation of the effective pedal force is provided in Figure 4-6. The leg mass normalized effective force integral over a pedal cycle was similar between conditions (ROAD approximately 22 ± 6 N·s/kg; TRI 17 ± 8 N·s/kg; $F = 2.0$, $p > 0.05$). There was large effective force (peaking approximately at 20 N/kg for both conditions) during the propulsive phase; however, the force was mostly negative during the up phase indicating that the force was directed opposite of movement of the crank arm. There was a 9°-shift in timing of effective pedal force application between seat post angle conditions. The onset of the effective force occurred later with steeper seat post angle (TRI) condition. The index of pedaling effectiveness averaged over one pedal cycle were not significantly different between conditions (on average ROAD 32 %; TRI 33 %, Wilcoxon Z between -1.3 & 0, $p > 0.05$). Difference in the index of effectiveness was not detected even when the propulsive and recovery phases were compared separately. The index of pedaling effectiveness for the propulsive phase was 66 ± 4 % and 64 ± 5 % for ROAD and TRI, and for the recovery phase was -49 ± 16 % for ROAD and -42 ± 27 % for TRI. The pedaling effectiveness measures, both effective force integral and index, were similar at 5 different time points during the cycling session.

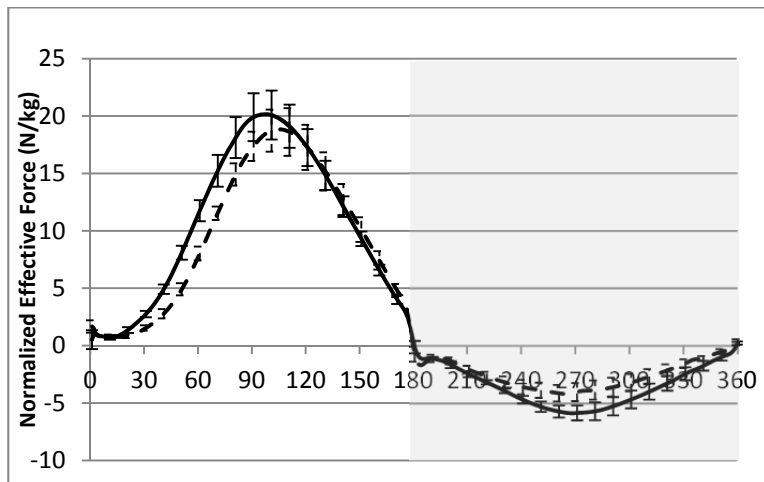


Figure 4-6: Normalized effective pedal force across 5 time points during a 20-km simulated cycling session with two different seat post angles.

The vertical axis for the effective force is the force magnitude normalized by the estimated leg mass (N/kg). The horizontal axis is the pedal cycle (deg), 0° - 360° . The each ROAD and TRI data include average of trials of 12 participants over 5 time points (1 km, 5 km, 10 km, 15 km, and 19 km). Each participant's data are the mean of the full pedal revolutions during a 10 second period. The solid line (—) is ROAD condition and the dotted line (---) is TRI condition. The error bars represents $\pm 1\text{SD}$.

Joint Moments

In both cycling conditions, the magnitude of joint moment was related to the size of the joints themselves. The largest joint the hip had the greatest, and the smallest the ankle had the least amount. The seat position affected the amount of the net moment as well as the moment at individual leg joints. The normalized net moment of the leg (sum of the time-integral of joint moment at 3 joints) for the TRI condition was significantly lower than for the ROAD condition at 1-km, 15-km, and at 19-km ($p < 0.05$; 16 ± 2 Nm/kg v. 12 ± 3 Nm/kg at 1-km, 16 ± 3 Nm/kg v. 13 ± 3 Nm/kg at 15-km, and 17 ± 3 Nm/kg v. 13 ± 4 Nm/kg at 19-km for ROAD and TRI respectively). This change was as the result of reduced hip moment occurred with TRI condition ($p < 0.05$ at 1-, 5-, 15-, and 19-km; ROAD 12 ± 3 Nm/kg; TRI 8 ± 3 Nm/kg on average). Joint moment increased at the knee for TRI condition ($p < 0.05$ at 5-, 10-, 15-, and 19-km; ROAD 3 ± 1 Nm/kg; TRI 4 ± 1 Nm/kg on average). The change at the ankle joint was statistically different ($p < 0.05$; ROAD 0.3 ± 0 Nm/kg v. TRI 0.2 ± 0 Nm/kg on average), but the ankle had far less contribution to the net moments of the leg. The joint moment data are included in the Figure 4-7. Cross correlation analysis revealed delayed change in joint moment with TRI at the hip (12°), knee (9°), and ankle (9°).

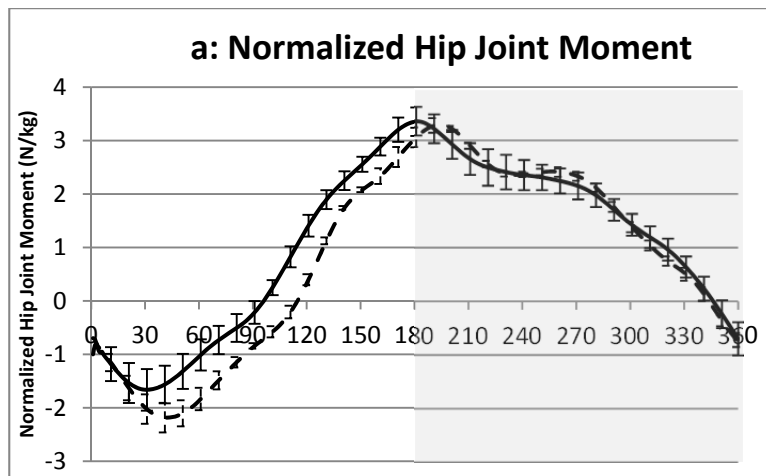


Figure 4-7a: Normalized hip joint moment across 5 time points during a 20-km simulated cycling session with two different seat post angles.

The vertical axis is the joint moment normalized by the estimated leg mass (N-m/kg); the horizontal axis is the pedal cycle (deg) 0° - 360° . Positive on vertical axis corresponds to flexion at hip. The each ROAD and TRI data include average of trials of 12 participants over 5 time points (1 km, 5 km, 10 km, 15 km, and 19 km). Each participant's data are the mean of the full pedal revolutions during a 10 second period. The solid line (—) is ROAD condition and the dotted line (---) is TRI condition. The error bars represents $\pm 1\text{SD}$. *Note that the vertical axis scaling for the ankle joint moment (c) is different from the other two to show the details.

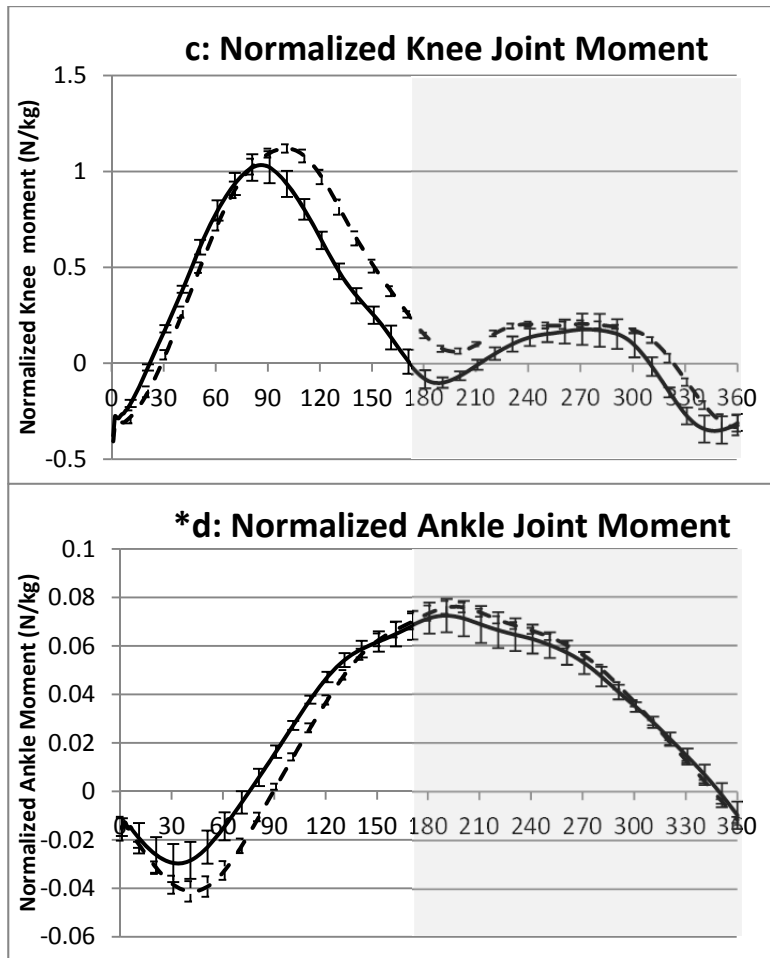


Figure 4-7b – c: Normalized knee and ankle joint moments across 5 time points during a 20-km simulated cycling session with two different seat post angles. The vertical axis is the joint moment normalized by the estimated leg mass (N-m/kg); the horizontal axis is the pedal cycle (deg) 0° - 360°. Positive on vertical axis corresponds to extension at knee (b) and plantar flexion at ankle (c). The each ROAD and TRI data include average of trials of 12 participants over 5 time points (1 km, 5 km, 10 km, 15 km, and 19 km). Each participant's data are the mean of the full pedal revolutions during a 10 second period. The solid line (—) is ROAD condition and the dotted line (- - -) is TRI condition. The error bars represents $\pm 1\text{SD}$. *Note that the vertical axis scaling for the ankle joint moment (c) is different from the other two to show the details.

Muscle Activation

Visual inspections of the EMG signal-time plots (Figure 4-8a – c) indicated similar general activation pattern of 7 monitored leg muscles during a pedal cycle. All, but tibialis anterior (TA), were more active primarily during the power phase (sector 2) in both conditions. Both quadriceps muscles (rectus femoris, RF and vastus lateralis, VL) were also highly active when the pedal was near top (sector 1), approximately, 50 - 60 %MVIC and 30 - 100 %MVIC respectively. Both calf muscles (Gast and SOL) were more active than other muscles through transition between the propulsive phase to the recovery phase (near BDC, sector 3). The other ankle muscle, TA, was also active during the sector 3; however, its highest activation occurred during the later recovery phase (later sector 4 and beginning of sector 1). The activation of the muscles was evaluated quantitatively by comparing the mean EMG RMS values over each of the 4 sectors (Table 4-3). The muscle activation levels among the sectors were significantly different within each of the 7 muscles ($p < 0.05$). Between two cycling positions, differences were detected for Gmax (ROAD 10 ± 8 %MVIC; TRI 6 ± 9 %MVIC; Wilcoxon $Z = -2.27$) and biceps femoris (BF) (ROAD 13 ± 7 %MVIC and TRI 7 ± 5 %MVIC) during the sector 1 and SOL during the sector 2 (ROAD 70 ± 39 %MVIC and TRI 43 ± 22 %MVIC).

Two of the larger muscles that act as the hip extensors, Gmax and BF, worked at a smaller capacity level relative to their maximal potentials. Even at their highest level of activation that occurred during the sector 2, these hip extensors' activation levels are at 24 – 35 %MVIC and 28 – 41 %MVIC, respectively. Additionally, these larger extensor muscles were relatively unused during the upstroke of the pedal cycle. Conversely, a uniarticular knee extensor (VL) worked at higher capacity during the second sector (96 – 108 %MVIC), and it only had a short period when it was minimally active (sector 3). Gastrocnemius (Gast) was another muscle that exhibited higher activation. In addition to its highest activation during the sector 2, the muscle was relatively active through the following sector into the first half of the sector 4.

The differences in muscle activation patterns were indicated by the results of cross correlation coefficient analysis (example shown in Figure 4-9). Although the patterns of activation were similar in all 7 muscles, activation timing was different between two seat conditions (Table 4-4). Of the 7 muscles, Gmax, BF, VL, and TA were associated with higher linearity between conditions, the assumption associated with cross correlation analysis. Activation timing of all, but BF occurred later with TRI condition (14° , 15° , and 20° delay for Gmax, VL, and TA). The time shift for BF occurred in the opposite direction – the activation of BF occurred earlier by 20° with TRI condition.

Table 4-3: Mean activation level of selected leg muscles during 4 sectors of pedal cycle during cycling in ROAD and TRI conditions at 1-km.

Activation is represented as the mean value for the normalized EMG (%MVIC) in a sector. Sector 1: 313° - 13°; sector 2: 13° - 133°; sector 3: 133° - 193°; and Sector 4: 193° - 313° of a pedal cycle. Gmax, gluteus maximus; BF, biceps femoris long head; RF, rectus femoris; VL, vastus lateralis; Gast, gastrocnemius lateral head; SOL, soleus; TA, tibialis anterior. “*” denotes a significant difference between ROAD and TRI conditions ($p < 0.05$).

Sector	Gmax		BF		RF		VL		Gast		SOL		TA		
	ROAD	TRI	ROAD	TRI	ROAD	TRI	ROAD	TRI	ROAD	TRI	ROAD	TRI	ROAD	TRI	
1	Activation	*10.2	*6.3	*12.9	*7.4	45.9	47.6	98.1	66.1	14.0	6.3	12.5	9.6	33.0	35.0
	SD	8.2	8.6	7.1	5.0	48.9	23.8	56.2	35.6	15.6	2.0	10.5	8.5	27.6	49.4
2	Activation	23.9	34.9	40.7	27.7	28.6	34.3	95.6	107.5	96.1	66.7	*66.9	*42.7	8.9	9.0
	SD	16.0	41.6	27.5	16.7	25.1	19.6	49.0	47.2	47.8	22.5	38.8	21.9	5.4	11.4
3	Activation	4.9	2.1	30.8	26.8	5.9	4.2	8.1	4.8	46.0	37.9	36.2	20.2	14.4	12.3
	SD	7.9	1.3	26.9	27.0	5.1	3.8	13.4	3.6	41.4	27.9	32.2	17.8	11.1	17.6
4	Activation	7.3	3.2	7.9	11.5	40.8	32.8	20.1	11.7	33.1	19.1	15.8	9.9	24.3	19.7
	SD	6.4	2.1	6.8	19.0	45.7	29.5	23.4	11.6	23.7	9.7	12.9	5.4	20.5	19.1

Table 4-4: Time shift, coefficient of cross correlation, and linearity of EMG signal of selected leg muscles between two seat positions at 1-km.

The EMG RMS linear envelope signals were used for cross correlation. Gmax, gluteus maximus; BF, biceps femoris long head; RF, rectus femoris; VL, vastus lateralis; Gast, gastrocnemius lateral head; SOL, soleus; TA, tibialis anterior. The negative time shift denotes later onset of the muscle with TRI condition.

	GMAX	BF	RF	VL	GAST	SOL	TA
Time Shift (deg)	-14	20	-7	-15	-13	-16	-21
Cross Correlation (r)	0.9261	0.9099	0.9774	0.9789	0.9847	0.9769	0.8826
Linearity (R^2)	0.8786	0.8189	0.0243	0.8998	0.4107	0.3118	0.8613

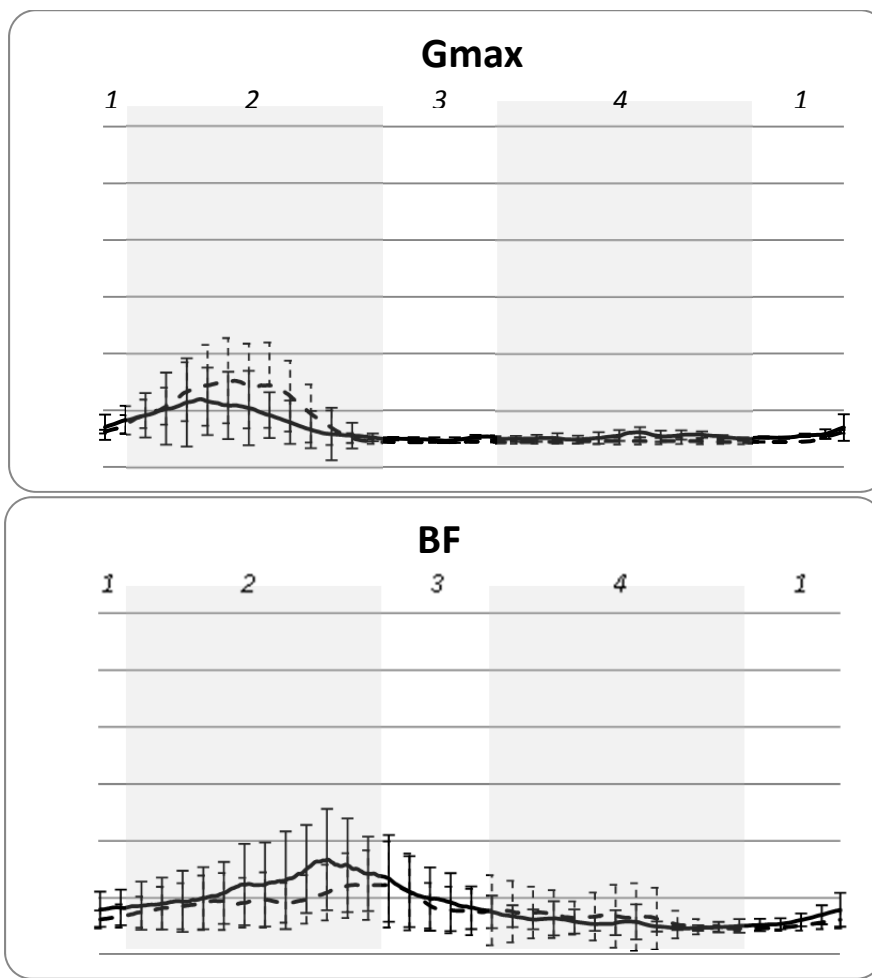


Figure 4-8a: Normalized EMG linear envelopes of gluteus maximus and biceps femoris at 1-km of a 20-km simulated cycling session with two different seat post angles.

Curves of EMG RMS linear envelop for gluteus maximus (Gmax) and biceps femoris (BF) muscles for two seat post angle positions. The linear envelop curves are the average of the 12 athletes with the number of full pedal revolutions in 10 seconds at 1-km. The magnitude is shown in %MVIC. The solid line (—) is ROAD condition and the dotted line (---) is TRI condition. The error bars represents $\pm 1\text{SD}$. The areas 1 – 4 represent different sectors of the pedaling cycle, $313^\circ - 13^\circ$, $13^\circ - 133^\circ$, $133^\circ - 193^\circ$, and $193^\circ - 313^\circ$, respectively.

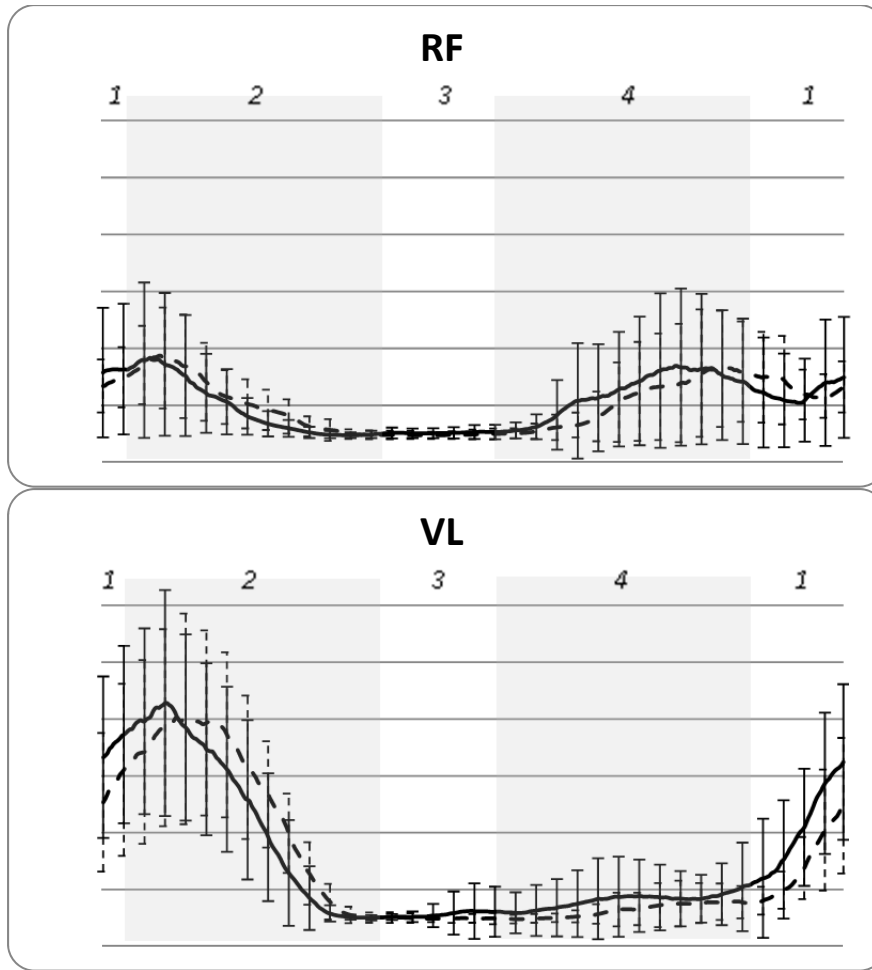


Figure 4-8b: Normalized EMG linear envelopes of rectus femoris and vastus lateralis at 1-km of a 20-km simulated cycling session with two different seat post angles.

Curves of EMG RMS linear envelop for rectus femoris (RF) and vastus lateralis (VL) muscles for two seat post angle positions. The linear envelop curves are the average of the 12 athletes with the number of full pedal revolutions in 10 seconds at 1-km. The magnitude is shown in %MVIC. The solid line (—) is ROAD condition and the dotted line (---) is TRI condition. The error bars represents $\pm 1\text{SD}$. The areas 1 – 4 represent different sectors of the pedaling cycle, $313^\circ - 13^\circ$, $13^\circ - 133^\circ$, $133^\circ - 193^\circ$, and $193^\circ - 313^\circ$, respectively.

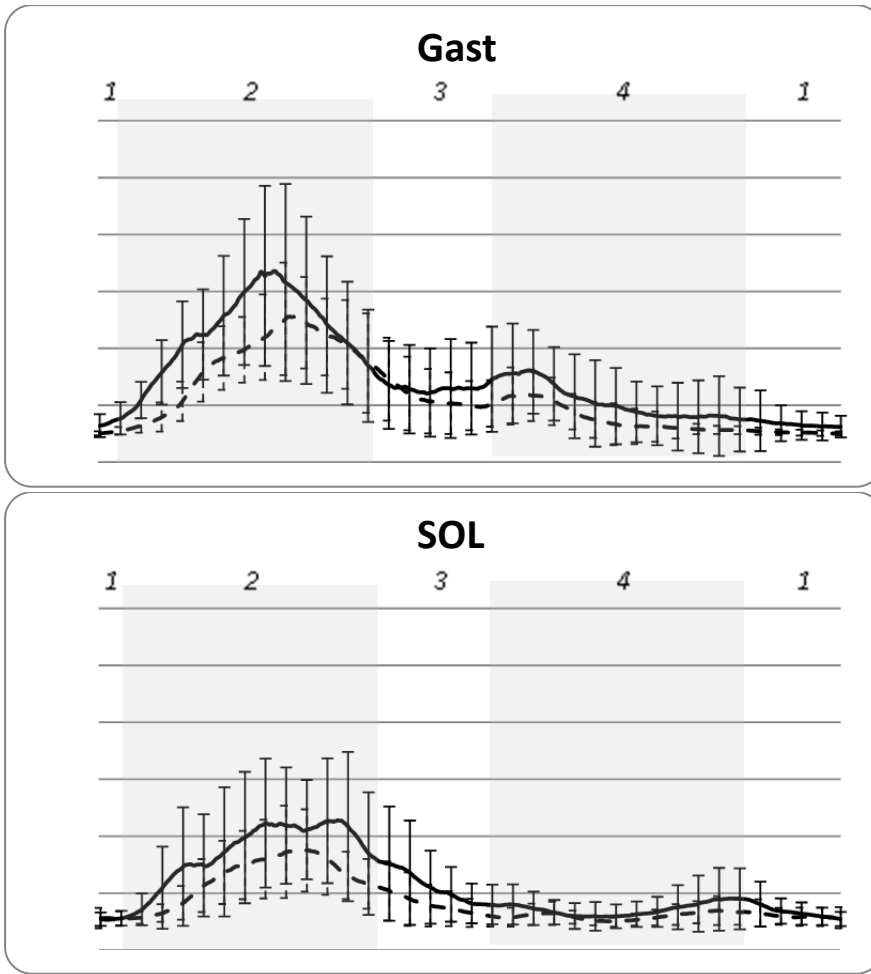


Figure 4-8c: Normalized EMG linear envelopes of gastrocnemius and soleus at 1-km of a 20-km simulated cycling session with two different seat post angles.

Curves of EMG RMS linear envelop for gastrocnemius lateral head (Gast) and soleus (SOL) muscles for two seat post angle positions. The linear envelop curves are the average of the 12 athletes with the number of full pedal revolutions in 10 seconds at 1-km. The magnitude is shown in %MVIC. The solid line (—) is ROAD condition and the dotted line (---) is TRI condition. The error bars represents $\pm 1\text{SD}$. The areas 1 – 4 represent different sectors of the pedaling cycle, $313^\circ - 13^\circ$, $13^\circ - 133^\circ$, $133^\circ - 193^\circ$, and $193^\circ - 313^\circ$, respectively.

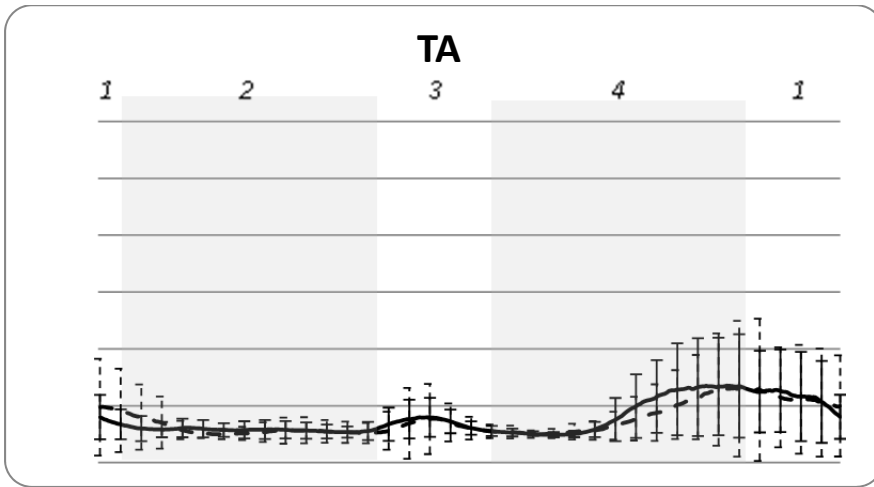


Figure 4-8d: Normalized EMG linear envelopes of tibialis anterior at 1-km of a 20-km simulated cycling session with two different seat post angles.

Curves of EMG RMS linear envelop for soleus (SOL) and tibialis anterior (TA) muscle for two seat post angle positions. The linear envelop curves are the average of the 12 athletes with the number of full pedal revolutions in 10 seconds at 1-km. The magnitude is shown in %MVIC. The solid line (—) is ROAD condition and the dotted line (---) is TRI condition. The error bars represents $\pm 1\text{SD}$. The areas 1 – 4 represent different sectors of the pedaling cycle, $313^\circ - 13^\circ$, $13^\circ - 133^\circ$, $133^\circ - 193^\circ$, and $193^\circ - 313^\circ$, respectively.

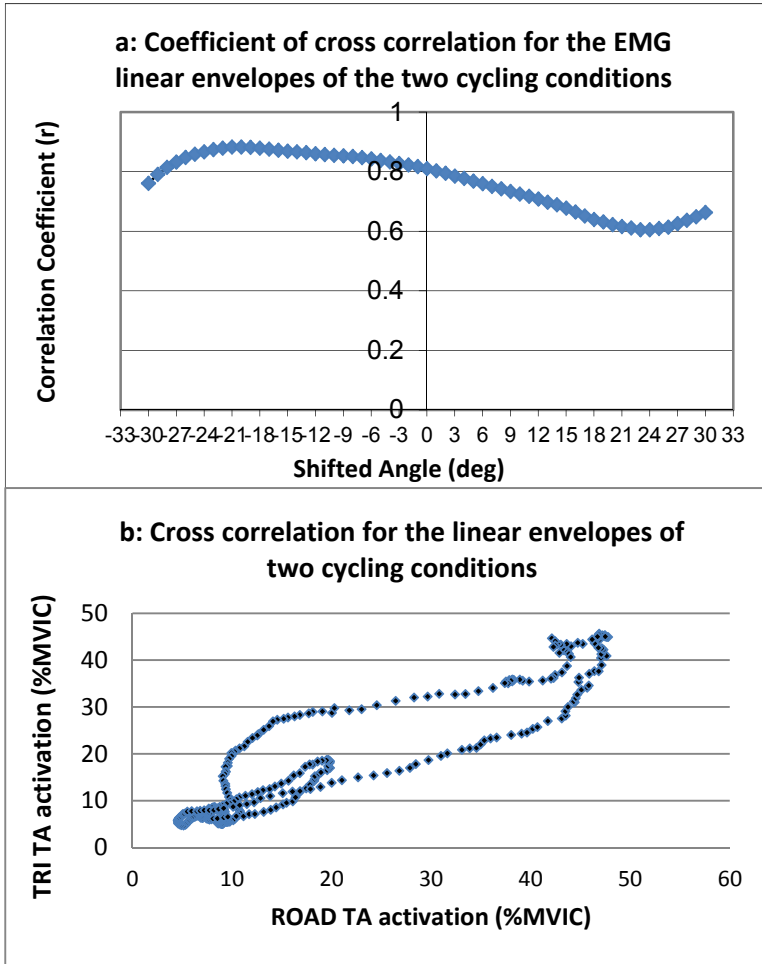


Figure 4-9: Cross correlation for the EMG linear envelopes of the two cycling conditions.

a): The coefficient of cross correlation for the tibialis anterior's (TA) EMG linear envelopes of the ROAD and TRI cycling conditions. The x-axis represents time shift expressed as the degree of pedaling cycle. the y-axis represents the correlation coefficient. The highest correlation coefficient occurred at -21, indicating that there was a 21° delay with TRI condition. b): Cross correlation for the TA linear envelopes for the ROAD and TRI conditions are represented graphically. The x-axis and the y-axis represent % MVIC muscle activation level (linear envelop) of TA with the ROAD and TRI conditions. TA exhibited high linearity (R^2) of 0.86.

Aerodynamics

On average, mean estimate for the projected frontal area for ROAD and TRI conditions were essentially the same ($0.29 \pm 0.03 \text{ m}^2$ for both). As the results, the estimated drag force between conditions did not differ neither (ROAD $131 \pm 7 \text{ N}$; TRI $133 \pm 5 \text{ N}$).

Performance

The time to complete the course was not significantly different between seat post angle conditions (ROAD $39:05 \pm 4:23$; TRI $38:23 \pm 6:25$), but the finish time was moderately influenced by the seat post angle modification ($d = 0.54$). The 42 second difference was not statistically significant; however, it can be practically meaningful. The participants' finish times and their preferred bike types are summarized in Table 4-5. Of 12 tested, 2 (sub 3 and 9) completed faster with ROAD condition. Both of these participants regularly rode a bike similar to ROAD condition. 2 others (sub 4 and 8) completed the course in about the same time. The rest (8 participants) completed the course faster with TRI seat post setting.

Table 4-5: Finish times of a 20-km simulated course using two different seat post angle settings and bike-type preferences of 12 study participants

The participants' own bike (bike pref.) was categorized to RAOD and TRI with the seat post angle <75° and ≥ 75° respectively. A positive percent difference (% diff.) value corresponds to faster finish time with TRI condition.

Finish Time			
Bike Pref	ROAD	TRI	% diff.
RAOD	32:11:00	32:18:00	-0.4
	33:09:00	33:56:00	-2.4
	37:12:00	34:15:00	7.9
	38:09:00	36:49:00	3.5
	44:10:00	43:28:00	1.6
	46:12:00	42:19:00	8.4
TRI	50:45:00	54:40:00	-7.7
	32:39:00	32:11:00	1.4
	36:11:00	34:40:00	4.2
	36:46:00	35:08:00	4.4
	39:46:00	39:46:00	0.0
Mean	41:44:00	40:59:00	1.8
	39:05:00	38:23:00	1.9
	SD	4:23	6:25

Summary of Results

The kinematics, kinetics, and muscle activation between two seat positions during cycling were different in certain biomechanical variables. The most differences were observed with segmental orientations. With forward seat position (TRI), the thigh was positioned more vertically, and that resulted in more horizontal shank orientation. Coincided with these segmental changes with TRI condition, the pedal was tilted more anteriorly, but the pedaling effectiveness was unchanged at 64 – 66 % during the propulsive phase. The joint moment at the hip and the ankle was reduced with the steeper seat post angle, but at the knee, it was greater. This made the total leg joint moments lesser approximately by 4 Nm/kg for the TRI condition. Significantly higher activation of Gmax and BF during the sector 1 (near TDC) was also associated with TRI cycling condition. There was delay in some muscle activation and pedal force application when cyclists cycled in TRI position. There was a small improvement, 42 seconds faster in finish time with TRI condition that could be practically meaningful. Several of the study participants reported some discomfort associated with ROAD condition.

Chapter Five

Discussion

Introduction

The aim of this study was to examine how fore-aft seat position modification influences the cycling mechanics. Altered fore-aft position of the seat changes seat's relative location to the crank axis, thus, the seat position angle. This type of geometrical modification in cycling has been adopted by many triathletes due to the anecdotal testimonials that cycling in more forward position is beneficial in triathlon performance. However, there are limited sources supporting positive effects of forward seating in cycling, and the consequences of such a change have not been thoroughly evaluated. In this study, biomechanical characteristics during cycling using two seat position settings were investigated. The research hypotheses examined kinematic, kinetic, and muscle activation variables that could be influenced by the seat position. The hypotheses were structured in the way that changed leg alignment relative to the crank axis (segmental kinematics) would lead to altered joint kinematics in certain joints. Further, these kinematic changes would potentially influence pedaling kinetics and muscle activation.

Seat Post Angle Effects

Kinematics

Changing the fore-aft position of the seat by 10 cm (ROAD = 5 cm behind and TRI = 5 cm forward of the crank axis) resulted in some kinematic changes. The actual sitting position was measured as the horizontal distance between the greater trochanter and the crank axis. The measured sitting position of the participants changed from 18.5 cm (ROAD) to 7.4 cm (TRI) behind the crank axis; therefore, the actual sitting position of the participants was modified by changed fore-aft seat position. The forward seat position in TRI condition increased the seat post angle (SPA) by 8° (ROAD 64±1°; TRI 72±1°), making the cyclist sit on a seat with its anterior-posterior center located above the crank arm rather than behind as with ROAD condition. Theoretically, with this change, the angle between the seat post and the horizontal line at the base of the seat would increase. Limited evidence [72, 111] suggested that this change caused the body to rotate forward about the crank axis positioning the leg in a more vertical orientation. Therefore, it was predicted that as the result of the seat position modification performed in this study, the leg orientation would become more vertical. The results indicated that most notable kinematic changes existed in segmental orientations. TRI position resulted in greater anterior tilt of the pelvis approximately by 7° with a minimal time shift of 1° of the pedaling cycle. The minimal time shift between ROAD and TRI conditions was because the participants' upper body was fixed (aerodynamic riding position) during the cycling session. With this increase in the anterior pelvic tilt among the cyclists, there

would be practical consequences concerning cycling performance. Previous research had found an association between the ability to actively position the pelvis in anterior tilt and cycling performance level. In these studies, the cyclists' ability to tilt the pelvis was measured statically using the long sit position, a commonly accepted way to assess the ability to assume more aggressive aerodynamic position in cycling community. Although, the applicability of this static measure to the dynamic situation (actual cycling) was inconclusive, the association between the ability to tilt the pelvis and the performance level had been established in different populations [112-115]. In the present study, the participants, on average, cycled 38 seconds faster when their pelvis was more anteriorly tilted (TRI condition). Although this was not statistically significant, this finding may imply that the positive association between anterior pelvic tilt and cycling performance is present in the dynamic (cycling) situation.

The average difference in thigh angle resulting from the seat position change was approximately 7°, TRI with smaller thigh angle, indicating that the participants did not pick up the distal thigh (i.e. the knee) as much when their bodies were more vertically aligned with the crank axis. A more vertically positioned thigh would theoretically 'open-up' the hip (reduction of hip flexion) [19, 20]. However, both the minimal hip flexion angle that occurred near the bottom dead center (BDC) and the maximal hip flexion angle that occurred near the top dead center (TDC) did not change significantly between conditions. Furthermore, the range of motion (ROM) of the hip joint during a single pedal cycle did not differ between conditions. This result does not fully support some previous research that reported decreased hip flexion angle with more vertical SPA [20, 73, 116]. This was possibly due to the orientation change that occurred with the pelvis. The thigh angle on average differed between conditions by 7°, and the anterior tilt angle of the pelvis also differed by 7°. As a result, the effect of segmental orientation differences between conditions was 'canceled out,' leading to no difference in the hip flexion angle. The more vertical sitting position associated with TRI setup resulted in tilting the pelvis and the thigh together as a unit. Additionally, unlike previous studies, the fore-aft position of the handlebars was moved with the seat position (i.e. the reach length, the distance between the seat and the handlebar, was maintained) in the present study. Therefore, the orientation relationship between the pelvis and the thigh was minimally affected. The hypothesis that the steeper seat post angle would result in a reduced hip flexion was not supported. Changing the seat post angle while maintaining the other geometrical measurements of the bike did not affect in hip flexion angle.

Knee flexion angle was not expected to change with the seat position modifications. Cycling movement involves a mechanically constrained environment. The knee angle is directly related to the orientation of two adjacent segments, the thigh and the shank. As indicated previously, the thigh angle was significantly more vertical with TRI condition. The shank angle, on the other hand was more horizontal with TRI condition. While the participants lifted their thigh anteriorly (thus, the knee) less, they lifted the shank (i.e. the heel) posteriorly more to compensate. As the crank arm length (i.e. the distance between the foot/pedal and the crank axis) was the same in both conditions, the participants were required to pick up their foot up to drive the pedal on the circle with a fixed radius. The more vertical orientation of the thigh was accounted for

by the more horizontally orientated shank segment, resulting in a conserved knee flexion angle. As previously reported, the knee angle and range of motion are minimally affected as long as the seat post length (SPL) stay unchanged [20, 25, 28, 111]. Knee flexion angle and the SPL have an inverse relationship. The knee undergoes greater amount of flexion with shorter SPL [5, 117, 118]. In the current set up, each participant's individual preferred SPL (69 ± 4 cm) was replicated in both experimental conditions; therefore, it was probable that the participants cycled with similar knee angle as with their own bike. The resulting mean knee flexion angle over a pedaling cycle was $77 \pm 4^\circ$ and $79 \pm 5^\circ$ for the ROAD and TRI conditions respectively. As the knee flexion angle was systematically similar in both conditions, the similar mean knee flexion angle across the pedaling cycle would reflect similar minimal and maximal knee flexion angle. The relatively small variability associated with the mean knee flexion angle indicated a highly consistent pattern of knee joint angle among participants in both conditions.

A notable kinematic change occurred with the foot-pedal segment. The ROM of the anterior-posterior tilt of the foot-pedal segment was comparable to previously published data [4] and was similar in both conditions ($44 \pm 4^\circ$ and $46 \pm 6^\circ$ for ROAD and TRI). As previously reported [25, 72, 73], the pedal was more anteriorly tilted throughout the pedal cycle with TRI condition (mean pedal angle: ROAD $14 \pm 5^\circ$; TRI $22 \pm 5^\circ$). This can be explained by the reduced need for driving the pedal forward from behind. Since the body was already above the crank axis the cyclist could focus on pushing the pedal downward. This modification in pedal angle was also related to the ankle joint angle that did not differ between conditions. More horizontal shank offset the modified orientation of the foot-pedal segment. With the steep SPA (TRI), the participants needed to pick up the heel more posteriorly that made the shank more horizontally oriented. The increase in anterior tilt of the pedal/foot was necessary to maintain similar angle at the ankle joint. With both forward and backward seat positions, the ankle was in moderate plantar flexion on average over a pedal cycle (mean ankle angle: ROAD $19 \pm 7^\circ$; TRI $17 \pm 5^\circ$). Previous research reported small changes in ankle kinematics with modification in cycling geometry [20, 28], and ankle joint kinematics has been documented as a relatively consistent component of the cycling mechanics. The consistency with the ankle angle is thought to be related to its function in energy transfer. The ankle stiffness is critical as the joint is located immediate to where the energy transfer from the body to the bicycle occurs [4, 5, 44, 119, 120]. Particularly, during the propulsive phase of the pedaling cycle, the ankle needs to be stiff and to be angled in a way to transfer the force generated by the leg muscles effectively [29, 32, 52]. The participants of this study allowed relatively small ankle ROM of approximately 17° in both conditions, much less than the ROM of the hip (approximately 46°) and the knee (approximately 77°). Additionally, the ankle was placed in anatomically more stable position at the closest to the neutral (0° of plantar or dorsiflexion) when the applied pedal force reached its peak. As all of the participants were accustom to a cycling task, they were able to establish the ankle angle that they typically use to deliver the force to the pedal effectively.

The effects of fore-aft seat position modification on cycling kinematics existed only in the segmental orientations. As the participants modified the segmental orientations accordingly with changed cycling position, relatively similar joint kinematics

were maintained during cycling. The changes in the foot-pedal segment and the shank orientations combined allowed the ankle joint angle to be preserved. The same type of events occurred between the shank and the thigh and between the thigh and the pelvis segmental orientation changes to maintain the knee and the hip joint angles. As suggested previously, it appeared that the cyclists were able to preserve their usual kinematic strategies even with altered cycling positions [25, 28, 121]. Cyclists were capable of making necessary adjustments to attain the projected outcome, such as force applied to the pedals [25, 28, 121]. Heil found that when cyclists rode an experimental bike (different geometry from their own bike), they preferred to maintain the hip angle the same as when they rode their own bike [116]. The preferred hip angle was associated with the lowest physiological demand (low oxygen consumption). Therefore, it is possible that the participants in the current study employed the kinematic strategies so that they could ride with better physiological efficiency.

Kinetics

The pedal force magnitudes were evaluated using the leg mass-normalized pedal forces to account for the effect of the leg mass as it has been shown that the inertial effect of the leg contributes to the applied force. [46, 122]. The variability of the force data was reduced with the normalization compared to non-normalized forces, making the interpretation of the results more appropriate. Separate analysis of the pedal forces by genders indicated that females applied approximately 17 - 21% less resultant forces than males when the force was not normalized, but leg mass-normalization of the resultant force showed 3 % difference (more in ROAD and less in TRI for females) between genders.

The overall pedal forces during a single pedal cycle were compared based on the impulse (integral of pedal force over the time spent for a pedal cycle). The impulse of the two components of the pedal force, normal and tangential forces were similar between conditions, indicating that amount of tangential and normal impulse applied did not change with seat position modification. Normal and tangential pedal forces peaked during the propulsive phase; however, the peak of tangential force occurred earlier (approximately 80° - 90° of the pedal cycle) than that of the normal force (110° - 120° of the pedal cycle). This supports the results from De Groot [25]. The time shift between these two forces was related to the direction of the pedal movement during the time of the pedal cycle. Moving from the TDC (0° of pedal cycle), the cyclist drove the pedal forward during the early propulsive phase using the tangential pedal force, but once the pedal reached near the front most of the pedal path (i.e. 90° of pedal cycle), the cyclist switched the direction of applied force into more downward direction. The different timings of the peak pedal forces for the different seat post angles were the result of the time shift occurring in the pedal angle. Making the seat post angle more vertical resulted in 7°-delay in pedal angle change, 2 % time of the full pedaling cycle. Delaying the force application was used as a strategy by the cyclists in the current study to maintain a consistent force applied to the pedal. The normal force peaked when the pedal was

oriented most horizontally, approximately at 100° for ROAD and 110° for TRI. The delay in the peak force associated with the TRI condition was the direct result of the delay in the pedal angle change. The most horizontally oriented pedal angle occurred later with TRI condition. The individual cyclists also appeared to use different techniques to maintain the resultant force. A large standard deviation was particularly noticeable around the peak force for both the normal and the tangential pedal forces, indicating that participants employed different technique to apply the force to the pedal. For the normal force, the inter-individual variation also became larger right before TDC.

When cycling with ROAD set up, the tangential force became negative approximately at 150° of the pedal cycle, indicating that the pedal force applied was directed more posteriorly relative to the pedal surface. The participants utilized more tangential force to drive the pedal backward until about 220° of the pedal cycle. With the TRI condition, however, the change in the direction of the tangential force never occurred. The tangential force was near-zero approximately at the BDC, but the tangential force remained positive over the entire pedal cycle. Since the pedal was more anteriorly tilted with TRI position, force applied vertically to the pedal surface (normal force) contributed to moving the pedal backward. In fact, from 150° of the pedal cycle to the BDC, the normal force for TRI condition showed a smaller decline than for ROAD condition.

During the recovery phase, the normal force for both conditions was considerably smaller than during the propulsive phase, but it remained positive indicating that force perpendicular to the pedal surface was still present. Part of this force acted to generate the torque that was opposed the crank revolution; however, at least during the initial portion of the recovery phase, the positive normal force was possibly applied in attempt to drive the crank posteriorly as the pedal was anteriorly tilted. When the time series of the normal pedal force is visually inspected, the effect of the seat post angle on the normal force seemed smaller during most of the recovery phase. This supports Price and Donne [73] who suggested that the seat post angle change would have a minimal effects on the pedal forces during the recovery phase. During the last portion of the recovery phase (330° - 360°), the tangential force became increasingly positive to start driving the pedal forward as it approached TDC. It appeared that both tangential and normal force magnitudes were relatively similar between conditions at the TDC. The patterns of tangential and normal forces were similar to the data documented in literature [4, 5], but the magnitudes of the forces in the current study were smaller (non-normalized normal: 300 N v. 350 - 400 N; non-normalized tangential 25 N v. 80 N, current study v. previous study respectively). This was likely due to difference in study samples. The previous study included all male high-level cyclists, whereas the current study included cyclists of both genders who were mostly recreational-level participants. The pedal force is one of the two elements that determines the pedal power (pedal power = the product of pedal force and angular displacement over time) [48]. If cycling at the same cadence with the same crank arm length, the pedal force is the only factor that determines the pedal power. The pedal power is positively related to the cycling speed [5, 48]; therefore, higher level cyclists who can cycle faster are able to generate greater pedal force. The cyclists in the current study were mostly recreational athletes, so they

had less force generating capability. Additionally, as indicated earlier, the leg mass was also related to the non-normalized pedal force. The gender difference in the pedal force was nearly 20 % before normalization in this study. As the current study included female cyclists, it would also contribute to the smaller pedal force magnitudes.

The similarities between the tangential and normal forces, however, resulted in statistically different resultant (F_{RES}) impulses between two seat conditions. The leg mass-normalized F_{RES} impulse over the entire pedal cycle for ROAD was 57 ± 17 N·s/kg and for TRI it was 49 ± 13 N·s/kg, indicating that overall force application was greater with ROAD condition. As occurred in tangential and normal forces, the majority of the force was applied during the propulsive phase of the pedal cycle. The timing of the onset and the offset of the force applications was also different between conditions. Very similar force magnitude and the pattern occurred, but the onset of the force was later in TRI condition. Previous research suggested that cyclists tend to alter the pedaling mechanics, such as force application timing to offset the effect of the changed pedal angle, to attain the consistent resultant pedal force [25]. However, the current results suggested that the net force applied to the pedal was affected by the change in cycling position relative to the crank axis. The current results may also suggest that F_{RES} impulses, the total pedal force over a pedal cycle, are not an appropriate variable to assess the cycling performance. Despite of the smaller F_{RES} impulse, the finish time was better with TRI condition. This could be because the resultant (or total applied) pedal force does not distinguish the useful force (i.e. effective force) from useless force (ineffective force) in driving the crank arm. Measures that differentiate useful force and useless force are more appropriate in examining cycling performance.

In the present study, the analysis focused on right leg mechanics; however, in reality, crank movement occurs due to the combined effect of the effective force from both right and left pedals. Therefore, the discussion of pedal effectiveness should be interpreted with caution. The effective pedal force (F_{EFF}) is often considered as the ‘useful’ pedal force since it actually contributes to crank torque. F_{EFF} that is positive drives the crank, whereas the negative value hinders the movement of the crank arm. The overall F_{EFF} for both ROAD and TRI conditions did not differ significantly. The normalized F_{EFF} impulses over the entire pedal cycle for ROAD and TRI conditions were 22 ± 6 N·s/kg and 17 ± 8 N·s/kg respectively. The majority of the driving force was applied to the crank during the propulsive phase, reaching the peak magnitude approximately at 100° for the ROAD and approximately at 110° for TRI. This supports previously published data showing that most of the torque-generating force is applied during the power phase, between 60° and 120° of the pedaling cycle [4, 6, 7, 32, 40, 52, 53, 57, 123, 124]. The F_{EFF} for the ROAD appeared slightly greater than that for the TRI during the propulsive phase. When the maximal magnitudes of the F_{EFF} and F_{RES} was compared, it became clear that majority of the F_{RES} was used to drive the crank arm. This high pedaling effectiveness was confirmed by the index of pedaling effectiveness (I_{EFF}). The average I_{EFF} during the propulsive phase was 66 ± 4 % and 64 ± 5 % for ROAD and TRI respectively.

During the recovery phase, F_{EFF} was negative indicating that the pedal force caused torque that acted against crank movement. This negative F_{EFF} was exhibited in

cyclist of different levels, including elites [4]. There is a common belief that ‘pulling up’ the pedal during the recovery phase reduces the amount of negative effective force that hinders the crank movement, thereby improving the cycling efficiency. Some commercially available independent crank arms (require each leg to work individually) are intended to improve the F_{EFF} by training the body to intentionally pull up the leg during the recovery. An investigation on the training effects of the independent crank arms reported that proportion of work performed between 45° and 135° of the pedal cycle (including the power phase) relative to the net work over an pedal cycle was reduced post-training, possibly indicating reduction of negative torque during the recovery phase [40]. Examination of different pedaling strategies confirmed that intentional pull up effort during the recovery phase in fact reduces the amount of negative torque during that phase and resulted in better pedaling effectiveness [58]. However, this particular pedaling strategy increased the physiological demand during cycling. In the current study, TRI condition was associated with slightly less negative F_{EFF} than ROAD during recovery. However, the overall F_{EFF} with TRI was not greater as the F_{EFF} was less during the propulsive phase.

Neptune and Herzog [122] examined the relationship between the F_{EFF} and the muscular and non-muscular components of the pedal force. During a steady-state cycling at 90 rpm, the primary source of the ineffectiveness in the pedal force was the non-muscular components of the force, and it increased with increased cadence. The primary cause of the non-muscular component of the force is related to the inertial property and the weight of the body segments [46]. In the current study, while the participants cycled at cadence of 89 rpm and 90 rpm for ROAD and TRI conditions. There was no significant difference in I_{EFF} in two seat conditions, suggesting that there was no change in amount of ineffectiveness in pedal force application. This could imply that possibly, the 8-degree change in seat post angle only minimally affected the amount of the ineffective force resulted from the inertial properties of the leg segments. Similarity, in overall F_{EFF} associated with different seat post angle condition may be the implication that even with some changes in segmental kinematics with different seat post angles the effectiveness of pedal force application is preserved, on contrary to the common beliefs that suggest that a steeper seat post angle improves the mechanical effectiveness of the pedaling movement through altering the orientation of the leg segments.

Examination of joint moments provides some insight to what happens in muscular functions. In the current study, time-integral of the joint moment data (normalized to leg mass) over a pedal cycle were used to represent the total joint moment during a pedal cycle. Some similarities and differences in joint moments were observed when two different seat post angles were compared. In both seat post angle conditions, the hip contributed the greatest and the ankle contributed the least to the net joint moment. Since the joint moment indicates the net effects of the muscles (plus small effects of passive structures such as ligaments) at the particular joint, the greatest contribution of the hip to net moment suggests that the greatest work contribution was made by hip musculature in the pedaling movement. The seat post angle modification did not alter the order in which the three leg joints contributed to the net joint moment;

however the amount of contribution each of these joints made were different. When the cyclists rode in ROAD condition, the hip moment accounted for 78±5% (leg mass-normalized, 12±3 N.m/kg) of the net moment, the knee moment accounted for 21±5% (3±1 N.m/kg), and the ankle accounted for 2±0.3 % (0.3±0.05 N.m/kg). Cycling with a steeper seat post angle (TRI), the hip's contribution decreased to 67±10 % (9±3 N.m/kg), whereas the knee's contribution increased to 31±10 % (4±1 N.m/kg). The contribution of the ankle joint was also affected (TRI 2±1%, 0.2±0.05 N.m/kg). However, the contribution of the ankle was small in both conditions, so it would have relatively smaller effect on the net joint moment. These results indicated that a steeper seat post angle shift the work distribution to the knee from the hip. This finding was in agreement with Browning et al. [72] who found the same trend of reduced hip contribution accompanied by increased knee contribution with increased seat post angle. The steeper seat post angle also decreased the net joint moments (ROAD 16±3 N.m/kg v. TRI 13±3 N.m/kg), which also support the aforementioned study [72]. The authors concluded that a steeper seat post angle resulted from moving the seat forward would also allow cyclists to ride in the aerodynamic position with enhanced cycling mechanics. The modification on the seat post angle in the current study did not, however, result in significant difference in the estimated aerodynamic force (ROAD 131±7 N; TRI 133±5 N).

In the current study, the participants were asked to ride the identical course at the same intensity. In that sense, the participants were required to apply the same amount of effective pedal force. Since the cadence was unchanged, it could be implied that the torque, angular velocity, thus, the power of the crank were not considerably different in two cycling conditions tested. Therefore, any changes in joint moment could occur as the result of a change in: 1) the amount of force that act upon the joint, 2) the length of the moment arm of the force that act on the joint, or 3) combination of these two elements. Reduced net joint moment and altered contributions by the hip and the knee joints with TRI condition could be partially explained by the effect of the segmental weight vectors [73]. Modification of seat post angle altered the orientation of the segmental weight vectors relative to the leg joint axes. For example, the thigh was more vertically positioned, and that could make the moment arm length of the thigh weight vector relative to the hip joint axis smaller, thereby reduced the resulting the moment at the hip. Additionally, if the sum of the weight vectors of the segments were aligned more vertically relative to the bicycle pedal, the weight of the leg itself could add the passive force applied to the pedal that could offset the amount of the muscle engagement in pedal force application. This way, lesser net joint moments could result in similar amount of pedal force.

Time Effects

Overall, the joint and segmental kinematics were maintained closely during the 20-km cycling session. There were few variables that were different across 5 different time points (1-km, 5-km, 10-km, 15-km, and 20-km). The amount of anterior pelvic tilt

was significantly different during the initial portion of the cycling session (1-km), but the difference in angle was small enough (1°) to be considered as an error associated with the motion capture system [125]. The orientation of the thigh in the two conditions were also significantly different; however, the differences were small (1°), and there was no pattern in the trend of change. Therefore, the effects of the time on the kinematic variables appeared to be practically meaningless. Kinetically, the resultant force showed gradual increase with the cycling time for ROAD condition. At 1-km, cyclists applied 50 ± 17 N·s/kg, but at 19-km, they applied 61 ± 19 N·s/kg average over a pedal cycle. One of the possibilities for the increased impulse is different pedaling rate. With the given pedal force, a slower pedaling rate (more time spend for the full revolution of the pedal cycle) would result in greater impulse. The mean crank angular velocity at 19-km was 3% slower than that at 1-km. This small reduction in the pedaling rate could possibly lead to the increase in the impulse. However, neither the amount of the effective force nor the index of pedaling effectiveness changed across the time point. Therefore, it did not seem to impact the cycling mechanics practically. Based on these results, the impulse over a pedal cycle may not be a preferable variable when examining cycling performance.

Muscle Activations

Any forces that act relative to the joint axis have effects on the joint moments, the rotation effect at the joint. The muscles are the primary source of generating the internal force in the body [51]; therefore, evaluation of the muscle activation further facilitates the understanding of the movement and potentially explain the differences observed in joint moments. Comparison of the muscle activation between two seat positions showed that overall activation pattern of 7 muscles monitored did not differ drastically. However, examination of activation by different sectors revealed that muscle activation levels were higher with ROAD in a few muscles.

Pattern of muscle activation during cycling has been studied extensively in previous research. Most of the leg muscles are active during the propulsive phase of the pedal cycle as this is where the majority of the pedal forces are being generated and applied. The electromyography (EMG) used to examine the muscle activation measures the electrical activity a muscle, thereby indicating the time when the muscle is active. The actual muscle contraction due to the activation seen as the EMG signal occurs later. To consider the timing when the muscle activation takes an actual effect, this delay, electromechanical delay (EMD), of 40 ms should be considered [62]. For the current study, the participants pedaled approximately at 90 rpm for both condition. Therefore, the actual time when a muscles' action appear mechanically was 17° after the muscle's activation seen in EMG. Gmax and vastii muscles were active during the propulsive phase to extend the hip and the knee respectively [3, 62]. Rectus femoris (RF) typically began its activation slightly before the beginning of the pedal cycle (i.e. TDC), slightly earlier than the onset of the vastii [3, 62]. With EMD, the onset of actual shortening, or the force production of the RF would correspond to 17° after the TDC or near the

beginning of the power phase. SOL was also active during the propulsive phase, but later, approximately from 45° to 135° [3, 62], and mechanically, it was effective from 62° to 152°, during the power phase when stiffness of the ankle is critical in transmission of the muscle force to the pedal [5, 7]. There are two patterns in activation of the hamstring muscles that have been reported, and they are considered as the results of either or a combination of 1) inter-individual pedaling techniques, 2) the effects of changed mechanical constraints in cycling movement, and 3) different definitions used to identify the onset and the offset of the muscle activation [1]. The hamstring muscles are generally active during the propulsive phase to act as the hip extensors [3, 62], and possibly as to facilitate concurrent knee hip and knee flexion during the first part of the recovery phase (BDC to 270°) [62]. Tibialis anterior (TA) muscle acts during the second half of the recovery phase (approximately from 270°) to slightly past TDC, slightly into the subsequent pedal cycle [3, 62]. It functions to dorsiflex the ankle to clear the foot over TDC.

In the current study, the muscle activations were evaluated by determining the mean activation level for 4 different sectors: forward (1), downward (2), backward (3), and upward (4) movements of the crank arm. From visual inspection of the RMS linear envelope plots, the general patterns of muscle activation described above were observed in both experimental conditions. Extensors of the leg were active during the propulsive phase. When the plots of the two hip extensors, Gmax and BF, were compared, the timing of activation of BF was delayed relative to Gmax activation. This was related to their different roles in pedaling motion. It has been documented that two types of muscles, namely, the monoarticular and biarticular muscles, have different functions in cycling movement. The monoarticular muscles, which cross a single joint, primarily function as the energy producer [61, 62] whereas the biarticular muscles that cross two joints act to facilitate energy transfer between segments [4, 5, 61]. Of the 7 muscles monitored in this study, Gmax, vastus lateralis (VL), SOL and TA were the monoarticular muscles. The pedal force data showed that a majority of the effective pedal force occurred during the propulsive phase, more specifically, between 25° and 160° (power phase [3]) of the pedal cycle as reported previously, and with consideration of EMD, the muscle activation between 18° and 143° (sector 2) would be related to that large magnitude of the force. Most monoarticular muscles, with exception of VL and TA, exhibited the highest activation level during this period in both ROAD and TRI conditions, suggesting that they functioned primarily to produce the force to drive the crank arm.

When the hip was extending during the power phase (sector 2), Gmax (monoarticular muscle) was contracting concentrically to cause the movement at the hip. As the BF started to gradually increase its activation during the sector 2, it was acting to produce hip extensor moment like Gmax. Unlike Gmax, the BF maintained relatively high activity level through the sector 3, as it facilitated to transfer the energy produced at the hip to the knee joint during the directional change occurred with the crank arm movement. Changing the seat post angle did not alter the roles of these muscles significantly. The mean magnitude for Gmax and BF were similar between ROAD and TRI conditions. Although a significantly larger hip moment was associated with ROAD

condition, the difference was not due to the activation level of the hip extensors during the power phase. Instead, difference in the activation level of the hip extensors occurred prior to the power phase. While the crank was moving in the forward direction near the TDC (sector 1), the activation level of both Gmax and BF was reduced with TRI condition. Different cycling positions have been shown to have some effects in activation level of the hip extensors. Greater activation of the Gmax was associated with greater amount of hip flexion angle [3], which would make the length of the muscle be greater resulting in increased the contribution of non-contractile tissue in developing total muscle tension. However, in the current study, the hip flexion angle did not differ between two cycling conditions. Previously published data [23] suggested decreased BF activation with a greater seat post angle (82°) during an all-out effort cycling. The current results indicated that reduced BF activation also occurred in submaximal cycling, at least during the sector 1. The greater activity level of the hip extensors with ROAD near the TDC could explain the greater amount of hip moment with ROAD condition. The reduced BF activation was not present in any other sectors. Therefore, a role of BF as an intersegmental link for force transfer, particularly critical during the sector 3, was preserved with the seat post modification. Reduced activation of the BF without compromising pedaling effectiveness could benefit the triathletes to cycle more efficiently as well as to save the leg muscles for the run segment.

The knee extensors (RF and VL) were also contracting considerably to extend the knee to produce the knee extensor moment during the power phase. VL, a monoarticular muscle, activated earlier with a higher intensity than RF to maximize the generated force when the effective force was at its peak. Between the two seat post conditions, the magnitudes of their activations were similar, but the onsets of activation were noticeably different. As it occurred with the hip extensors, the activation of VL took place later in TRI condition. The later activation of VL was to accommodate the timing of Gmax activation. As the co-contraction of the agonists (RF and VL) and the biarticular antagonist (BF) during this final knee extension period (sector 2 to 3) was critical in effective force transfer from the hip to the knee [61] while providing joint stability [126], alteration of the timing of activation in these muscles was essential. As the power phase came to the end with a quick decrease in the activation of the knee extensors, the knee flexor (BF) increased its activation level, its role switched to cause the knee flexor moment to prepare for the switch in knee movement from extension to flexion at the bottom of the pedal cycle.

In the current study, EMD of 20 ms or 17° was considered to interpret the mechanical events related to the EMG signals. EMD is shown constant regardless of the preceding contraction state of the muscle [92]; although, the MU activations appeared to be affected [93]. Gast peaked its activation magnitude approximately at 85° (ROAD) and at 100° (TRI) of the pedal cycle. With EMD, the mechanical effect of this muscle took place approximately at 102° and 117° , when the pedal-foot segment was oriented most horizontally. At this time it was also at near the peak magnitude of the resultant pedal force. Since Gast is a biarticular muscle that is responsible for transferring the force generated in other leg muscles, the timing of activation of this muscle is important. Therefore, the timing of muscle activation can be interpreted as the cyclists' effort to

maximize the amount of the force transferred from the segments to the pedal. A monoarticular plantarflexor, soleus (SOL) was also very active in the power phase, but the timing of the activation onset was slightly later than that of Gast in both conditions. SOL, however, was significantly more active for ROAD than for TRI during the power phase. This could explain increased ankle joint moment associated with ROAD condition. The shallow seat post angle seen in ROAD condition positioned the pedal and the foot in less anteriorly tilted position, and the direction of the tangential force switches from anteriorly-directed to posteriorly-directed shortly after the sector 2. Therefore, increased SOL activation might be preparatory to the switch in direction.

There were relatively small changes in muscle activation levels with modification of seat post angle. Most of the muscle activation data in the current study indicated high intersubject variability. It has been shown that high variability in muscle activation data was present even among elite cyclists [106, 127]. Hug et al. found that all biarticular muscles and a few monarticular muscles (soleus [127] and tibialis anterior [106]) were associated with high variability among similarly trained cyclists despite that power output and cadence were maintained the same. Additionally, the pedal force profiles and the index of pedaling effectiveness were unchanged when the muscle activation patterns varied among individuals [106]. Different combinations of muscle synergy are known to produce the same outcome. Therefore, it is likely that the participants in the current study employed different muscle synergy strategies. As the high intersubject variability associated with the EMG data might lead to non-significant statistical comparison, alternative data processing, reduction, and analysis may be appropriate. Another possible cause for not identifying the effects of cycling position may be related to a different part of the methodology. When the orientation of the entire body was altered while preserving joint angles, gravity's influence alone affected the activation level of the leg muscles in pedaling [22]. Perhaps, relatively unaffected muscle activation levels in this study were because the change in effects of the gravity was not significant enough. In the current setting, only the lower body orientation was changed. As suggested by De Groot [25], individuals with cycling experience seemed to have a capability to use a trained pattern of muscle activation to maintain the same applied pedal force, even with different cycling geometry.

Aerodynamics

One of the reasons for using a bike with a steeper seat post angle is to be able to position the body to minimize the aerodynamic drag. Of the total aerodynamic drag, the portion associated with the cyclist's body account approximately for 70 % to 75 % [128], and the amount of the aerodynamic drag is largely dependent on the body positioning [8, 128-130]. Heil [8] reported that with the trunk angles comparable to the current study (72° - 74° relative to vertical), the projected frontal areas ranged between 0.322 m² and 0.323 m². The estimated projected frontal areas in the present study were slightly smaller, 0.29±0.03 m² for both conditions. Although it has been reported that greater seat post angle was associated with smaller projected frontal area, which is one of the

determinants of the aerodynamic drag [4, 8, 128], the current results did not show any difference between two seat post angle positions investigated. This was because the prediction equation [8] used trunk orientation. As bike's geometric measurements except the seat post angle were held constant in this study, the orientation of the trunk did not change significantly. Therefore, the estimated aerodynamic drag force did not differ between conditions.

Performance

The difference in times for the cyclists in the current study to complete the 20-km course was not statistically significant between two seat post angle conditions. However, these small changes can be practically significant. On average, there was a 42 seconds improvement comparing the ROAD to TRI (finish time: ROAD $39:05\pm4:23$; TRI $38:23\pm6:25$). The simulated course was 20 km, which is a typical bike segment for a sprint distance (shortest category) triathlon. Some of the study participants competed in triathlon races that are longer, such as a half-Ironman (89.6 km bike) and an Ironman distance (179.2 km bike). Potentially, an athlete can improve the bike time by 3 minutes and 6 minutes for these endurance events respectively. At the 2009 Ironman World Championship in Kona, the top 3 finishers in the 25 to 29 year old age group (armature) were within just over 2 minutes [131]. Therefore, this small difference in the finish time can be practically meaningful.

Additionally, several study participants reported discomfort associated with ROAD condition. It has been shown that more aggressive aerodynamic position with shallower seat post angle (73° in a published study) was not physiologically cost effective [74]. Although, limited changes in kinematics were observed between the two seat angle conditions tested in this study, it is possible that the shallower angle in ROAD condition had impacted the cyclists' performance. Even without the kinematic changes, the perceived discomfort alone could affect the performance outcome.

Summary of Chapter

The cyclists were able to retain relatively consistent pedaling mechanics over the 20-km simulated cycling course. Modified seat post angle, however, affected segmental orientations. This was primarily because the position of the cyclist was moved to be more directly on top of the crank axis with the steep seat post angle. Although there were changes in segmental orientations between two cycling conditions, the joint kinematics at the hip, knee and the ankle were maintained. This was likely because the other geometric features of the bicycle were preserved. The cyclists were cycling under relatively similar mechanical constraints in both experimental conditions. Additionally, there was a need for them to ride with the constant intensity and pedaling cadence. The study participants rode at their race intensity at their preferred cadence of approximately 90 rpm for both cycling conditions. This required the cyclist to apply the similar amount

of pedal force to drive the crank arm. There were differences in net joint moment of the leg, and how each of the joints contributed to the net moment. Some muscle activation levels explained the changes in joint moments. Two seat post angle conditions allowed the cyclists to pedal at the same mechanical effectiveness. This investigation on cycling mechanics between two seat post angle conditions provided some evidence that one riding position would be better mechanically. An improvement in the finish time of 42 seconds provided implications to practically meaningful results that could potentially impact the performance outcome. Also since many of the participants reported that ROAD setting put them in rather uncomfortable riding position, it may not be an ideal position for competition.

Chapter Six

Summary, Conclusions, Recommendations

Summary

The sport of triathlon has grown dramatically in the recent years [9]. A triathlon event includes three segments, swim, bike, and run. Across different distances of triathlon events, the bike (cycling) segment is typically the longest, followed by the run segment, and performance on those longer segments has been shown to be strongly related to the entire triathlon performance [10]. Many triathletes report that their run performances are negatively affected by the preceding cycling segment and many of the injuries associated with triathlon appeared to be related to the cycle-run transition [66]. Previous research has suggested preceding cycling affects stride and joint kinematics [12, 14, 17, 18, 132] as well as physiological parameters [15, 65, 68].

In attempting to minimize the adverse effects of the cycling bouts preceding the run, triathletes have adopted a newer, triathlon specific bike that is characterized by a more vertical seat post. Although it is commonly believed that this type of bike improves athletes' performance, there is limited evidence that supports positive effects of such bikes on performance [27, 115, 116]. Also, many of the studies that investigated the effects of the seat post angle involved experimental setups that were not transferrable to triathlon [20, 23]. A comprehensive evaluation of the effects of steeper seat post angle resembling the triathlon-specific bike is essential for triathletes and their coaches in choosing an appropriate bicycle to meet their performance goals. Therefore, the purpose of this study was to provide the evidence of which seat post angle is effective in performance. To meet this purpose, a comprehensive mechanical analysis of cycling with two different seat post conditions was conducted. The following main hypotheses were proposed to assess the effect of different seat post angles: 1) the sagittal pedal and joint kinematics will be influenced by seat post angle modification, 2) pedal kinetics will be affected by seat post angle modification, 3) the muscle activation pattern will be different between two seat post angle conditions, and 4) the time to complete the simulated course will be shorter for the steeper seat post angle condition.

A comprehensive analysis of cycling mechanics including segmental and joint kinematics, pedal and joint kinetics, and electromyography (EMG) was conducted using a stationary bicycle that was equipped with a pair of instrumented force pedals. 12 athletes (4 cyclists, 8 triathletes) who regularly trained as cyclists completed a 20-km simulated cycling course twice, each with a different seat post angle (steep and shallow). Five 30-second data trials were recorded during each ride. Dependent variables including segmental and joint kinematics and pedal and joint kinetics were compared using two-way ANOVA for repeated measures. The EMG data were tested for the effects of seat setting and for the different sectors of the pedal cycle using a series of non-parametric tests. The finish time was compared using paired t-tests ($p= 0.05$).

Results indicated that there were some effects of two different seat post angles on cycling mechanics. Although, joint kinematics were conserved with changing the seat post angle, the segmental kinematics (orientations) were affected. Additionally, the timing of the pedal force application and the muscle activation were affected by the modified seat post angle.

Conclusion

Based on the results of this study, the following conclusions are warranted:

- F) The sagittal pedal and joint kinematics will be influenced by seat post angle modification.
 - a. The pedal will be more tilted anteriorly with steeper seat post angle. This hypothesis was confirmed. The steeper seat post angle resulted in greater amount of the anterior tilt by 6° - 7° throughout the pedal cycle.
 - b. The hip joint flexion angle will be less with more vertically positioned legs relative to the crank axis associated with the steeper seat post angle. This hypothesis was rejected as both the minimal and maximal hip joint flexion angle between two seat post angle conditions The minimal and maximal hip flexion angles were approximately $37\pm3^\circ$ and $84^\circ - 82^\circ$ for both conditions.
 - c. Ankle dorsiflexion angle will be lesser during the propulsive phase while it will be greater during the recovery phase of the pedal cycle as a result of more vertically positioned legs with steeper seat post angle. This hypothesis was rejected. The ankle dorsiflexion angle was similar between two seat post angle conditions. The minimal and maximal plantar flexion angles were maintained at approximately at 10° and $26^\circ - 28^\circ$.
 - d. The knee joint kinematics will remain relatively unchanged since the seat post length remains the same. This hypothesis was confirmed. The knee joint kinematics was preserved with modification of seat post angle. The knee was flexed maximally to $114^\circ - 115^\circ$ near the top dead center and minimally flexed to $36^\circ - 38^\circ$ near the bottom dead center.
- G) Pedal kinetics will be affected by seat post angle modification.
 - a. A greater contribution of the tangential pedal force to the resultant pedal force throughout the pedaling cycle will be present with steeper seat post angle due to more anteriorly tilted pedal. This hypothesis was not confirmed as the contribution of the tangential pedal force did not differ between two seat post angle conditions. The tangential pedal force impulse over the pedal cycle remained similar with $2\pm2 \text{ N}\cdot\text{s}/\text{kg}$.
 - b. The portion of the resultant force used as the effective pedaling force will increase owing to changed contribution of tangential force with steeper

seat post angle arrangement. This hypothesis was not confirmed. Similar amount of the resultant force was used as the effective force in both seat post angle conditions.

- c. The index of pedaling effectiveness will improve with different seat post angle conditions. This hypothesis was not confirmed as the index of pedaling effectiveness remained unchanged with seat post angle modification. The overall effectiveness over a pedal cycle was 32% - 33%.
 - d. There will be a time-shift in the timing of pedal force application associated with steeper seat post angle. This hypothesis was confirmed. Steeper seat post angle resulted in delayed onset of pedal force application. The resultant pedal force was applied 12° of the pedal cycle later with the steeper seat post angle.
- 3) The muscle activation pattern will be different between two seat post angle conditions
- a. The biceps femoris activation level will decrease with the steep seat post angle. This hypothesis was confirmed. The activation level of the biceps femoris muscle decreased in the steep seat post angle conditions. Particularly, the mean activation of the biceps femoris was reduced when the pedal was moved forward by 5% of MVIC.
 - b. There will be a time-shift for onset and offset of the muscle activation due to the altered pedal with steep seat post angle. This hypothesis was confirmed. Steeper seat post angle was associated with later onset of muscle activation of some of the muscles tested. The activation timing for the gluteus maximus, vastus lateralis, and tibialis anterior were delayed by 14° - 20° when riding with the steeper seat post angle.
- 4) The time to complete the simulated course will be shorter for the steeper seat post angle condition. This hypothesis was not confirmed. The finish time between two seat post angle conditions were not statistically significant. However, the finish time of the 20-km ride was 42 seconds faster with the steeper seat post angle.

Recommendations

The results from the current study indicate changing seat post angle influenced certain cycling mechanics variables. More vertically aligned seat post angle resulted in changes in orientation of the lower extremity segments and more anteriorly tilted pedal, which appeared to be related to the time-shift (delay) in pedal force application and the timing of muscle activation. The contributions of the hip and knee joint moments were also altered associated with the seat post angle modification. As the joint moments are primarily related to the forces of the muscles associated with the joint, the current results of changed hip and knee moments may be an indication of neuromuscular events that were not clearly identified or detected. It has been suggested that muscle activation

patterns change solely due to changed segmental orientation [22]. Therefore, investigation of effects of the gravitational force on muscle activation will provide part of the missing link in the current findings. The current results indicated altered segmental orientations with changed seat post angle. This could change the effect of segmental weight acting as a passive joint moment that could either hinder or assist in pedaling movement.

In the current study, analyses were performed unilaterally. As cycling involves bilateral limb motion, and as the mechanics of a limb influences the mechanics of the contralateral limb, mechanical analyses including the bilateral limb would provide more accurate and comprehensive picture of cycling task. Additionally, kinetic and kinematic variables of cycling that occur in planes in addition to in the sagittal plane is highly beneficial, especially, non-sagittal mechanics are suggested to be related to overuse injuries associated with cycling [5].

The slight improvement in finish time associated with the steeper seat post angle can be interpreted as a practically meaningful. However, in the current study, the swim and the run portion were omitted. To obtain more valid data related to triathlon competition, the effects of prior swimming on cycling should be considered. Consequently, the future study should include a swim segment that is comparable to the actual competition.

The current study provided some evidence that steeper seat post angle may improve the cycling performance. With the steeper seat post angle, participants were able to complete the 20-km bike course more than a half-minute faster while reducing the activation level of one of the key muscles in running. Altering the seat post angle also resulted in different joint moment distributions. This may imply that some mechanical changes associated with steeper seat post angle typically seen in a triathlon-specific bike may have positive effects in cycling and possibly, in running performance.

Appendix A

The study participants' profiles and training/competition history.

Sub#	Gender	Age	Average Miles/week	Primary		Last Race	Next Race
				Sport	Level		
1	m	42	40	TRI/DU	2	10 days: Spr DU	2 mo: MAR; 3 mo: Spr DU
2	f	29	75	TRI	2	6 weeks; IM TRI	10 weeks MAR; 6 mo: Spr TRI
3	m	22	225	CY	2/Cat 3	3 mo: 35 min Cir CY	Cir
4	f	25	30	TRI	4	6 mo: Spr TRI	6 mo: Tour CY & Spr TRI
5	m	33	30	TRI	3	2 mo: Spr TRI	6 mo: Spr TRI
6	m	30	50	TRI	1	3 weeks: 1/2 IM TRI	4 mo: Spr TRI
7	m	20	120	CY	3	3 mo: 172 mi CY	3 mo: Endur CY
8	m	24	75	CY	3/Cat 4	3 mo: 10 mi TT CY	2 mo: TT CY
9	f	27	35	TRI	3	5 mo: 1/2 IM TRI	3 weeks: OLY TRI
10	m	31	65	TRI	3	8 mo: IM TRI	3 weeks: Spr TRI; 4 mo: 1/2 IM TRI
11	f	28	60	TRI	3	3 weeks: Spr TRI	4 mo: 1/2 IM TRI
12	f	32	250	CY	2/Cat 3	12 days: 45 min Cir CY	3 days: 45 min Cir CY

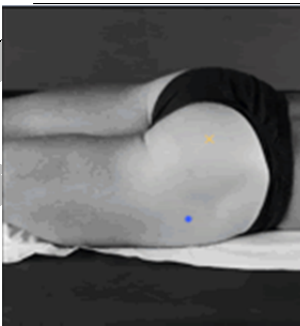
97

Sport: TRI - triathlon; DU - duathlon; CY - road cycling; **RACE:** Spr - sprint distance; IM - Ironman distance; 1/2 IM - half-Ironman distance; Cir - circuit race; TT - time trial; OLY - Olympic distance; Endur - endurance; **LEVEL:** 1 - elite (international level); 2 - sub-elite (top 10th percentile); 3 - high-recreational (top 30th percentile); 4 - middle-recreational (top 60th percentile); Cat 3 - USA Cycling Category 3; Cat 4 - USA Cycling Category 4

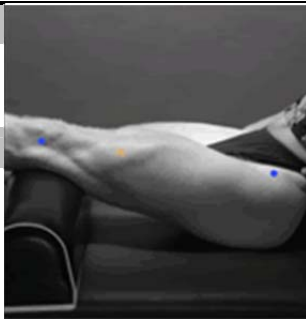
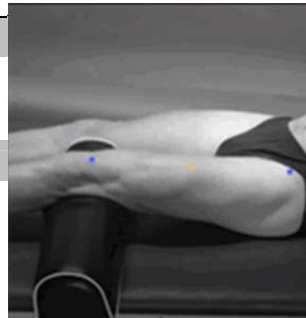
Appendix B

SENIAM EMG electrodes placements and MIVC testing methods. (with permission form SENIAM)

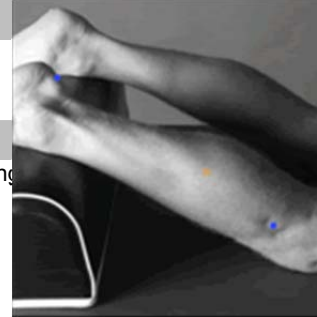
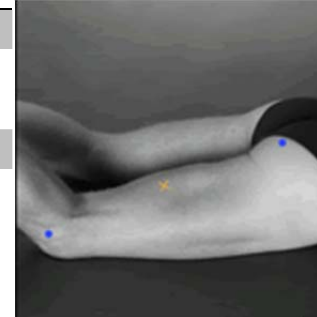
Muscle	
Name	GLUTEUS
Subdivision	MAXIMUS
Recommended sensor placement procedure	
Starting posture	Prone position, lying down on a table.
Electrode size	Maximum size in the direction of the muscle fibres: 10 mm.
Electrode distance	20 mm.
Electrode placement	
- location	The electrodes need to be placed at 50% on the line between the sacral vertebrae and the greater trochanter. This position corresponds with the greatest prominence of the middle of the buttocks well above the visible bulge of the greater trochanter.
- orientation	In the direction of the line from the posterior superior iliac spine to the middle of the posterior aspect of the thigh
- fixation on the skin	(Double sided) tape / rings or elastic band.
- reference electrode	On the proc. spin. of C7 or on / around the wrist or on / around the ankle.
Clinical test	Lifting the complete leg against manual resistance.



Muscle	
Name	Quadriceps Femoris
Subdivision	RECTUS FEMORIS
Recommended sensor placement procedure	
Starting posture	Sitting on a table with the knees in slight flexion and the upper body slightly bend backward.
Electrode size	Maximum size in the direction of the muscle fibres: 10 mm.
Electrode distance	20 mm.
Electrode placement	
- location	The electrodes need to be placed at 50% on the line from the anterior spina iliaca superior to the superior part of the patella
- orientation	In the direction of the line from the anterior spina iliaca superior to the superior part of the patella.
Clinical test	Extend the knee without rotating the thigh while applying pressure against the leg above the ankle in the direction of flexion.
Muscle	
Name	Quadriceps Femoris
Subdivision	VASTUS LATERALIS
Recommended sensor placement procedure	
Starting posture	Sitting on a table with the knees in slight flexion and the upper body slightly bend backward.
Electrode size	Maximum size in the direction of the muscle fibres: 10 mm.
Electrode distance	20 mm.
Electrode placement	
- location	Electrodes need to be placed at 2/3 on the line from the anterior spina iliaca superior to the lateral side of the patella.
- orientation	In the direction of the muscle fibres
Clinical test	Extend the knee without rotating the thigh while applying pressure against the leg above the ankle in the direction of flexion.

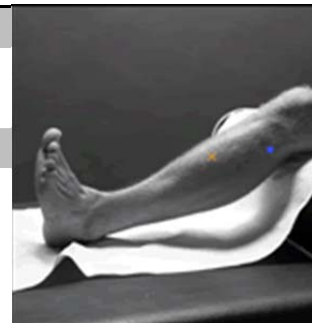
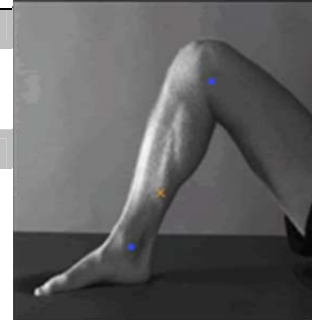


Muscle	
Name	BICEPS FEMORIS
Subdivision	LONG HEAD and short head
Recommended sensor placement procedure	
Starting posture	Lying on the belly with the face down with the thigh down on the table and the knees flexed (to less than 90 degrees) with the thigh in slight lateral rotation and the leg in slight lateral rotation with respect to the thigh.
Electrode size	Maximum size in the direction of the muscle fibres: 10 mm.
Electrode distance	20 mm.
Electrode placement	
- location	The electrodes need to be placed at 50% on the line between the ischial tuberosity and the lateral epicondyle of the tibia.
- orientation	In the direction of the line between the ischial tuberosity and the lateral epicondyle of the tibia.
Muscle	
Name	Gastrocnemius
Subdivision	Lateralis
Recommended sensor placement procedure	
Starting posture	Lying on the belly with the face down, the knee extended and the foot projecting over the end of the table.
Electrode size	Maximum size in the direction of the muscle fibres: 10 mm.
Electrode distance	20 mm.
Electrode placement	
- location	Electrodes need to be placed at 1/3 of the line between the head of the fibula and the heel.
- orientation	In the direction of the line between the head of the fibula and the heel.
Clinical test	Plantar flexion of the foot with emphasis on pulling the heel upward more than pushing the forefoot downward. For maximum pressure in this position it is necessary to apply pressure against the forefoot as well as against the calcaneus.



Muscle	
Name	Soleus
Subdivision	
Recommended sensor placement procedure	
Starting posture	Sitting with the knee approximately 90 degrees flexed and the heel / foot of the investigated leg on the floor.
Electrode size	Maximum size in the direction of muscle fibres: 10 mm.
Electrode distance	20 mm.
Electrode placement	
- location	The electrodes need to be placed at 2/3 of the line between the medial condylis of the femur to the medial malleolus.
- orientation	In the direction of the line between the medial condylis to the medial malleolus.
Clinical test	Put a hand on the knee and keep / push the knee downward while asking the subject / patient to lift the heel from the floor.
Muscle	
Name	Tibialis anterior
Subdivision	
Recommended sensor placement procedure	
Starting posture	Supine or sitting.
Electrode size	Maximum size in the direction of the muscle fibres: 10 mm.
Electrode distance	20 mm.
Electrode placement	
- location	The electrodes need to be placed at 1/3 on the line between the tip of the fibula and the tip of the medial malleolus.
- orientation	In the direction of the line between the tip of the fibula and the tip of the medial malleolus.
Clinical test	Support the leg just above the ankle joint with the ankle joint in dorsiflexion and the foot in inversion without extension of the great toe. Apply pressure against the medial side, dorsal surface of the foot in the direction of plantar flexion of the ankle joint and eversion of the foot.

Modified from “Recommendations for sensor locations in hip or upper leg muscles” <http://www.seniam.org>



Appendix C

The list of retro-reflective markers for 3D motion analysis and their placement locations.

Area	Name	Location
Bike	BK_F	Front of bike at middle front wheel axis
	BK_T	Front bike on handlebar stem
	R_WH	Right side rear wheel axis
Rear	L_WH	Left side rear wheel axis
Pedals	RPED	Lateral right pedal spindle
	LPED	Lateral left pedal spindle
Cyclist	HD1	Top of the head
	HD2	Right lateral head
	HD3	Left lateral head
	C7	Cervical 7 vertebrae, on spinous process
	RAC	Right acromioclavicular joint
	LAC	Left acromioclavicular joint
	OFFSET	Medial border of right scapula
	RRIB	Lateral most of right 12th rib
	LRIB	Lateral most of left 12th rib
	RELB	Right lateral elbow, lateral epicondyle
	R_WR	Right wrist, right radial styloid process
	LELB	Left lateral elbow, lateral epicondyle
	L_WR	Left wrist, left radial styloid process
	R_IL	Lateral most right iliac crest
	L_IL	Lateral most left iliac crest
	RASIS	Right anterir superior iliac spine
	LASIS	Left antero superior iliac spine
Pelvis	SAC	Superior border of sacrum
	RGTR	Right greater trochanter
	RTHP	Right proximal thigh
	RTHD	Right distal thigh
	RKNL	Right lateral knee, lateral femoral condyle
	RSHP	Right proximal shank/leg
R Shank	RSHD	Right distal shank/leg
	RAKL	Right lateral ankle, right lateral mallolus
R Foot	RTOE	Right toe, right 1st distal toe
	R5TH	Right base of 5th metatarsal
	RHEE	Right heel

Appendix C - Continued

The list of retro-reflective markers for 3D motion analysis and their placement locations.

Area	Name	Location	Area
Cyclist	L Thigh	LGTR	Left greater trochanter
		LTHP	Left proximal thigh
		LTHD	Left distal thigh
		LKNL	Left lateral knee, lateral femoral condyle
	L Shank	LSHP	Left proximal shank/leg
		LSHD	Left distal shank/leg
		LAKL	Left lateral ankle, left lateral mallolus
	L foot	LTOE	Left toe, left 1st distal toe
		L5TH	Left base of 5th metatarsal
	LHEE	Left heel	

Appendix D

Matlab code to convert raw pedal signals to usable force data.

```
clc;
clear all;

prompt={'Enter data set #:','Enter motion SF:'};
%data set "1" = rows 1-5; "2"=rows 6-10 etc...
title='Data start menu';
lines=1;
answer=inputdlg(prompt,title,lines);
row1=str2num(char(answer{1}));
if (row1==1)
    start_row=1;
end
if (row1>1)
    start_row=(row1-1)*5+1;
end

end_row=start_row+4;

SF_kine=str2num(char(answer{2}));
SF_force=SF_kine*10;

[num, txt]=
xlsread('G:\Dissertation\Methods\analysis\TRI_keyfile2.xls','sheet1','A2:AF121');

for aa=start_row
datapath=(['G:\Dissertation\Data\']);
filedir1=([txt{aa,9}]);
filedir2=([txt{aa,10}]);
filedir3=([txt{aa,11}]);
static = ([txt{aa,12}]);
dynamic1 =([txt{aa,13}]);%name (prefix)of dyn files
dynamic2 =num(aa,14); %dyn trial #
Rped1=([txt{aa,24}]);%zero offset at no tilt
Rped2=([txt{aa,25}]);%zero offset forward 90
Rped3=([txt{aa,26}]);%zero offset upside down
Rped4=([txt{aa,27}]);%zero offset backward 90

fileloc=char(strcat(filedir1,filedir2));
fileloc=strupr(fileloc,'none','');
data_path = [fileloc];
ped_cal_coeff=dlmread([datapath,'pedal_cal_coeff.txt']);
datafolder=char(strcat(datapath,filedir1,filedir2));
datafolder=strupr(datafolder,'none','');
datafolder=[datafolder,'C3D\'];
switch lower(filedir3)
    case {'\a'}
        datafolder=strupr(datafolder,'a\C3D\' , 'ANC\' );
    case {'\b'}
```

```

        datafolder=strrep(datafolder,'b\C3D\','ANC\');
    otherwise
        datafolder=strrep(datafolder,'C3D\','ANC\');
end

raw_R_ped=dlmread([datafolder Rped1,'.anc'],'\t', 11,1);
Rped1sh=raw_R_ped(:,2);%R shear zero tilt
Rped1norm=raw_R_ped(:,3);%R normal zero tilt

raw_R_ped=dlmread([datafolder Rped2,'.anc'],'\t', 11,1);
Rped2sh=raw_R_ped(:,2);%forward 90
Rped2norm=raw_R_ped(:,3);

raw_R_ped=dlmread([datafolder Rped3,'.anc'],'\t', 11,1);
Rped3sh=raw_R_ped(:,2);%upside down
Rped3norm=raw_R_ped(:,3);

raw_R_ped=dlmread([datafolder Rped4,'.anc'],'\t', 11,1);
Rped4sh=raw_R_ped(:,2);%backward 90
Rped4norm=raw_R_ped(:,3);

%%%average, single value as offset by averaging middle 1/3 of
data
zero_offset=[ ];
zero_offset(1,1)=-1*pi; %R1= -180deg
zero_offset(2,1)=-0.5*pi; %R2= -90deg
zero_offset(3,1)=0;%R3
zero_offset(4,1)=0.5*pi; %R4= 90deg
zero_offset(5,1)=1*pi; %R5= 180deg
zero_offset(6,1)=1.5*pi; %R6= 270deg
zero_offset(7,1)=2*pi; %R7= 360deg
%setting 1st column with angle(rad)

[rrr ccc]=size(raw_R_ped);
start=rrr/4+1; %frame# (force)at 1/3
stop=rrr/4*3; %frame# at 2/3

%filling rest of the zero_offset data (c2=Rshe;c3=Rnorm)
zero_offset(1,2)=mean(Rped3sh(start:stop,1));%R1=-180deg=180deg
zero_offset(1,3)=mean(Rped3norm(start:stop,1));
zero_offset(2,2)=mean(Rped4sh(start:stop,1));%R2=-90 deg=270deg
zero_offset(2,3)=mean(Rped4norm(start:stop,1));
zero_offset(3,2)=mean(Rped1sh(start:stop,1));%R3=zero deg
zero_offset(3,3)=mean(Rped1norm(start:stop,1));
zero_offset(4,2)=mean(Rped2sh(start:stop,1));%R4=90 deg
zero_offset(4,3)=mean(Rped2norm(start:stop,1));
zero_offset(5,2)=mean(Rped3sh(start:stop,1));%R5=180deg
zero_offset(5,3)=mean(Rped3norm(start:stop,1));
zero_offset(6,2)=mean(Rped4sh(start:stop,1));%R6=270deg
zero_offset(6,3)=mean(Rped4norm(start:stop,1));
zero_offset(7,2)=mean(Rped1sh(start:stop,1));%R7=360 deg
zero_offset(7,3)=mean(Rped1norm(start:stop,1));

```

```

params_all=[ ];
[rr cc]=size(zero_offset);
for j=2:cc
yin=zeros_offset(:,j);
t=zeros_offset(:,1);
f=1.8;
[params,yest,yres,rmserr]= sinefit(yin,t,f,0,1);
phase=params(1,1);
amp=params(1,2);
freq=params(1,3);
theta=params(1,4);

params_all(1,j-1)=phase;
params_all(2,j-1)=amp;
params_all(3,j-1)=freq;
params_all(4,j-1)=theta;
end

Rsh_phase=params_all(1,1);
Rsh_amp=params_all(2,1);
Rsh_freq=params_all(3,1);
Rsh_theta=params_all(4,1);
Rnor_phase=params_all(1,2);
Rnor_amp=params_all(2,2);
Rnor_freq=params_all(3,2);
Rnor_theta=params_all(4,2);

end

for a = start_row:end_row;
errorcheck = sum(isnan(num(a,1:4)));
if errorcheck==0;

datapath=([ 'G:\Dissertation\Data\' ]);
filedir1=([txt{a,9}]);
filedir2=([txt{a,10}]);
filedir3=([txt{a,11}]);
static = ([txt{a,12}]);
dynamic1 =([txt{a,13}]);%name (prefix)of dyn files
dynamic2 =num(a,14); %dyn trial #
Rped1=([txt{a,24}]);%zero offset at no tilt
Rped2=([txt{a,25}]);%zero offset forward 90
Rped3=([txt{a,26}]);%zero offset upside down
Rped4=([txt{a,27}]);%zero offset backward 90
SHEgain=num(a,32);%shear pedal gain setting

fileloc=char(strcat(filedir1,filedir2));
fileloc=strrep(fileloc,'none','');
data_path = [fileloc];

datafolder=char(strcat(datapath,filedir1,filedir2));

```

```

datafolder=strrep(datafolder,'none',' ');
datafolder=[datafolder,'C3D\'];
ped_data=dlmread([datafolder,'ped_data.txt']);

switch lower(filedir3)
    case {'\a'}
        datafolder=strrep(datafolder,'a\C3D\', 'ANC\' );
    case {'\b'}
        datafolder=strrep(datafolder,'b\C3D\', 'ANC\' );
    otherwise
        datafolder=strrep(datafolder,'C3D\', 'ANC\' );
end
end

if SHEgain==10000
    RSHEcoeff=ped_cal_coeff(:,2);%for SHEgain==10000, coeff on C2
else RSHEcoeff=ped_cal_coeff(:,3);%for SHEgain==20000, coeff on
C3
end

RNORA=ped_cal_coeff(1,1);%coeff 'a' for RNOR @40000 gain
RNORB=ped_cal_coeff(2,1);%coeff 'b' for RNOR @40000 gain
RNORC=ped_cal_coeff(3,1);%coeff 'c' for RNOR @40000 gain
RNORD=ped_cal_coeff(4,1);%coeff 'd' for RNOR @40000 gain
RNORE=ped_cal_coeff(5,1);%coeff 'c' for RNOR @40000 gain

RSHEa=RSHEcoeff(1,1);%coeff 'a' for RSHE
RSHEb=RSHEcoeff(2,1);%coeff 'b' for RSHE
RSHEc=RSHEcoeff(3,1);%coeff 'c' for RSHE
RSHEd=RSHEcoeff(4,1);%coeff 'd' for RSHE
RSHEe=RSHEcoeff(5,1);%coeff 'c' for RSHE

if dynamic2==1
    m=1+1;%'m' is for Rped angle C2, C5,...of ped_data
else
    m=((dynamic2-1)*3)+2;
end
%defining/extracting pedal angle data (tt)in eq,
phase+amp*cos(2*pi*tt*freq+theta)
Rtt_deg=ped_data(:,m);
Rtt=Rtt_deg*pi/180;

[row_ped col_ped]=size(Rtt);
Ped_offset=[];

analog_data=dlmread([datafolder,dynamic1,'.anc'],'\t', 11,1);
Rsh_raw_dyn=analog_data(:,1);
Rnor_raw_dyn=analog_data(:,2);
ped_new_name=['ped_new',num2str(dynamic2),'.txt'];
ped_new=[ ]; %'ped_new' includes offset-adjusted pedal data in
mV

```

```

for l=1:row_ped
    Rtt_sign=-1;%following right hand rule in matlab
    %opposite of ped angle convention in v3d)

RshPed_offset=Rsh_phase+Rsh_amp*cos(2*pi*Rtt(l,1)*Rsh_freq+Rsh_theta);
    Ped_offset1(l,1)=RshPed_offset;
    Ped_offset(l,1)=Ped_offset1(l,1)*Rtt_sign;

RnorPed_offset=Rnor_phase+Rnor_amp*cos(2*pi*Rtt(l,1)*Rnor_freq+Rnor_theta);
    Ped_offset1(l,2)=RnorPed_offset*Rtt_sign;
    Ped_offset(l,2)=Ped_offset1(l,2);

ped_new(l,1)=Rsh_raw_dyn(l,1) - Ped_offset(l,1);
ped_new(l,2)=Rnor_raw_dyn(l,1) - Ped_offset(l,2);

%below, angle effect eq [SHE = a*sin(b*angle_rad)+c]is applied

RSHEeq1p(l,1)=RSHEa*sin(RSHEb*Rtt(l,1))*Rtt_sign+RSHEc;
    RSHEfin(l,1)=RSHEd*(ped_new(l,1)-
RSHEeq1p(l,1))+RSHEe;

RNOREq1p(l,1)=RNORA*sin(RNORB*Rtt(l,1))*Rtt_sign+RNORc;
    RNORfin(l,1)=RNORD*(ped_new(l,2)-
RNOREq1p(l,1))+RNORe;

    ped_fin=[];
    ped_fin(:,1)=RSHEfin;
    ped_fin(:,2)=RNORfin;
end
cd([datafolder]);
dlmwrite(ped_new_name,ped_fin);
end
disp 'FINISH!!';

```

Appendix E

Descriptions of pedal signal calibration and conversion

Calibration

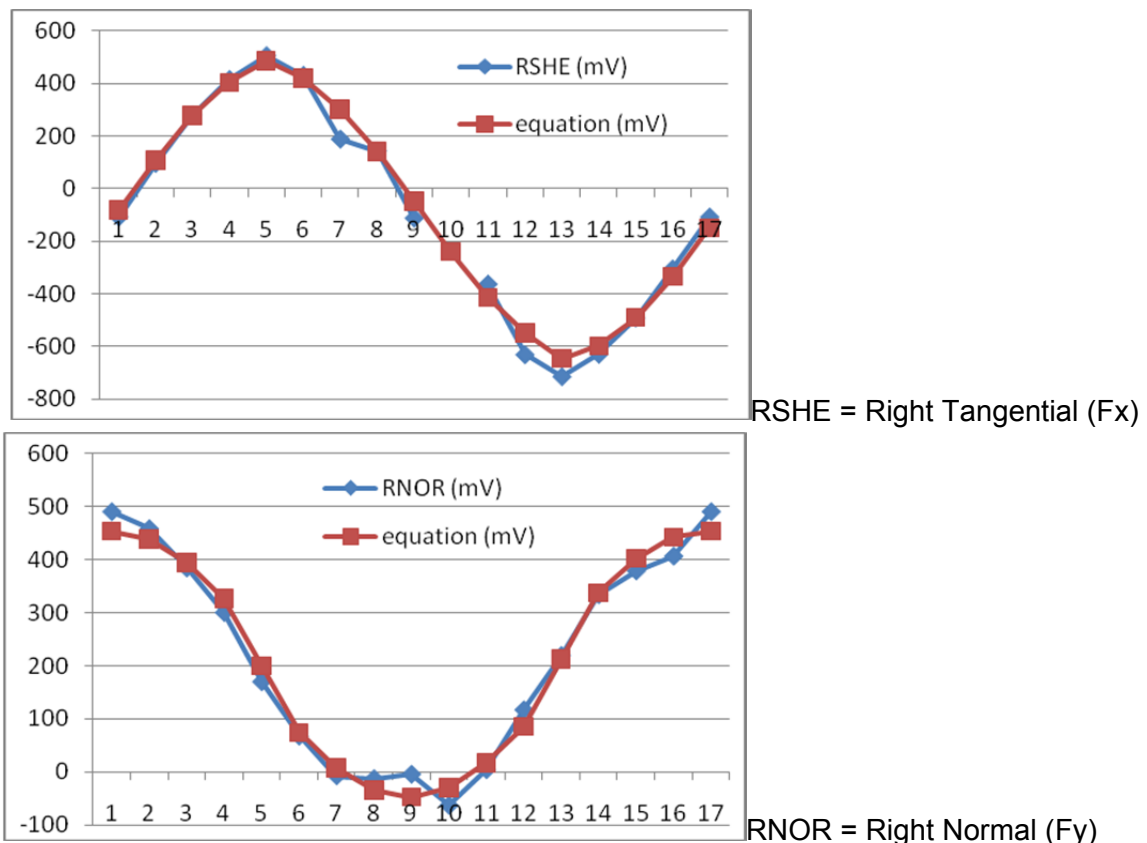
Determination of Angle Effect Equations

1. Zero-load at different pedal angles (10-degree increments – 35 trials) was recorded.
2. Using data signals of zero trial data, a curve was fitted to determine an equation (sin and cos equations for tangential and normal signal, respectively) to calculate the angle effect for any given pedal angles. Calibration coefficients, a, b, c were determined.

$$\text{Zero-offset for } F_x \text{ (mV)} = a * \sin(b * \text{ped_ang_rad}) + c \quad [1a]$$

$$\text{Zero-offset for } F_y \text{ (mV)} = a * \cos(b * \text{ped_ang_rad}) + c \quad [1b]$$

Graphical representation of fitted angle effect equations



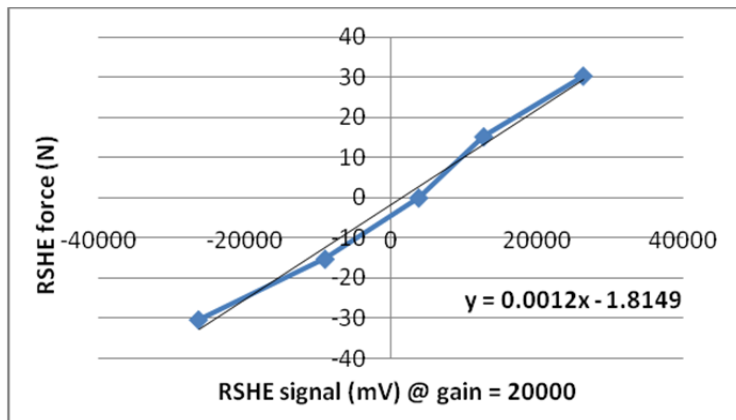
Determination of Load Effect Equations

1. Different combinations of 'loads x different pedal angle' trials were collected to determine the linear equation for the load effects of the pedal. Calibration coefficients, c and d were determined.

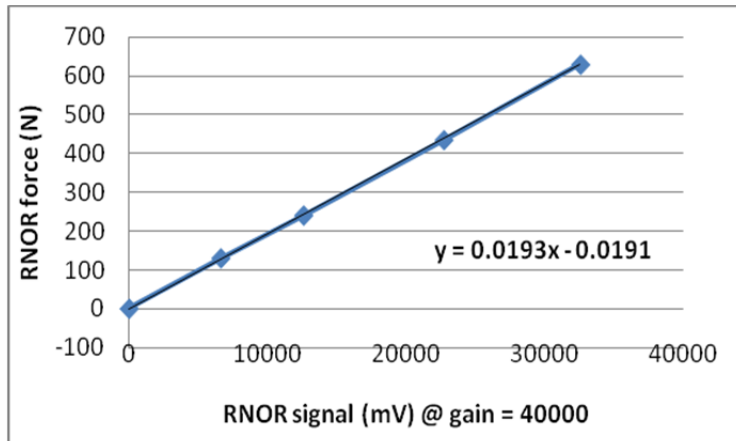
$$\text{Force (N)} = d * \text{zero-offset adjusted signal (mV)} + e$$

[2]

Graphical representation of fitted load effect equations



RSHE = Right tangential (Fx)



RNOR = Right normal (Fy)

<i>Calibration Equation Coefficients</i>			
ANGLE EFFECTS	RNOR40000	RSHE10000	RSHE20000
a	250.17	567.27	1243.59
b	1.01	0.98	1.01
c	203.04	-81.58	-38.94
LOAD EFFECTS	RNOR40000	RSHE10000	RSHE20000
c	0.02	0.00	0.00
d	0.02	2.01	-1.81

Pedal force determination for experimental trial data

For each subject-condition combinations -

1. Zero-load trial at 0 deg, 90 deg, 180 deg, and 270 deg of pedal angle was recorded.
2. Using these values, new sine equation was established for the subject-condition for each tangential and normal force data for zero offset values.
3. For each frame of data, the pedal angle value was applied to the angle effect equation and angle-effect offset values were subtracted.
4. Then the load effect equation was applied to the zero-offset signal to convert the signal to usable force data in Newton.

References

1. Hug, F. and S. Dorel, *Electromyographic analysis of pedaling: A review*. Journal of Electromyography and Kinesiology, 2009. **19**(2): p. 182-198.
2. Coyle, E.F., et al., *Physiological and biomechanical factors associated with elite endurance cycling performance*. Medicine and Science in Sports and Exercise, 1991. **23**(1): p. 93-107.
3. Dorel, S., Couturier, A., F. Hug, F., *Influence of different racing positions on mechanical and electromyographic patterns during pedaling*. Scandinavian Journal of Medicine & Science in Sports, 2009. **19**(1): p. 44-54.
4. Broker, J.P., *Cycling Biomechanics: Road and Mountain*, in *High-Tech Cycling*, E.D. Burke, Editor. 2003, Human Kinetics: Champaign, IL. p. 119 - 146.
5. Gregor, R.J. and F. Conconi, eds. *Road Cycling*. ed. R.J. Gregor and F. Conconi. 2001, Blackwell Science. 18 - 39.
6. Newmiller, J., M.L. Hull, and F.E. Zajac, *A mechanically decoupled 2 force component bicycle pedal dynamometer*. Journal of Biomechanics, 1988. **21**(5): p. 375-386.
7. Ericson, M.O. and R. Nisell, *Efficiency of pedal forces during ergometer cycling*. International Journal of Sports Medicine, 1988. **9**(2): p. 118-122.
8. Heil, D.P., *Body mass scaling of projected frontal area in competitive cyclists*. European Journal of Applied Physiology, 2001. **85**(3-4): p. 358-366.
9. USA Triathlon. *Demographics*. About USAT 2011 August, 2010 [cited 2011 March 24]; Available from: <http://www.usatriathlon.org/about-usat/demographics>.
10. Miura, H., K. Kitagawa, and T. Ishiko, *Economy during a simulated laboratory test triathlon is highly related to Olympic distance triathlon*. International Journal of Sports Medicine, 1997. **18**(4): p. 276-280.
11. Heiden, T. and A. Burnett, *The effect of cycling on muscle activation in the running leg of an Olympic distance triathlon*. Sports Biomechanics, 2003. **2**(1): p. 35-49.
12. Cala, A., et al., *Previous cycling does not affect running efficiency during a triathlon world cup competition*. Journal of Sports Medicine and Physical Fitness, 2009. **49**(2): p. 152-158.
13. Millet, G.P., et al., *Alterations in running economy and mechanics after maximal cycling in triathletes: Influence of performance level*. International Journal of Sports Medicine, 2000. **21**(2): p. 127-132.
14. Millet, G.P., G.Y. Millet, and R.B. Candau, *Duration and seriousness of running mechanics alterations after maximal cycling in triathletes: influence of the performance level*. Journal of Sports Medicine & Physical Fitness, 2001. **41**(2): p. 147-153.
15. Boussana, A., et al., *The effects of prior cycling and a successive run on respiratory muscle performance in triathletes*. International Journal of Sports Medicine, 2003. **24**(1): p. 63-70.
16. Farber, H.W., et al., *The endurance triathlon - metabolic changes after each event and during recovery*. Medicine and Science in Sports and Exercise, 1991. **23**(8): p. 959-965.
17. Bonacci, J., et al., *Change in running kinematics after cycling are related to alterations in running economy in triathletes*. Journal of Science and Medicine in Sport, 2010. **13**(4): p. 460-464.

18. Gottschall, J.S. and B.M. Palmer, *Acute effects of cycling on running step length and step frequency*. Journal of Strength and Conditioning Research, 2000. **14**(1): p. 97-101.
19. *Tri-Newbies Online: Road Bike vs. Tri-Bike...What Should I Buy?* 2011 [cited 2011; Available from: http://www.trinewbies.com/tno_cycling/tno_cyclearticle_02.asp.
20. Umberger, B.R., H.J. Scheuchenzuber, and T.M. Manos, *Differences in power output during cycling at different seat tube angles*. Journal of Human Movement Studies, 1998. **35**(1): p. 21-36.
21. Mestdagh, K.D., *Personal perspective: in search of an optimum cycling posture*. Applied Ergonomics, 1998. **29**(5): p. 325-334.
22. Brown, D.A., S.A. Kautz, and C.A. Dairaghi, *Muscle activity patterns altered during pedaling at different body orientations*. Journal of Biomechanics, 1996. **29**(10): p. 1349-1356.
23. Ricard, M.D., et al., *The effects of bicycle frame geometry on muscle activation and power during a Wingate anaerobic test*. Journal of Sports Science and Medicine, 2006. **5**(1): p. 25-32.
24. Rossato, M., et al., *Cadence and workload effects on pedaling technique of well-trained cyclists*. International Journal of Sports Medicine, 2008. **29**(9): p. 746-752.
25. De Groot, G., et al., *Power, muscular work, and external forces in cycling*. Ergonomics, 1994. **37**(1): p. 31-42.
26. Candotti, C.T., et al., *Effective force and economy of triathletes and cyclists*. Sports Biomechanics, 2007. **6**(1): p. 31-43.
27. Garside, I. and D.A. Doran, *Effects of bicycle frame ergonomics on triathlon 10-km running performance*. Journal of Sports Sciences, 2000. **18**(10): p. 825-833.
28. Chapman, A.R., et al., *The influence of body position on leg kinematics and muscle recruitment during cycling*. Journal of Science and Medicine in Sport, 2008. **11**(6): p. 519-526.
29. Candotti, C.T., et al., *Cocontraction and economy of triathletes and cyclists at different cadences during cycling motion*. Journal of Electromyography and Kinesiology, 2009. **19**(5): p. 915-921.
30. Delextrat, A., et al., *Does Prior 1500-m Swimming Affect Cycling Energy Expenditure in Well-Trained Triathletes?* Canadian Journal of Applied Physiology, 2005. **30**(4): p. 392-403.
31. Bentley, D.J., et al., *The effects of exercise intensity or drafting during swimming on subsequent cycling performance in triathletes*. Journal of Science and Medicine in Sport, 2007. **10**(4): p. 234-243.
32. Gregor, R.J.C., F., *Biomechanics, in Road Cycling*, R.J. Gregor, Editor. 2000, Oxford: Blackwell Science. p. 18-39.
33. Muraoka, T., et al., *Influence of tendon slack on electromechanical delay in the human medial gastrocnemius in vivo*. Journal of Applied Physiology, 2004. **96**(2): p. 540-544.
34. Cavanagh, P.R. and P.V. Komi, *Electro-mechanical delay in human skeletal-muscle under concentric and eccentric contractions*. European Journal of Applied Physiology and Occupational Physiology, 1979. **42**(3): p. 159-163.
35. Hobson, W., Campbell, C., Vickers, M., *Swim Bike Run*. 1 ed. 2001, Champaign, IL: Human Kinetics.
36. USAC (2008) *USA Cycling Bike Measurement*. 4 - 5.
37. Burke, E.D., Pruitt, A. L., *Body Positioning for Cycling*, in *High-Tech Cycling*, E.D. Burke, Editor. 2003, Human Kinetics: Champaign, IL. p. 69-92.

38. USATriathlon, *USA Triathlon Competitive Rules*. 2008: Colorado Springs, CO.
39. NSGA (2009) *2009 Sports Participation*.
40. Bohm, H., S. Siebert, and M. Walsh, *Effects of short-term training using SmartCranks on cycle work distribution and power output during cycling*. European Journal of Applied Physiology, 2008. **103**(2): p. 225-232.
41. Sanderson, D.J., E.M. Hennig, and A.H. Black, *The influence of cadence and power output on force application and in-shoe pressure distribution during cycling by competitive and recreational cyclists*. Journal of Sports Sciences, 2000. **18**(3): p. 173-181.
42. Bini, R.R. and F. Diefenthäler, *Mechanical work and coordinative pattern of cycling: a literature review*. Kinesiology, 2009. **41**(1): p. 25-39.
43. Chapman, A., et al., *Do differences in muscle recruitment between novice and elite cyclists reflect different movement patterns or less skilled muscle recruitment?* Journal of Science and Medicine in Sport, 2009. **12**(1): p. 31-34.
44. Wheeler, J.B., R.J. Gregor, and J.P. Broker, *The Effect of Clipless Float Design on Shoe/Pedal Interface Kinetics and Overuse Knee Injuries During Cycling*. Journal of Applied Biomechanics, 1995. **11**(2): p. 119-141.
45. Gonzalez, H. and M.L. Hull, *Multivariable optimization of cycling biomechanics*. Journal of Biomechanics, 1989. **22**(11-12): p. 1151-1161.
46. Kautz, S.A. and M.L. Hull, *A theoretical basis for interpreting te force applied to the pedal in cycling*. Journal of Biomechanics, 1993. **26**(2): p. 155-165.
47. Kautz, S.A. and R.R. Neptune, *Biomechanical determinants of pedaling energetics: Internal and external work are not independent*. Exercise and Sport Sciences Reviews, 2002. **30**(4): p. 159-165.
48. Broker, J.P., *Cycling Power: Road and Mountain*, in *High-Tech Cycling*, E.D. Burke, Editor. 2003, Human Kinetics: Champaign, IL. p. 147 - 179.
49. Sanderson, D.J., *The influence of cadence and power output on the biomechanics of force application during steady-rate cycling in competitive and recreational cyclists*. Journal of Sports Sciences, 1991. **9**(2): p. 191-203.
50. Bentley, D.J., et al., *Correlations between peak power output, muscular strength and cycle time trial performance in triathletes*. Journal of Sports Medicine and Physical Fitness, 1998. **38**(3): p. 201-207.
51. Winter, D.A., *Biomechanics and Motor Control of Human Movement* 3rd ed. 2000: Wiley.
52. Gregor, R.J., J.P. Broker, and M.M. Ryan, *The biomechanics of cycling*. Exercise & Sport Sciences Reviews, 1991. **19**: p. 127-169.
53. Caldwell, G.E., et al., *Pedal and crank kinetics in uphill cycling*. . Journal of Applied Biomechanics, 1998. **14**(3): p. 245-259.
54. Hanaki-Martin, S., Mullineaux, D. R., Underwood, T. M. *Effects of Independent Crank Arms and Slope on Pedaling Mechanics*. in *International Society of Biomechanics in Sports Annual Meeting*. 2009. Limerik, Ireland.
55. Lucia, A., et al., *Effects of the rotor pedaling system on the performance of trained cyclists during incremental and constant-load cycle ergometer tests*. International Journal of Sports Medicine, 2004. **25**(7): p. 479-485.
56. Lucia, A., et al., *In professional road cyclists, low pedaling cadences are less efficient*. Medicine and Science in Sports and Exercise, 2004. **36**(6): p. 1048-1054.
57. Loras, H., G. Ettema, and S. Leirdal, *The Muscle Force Component in Pedaling Retains Constant Direction Across Pedaling Rates*. Journal of Applied Biomechanics, 2009. **25**(1): p. 85-92.

58. Korff, T., et al., *Effect of pedaling technique on mechanical effectiveness and efficiency in cyclists*. Medicine and Science in Sports and Exercise, 2007. **39**(6): p. 991-995.
59. Robertson, D.G.E., Caldwell, G.E., Hamill, J., Karmen, G., Whittlesey, S.N., *Research Methods in Biomechanics* 2004, Urbana, IL: Human Kinetics.
60. Neptune, R.R., S.A. Kautz, and F.E. Zajac, *Muscle contributions to specific biomechanical functions do not change in forward versus backward pedaling*. Journal of Biomechanics, 2000. **33**(2): p. 155-164.
61. van Ingen Schenau, G.J., Boots, P.J.M, De Grood, G., Snackers, R.J., Van Woensel, W.W.L.M., *The constrained control of force and position in multi-joint movements*. Neuroscience, 1992. **46**: p. 197-207.
62. Ryan, M.M. and R.J. Gregor, *EMG profiles of lower-extremity muscle during cycling at constant workload and cadence*. Journal of Electromyography and Kinesiology, 1992. **2**(2): p. 69-80.
63. Dingwell, J.B., et al., *Changes in Muscle Activity and Kinematics of Highly Trained Cyclists During Fatigue*. Ieee Transactions on Biomedical Engineering, 2008. **55**(11): p. 2666-2674.
64. Prilutsky, B.I. and R.J. Gregor, *Strategy of coordination of two- and one-joint leg muscles in controlling as external force*. Motor Control, 1997. **1**(1): p. 92-116.
65. Millet, G.P. and V.E. Vleck, *Physiological and biomechanical adaptations to the cycle to run transition in Olympic triathlon: review and practical recommendations for training*. British Journal of Sports Medicine, 2000. **34**(5): p. 384-390.
66. Migliorini, S., *The triathlon: acute and overuse injuries*. Journal of Sports Traumatology & Related Research, 2000. **22**(4): p. 186-195.
67. Quigley, E.J. and J.G. Richards, *The effects of cycling on running mechanics*. Journal of Applied Biomechanics, 1996. **12**(4): p. 470-479.
68. Hausswirth, C., A.X. Bigard, and C.Y. Guezennec, *Relationships between Running Mechanics and Energy Cost of Running at the End of a Triathlon and a Marathon*. Int J Sports Med, 1997. **18**(05): p. 330-339.
69. Chapman, A.R., et al., *Does cycling effect motor coordination of the leg during running in elite triathletes?* Journal of Science & Medicine in Sport, 2008. **11**(4): p. 371-380.
70. Gottschall, J.S. and B.M. Palmer, *The acute effects of prior cycling cadence on running performance and kinematics*. Medicine and Science in Sports and Exercise, 2002. **34**(9): p. 1518-1522.
71. Suriano, R., et al., *Variable power output during cycling improves subsequent treadmill run time to exhaustion*. Journal of Science and Medicine in Sport, 2007. **10**(4): p. 244-251.
72. Browning, R.C., Gregor, R.J., Broker, J.P., *Lower extremity kinetics in elite athletes in aerodynamic cycling positions*. Medicine and Science in Sports and Exercise, 1992. **24**(5): p. S186.
73. Price, D. and B. Donne, *Effect of variation in seat tube angle at different seat heights on submaximal cycling performance in man*. Journal of Sports Sciences, 1997. **15**(4): p. 395-402.
74. Jackson, K., J. Mulcare, and R. Duncan, *The effects of bicycle seat-tube angle on the metabolic cost of the cycle-run transition in triathletes*. Journal of Exercise Physiology Online, 2008. **11**(1): p. 45-52.
75. Too, D., *The Effect of Hip Position Configuration on Anaerobic Power and Capacity in Cycling*. International Journal of Sport Biomechanics, 1991. **7**(4): p. 359-370.

76. Cappozzo, A., et al., *Human movement analysis using stereophotogrammetry - Part 1: theoretical background*. Gait & Posture, 2005. **21**(2): p. 186-196.
77. Wu, G. and P.R. Cavanagh, *ISB recommendations for standardization in the reporting of kinematic data*. Journal of Biomechanics, 1995. **28**(10): p. 1257-1260.
78. Wu, G., et al., *ISB recommendation on definitions of joint coordinate system of various joints for the reporting of human joint motion--part I: ankle, hip, and spine*. Journal of Biomechanics, 2002. **35**(4): p. 543-548.
79. Grood, E.S. and W.J. Suntay, *A joint coordinate system for the clinical description of 3-dimensional motions - application to the knee*. Journal of Biomechanical Engineering-Transactions of the Asme, 1983. **105**(2): p. 136-144.
80. Leardini, A., et al., *Human movement analysis using stereophotogrammetry - Part 3. Soft tissue artifact assessment and compensation*. Gait & Posture, 2005. **21**(2): p. 212-225.
81. Della Croce, U., A. Cappozzo, and D.C. Kerrigan, *Pelvis and lower limb anatomical landmark calibration precision and its propagation to bone geometry and joint angles*. Medical & Biological Engineering & Computing, 1999. **37**(2): p. 155-161.
82. Schwartz, M.H. and A. Rozumalski, *A new method for estimating joint parameters from motion data*. Journal of Biomechanics, 2005. **38**(1): p. 107-116.
83. Pohl, M.B., C. Lloyd, and R. Ferber, *Can the reliability of three-dimensional running kinematics be improved using functional joint methodology?* Gait & Posture, 2010. **32**(4): p. 559-563.
84. Donati, M., et al., *Enhanced anatomical calibration in human movement analysis*. Gait & Posture, 2007. **26**(2): p. 179-185.
85. Donati, M., et al., *Anatomical frame identification and reconstruction for repeatable lower limb joint kinematics estimates*. Journal of Biomechanics, 2008. **41**(10): p. 2219-2226.
86. Basmajian, J.V., De Luca, C J, *Muscle Alive: Their fucntions revealed by electromyography*. 5th ed. 1985, Baltimore: Williams & Wilkins.
87. Bigland, B. and O.C. Lippold, *The relation between force, velocity and integrated electrical activity in human muscles*. The Journal of physiology, 1954. **123**(1): p. 214-24.
88. De Luca, C.J., *The use of surface electromyography in biomechanics*. Journal of Applied Biomechanics, 1997. **13**(2): p. 135-163.
89. Woods, J.J. and B. Biglandritchie, *Linear and non-linear surface EMG force relationships in human muscles - an anatomical functional argument for the existence of both*. American Journal of Physical Medicine & Rehabilitation, 1983. **62**(6): p. 287-299.
90. Henneman, E., *Relation between size of neurons and their susceptibility to discharge*. Science (New York, N.Y.), 1957. **126**(3287): p. 1345-7.
91. Lawrence, J.H. and C.J. De Luca, *Myoelectric signal versus force relationship in different human muscles*. Journal of Applied Physiology, 1983. **54**(6): p. 1653-1659.
92. Staudenmann, D., et al., *Methodological aspects of SEMG recordings for force estimation - A tutorial and review*. Journal of Electromyography and Kinesiology, 2010. **20**(3): p. 375-387.
93. Uematsu, A., et al., *Contraction history produced tasks-specific variations in spinal excitability in healthy human soleus muscle*. Muscle & Nerve, 2011. **43**(6): p. 851-858.

94. Burden, A., *How should we normalize electromyograms obtained from healthy participants? What we have learned from over 25 years of research*. Journal of Electromyography and Kinesiology, 2010. **20**(6): p. 1023-1035.
95. Allison, G.T., R.N. Marshall, and K.P. Singer, *EMG singal amplitude normalization technique in stretch-shortening cycle movements*. Journal of Electromyography and Kinesiology, 1993. **3**(4): p. 236-244.
96. Nieminen, H., E.P. Takala, and E. Viikarijuntura, *Normalization of electromyogram in the neck-shoulder region*. European Journal of Applied Physiology and Occupational Physiology, 1993. **67**(3): p. 199-207.
97. Mirka, G.A., *The quantification of EMG normalization error*. Ergonomics, 1991. **34**(3): p. 343-352.
98. Clarys, J.P., *Electromyography in sports and occupational settings: an update of its limits and possibilities*. Ergonomics, 2000. **43**(10): p. 1750-1762.
99. Yang, J.F. and D.A. Winter, *Electromyographic amplitude normalization methods - improving their sensitivity as diagnostic tools in gait analysis*. Archives of Physical Medicine and Rehabilitation, 1984. **65**(9): p. 517-521.
100. Rouffet, D.M. and C.A. Hautier, *EMG normalization to study muscle activation in cycling*. Journal of Electromyography and Kinesiology, 2008. **18**(5): p. 866-878.
101. CSEP, *Physical Activity Readiness Questionnaire - PAR-Q (A Questionnaire for People Aged 15 to 69)*, C.S.f.E. Physiology, Editor. 2002: Ottawa.
102. SENIAM, *The SENIAM project (Surface ElectroMyoGraphy for the Non-Invasive Assessment of Muscles): Recommendations*. 2006.
103. Dempster, W.T., *The space requirements of the seated operator*, in *WADC Technical Report 55-159*. 1955, University of Michigan.
104. Hanavan, E.P., *Mathematical model of the human body*. 1964, Writ-Patterson Airforce Base, OH.
105. c-motion. *Inverse Dynamics*. c-motion Online Wiki 2010 November 30 [cited 2011; Available from: http://www.c-motion.com/v3dwiki/index.php?title=Inverse_Dynamics.
106. Hug, F., et al., *Interindividual variability of electromyographic patterns and pedal force profiles in trained cyclists*. European Journal of Applied Physiology, 2008. **104**(4): p. 667-678.
107. Pugh, L., *RELATION OF OXYGEN INTAKE AND SPEED IN COMPETITION CYCLING AND COMPARATIVE OBSERVATIONS ON BICYCLE ERGOMETER*. Journal of Physiology-London, 1974. **241**(3): p. 795-808.
108. Cutnell, J.D., Johnson, K. W., *Physics*. 5th ed. 2001, New York: John Wiley & Sons.
109. Li, L. and G.E. Caldwell, *Coefficient of cross correlation and the time domain correspondence*. Journal of Electromyography and Kinesiology, 1999. **9**(6): p. 385-389.
110. Paolo, d.L., *Adjustments to Zatsiorsky-Seluyanov's segment inertia parameters*. Journal of Biomechanics, 1996. **29**(9): p. 1223-1230.
111. Savelberg, H., I.G.L. Van de Port, and P.J.B. Willems, *Body configuration in cycling affects muscle recruitment and movement pattern*. Journal of Applied Biomechanics, 2003. **19**(4): p. 310-324.
112. Bressel, E. and B.J. Larson, *Bicycle seat designs and their effect on pelvic angle, trunk angle, and comfort*. Medicine and Science in Sports and Exercise, 2003. **35**(2): p. 327-332.
113. McEvoy, M.P., K. Wilkie, and M.T. Williams, *Anterior pelvic tilt in elite cyclists - A comparative matched pairs study*. Physical Therapy in Sport, 2007. **8**(1): p. 22-29.

114. Mueller, P., M. McEvoy, and S. Everett, *The long sitting screening test in elite cyclists*. Journal of Science and Medicine in Sport, 2005. **8**(4): p. 369-374.
115. Usabiaga, J., et al., *Adaptation of the lumbar spine to different positions in bicycle racing*. Spine, 1997. **22**(17): p. 1965-1969.
116. Heil, D.P., T.R. Derrick, and S. Whittlesey, *The relationship between preferred and optimal positioning during submaximal cycle ergometry*. European Journal of Applied Physiology and Occupational Physiology, 1997. **75**(2): p. 160-165.
117. Rankin, J.W., Neptune R. R. *Determination of the optimal seat position that maximizes average crank power: a theoretical study*. in *North American Congress on Biomechanics*. 2008. Ann Arbor, Michigan, USA.
118. Bini, R.R., A.C. Tamborindeguy, and C.B. Mota, *Effects of Saddle Height, Pedaling Cadence, and Workload on Joint Kinetics and Kinematics During Cycling*. Journal of Sport Rehabilitation, 2010. **19**(3): p. 301-314.
119. Gruben, K.G. and C. Lopez-Ortiz, *Characteristics of the force applied to a pedal during human pushing efforts: Emergent linearity*. Journal of Motor Behavior, 2000. **32**(2): p. 151-162.
120. Mornieux, G., et al., *Effects of Pedal Type and Pull-Up Action during Cycling*. International Journal of Sports Medicine, 2008. **29**(10): p. 817-822.
121. Minetti, A.E., J. Pinkerton, and P. Zamparo, *From bipedalism to bicyclism: evolution in energetics and biomechanics of historic bicycles*. Proceedings of the Royal Society of London Series B-Biological Sciences, 2001. **268**(1474): p. 1351-1360.
122. Neptune, R.R. and W. Herzog, *Adaptation of muscle coordination to altered task mechanics during steady-state cycling*. Journal of Biomechanics, 2000. **33**(2): p. 165-172.
123. Davis, R.R. and M.L. Hull, *Measurement of pedal loading in bicycling: II. Analysis and results*. Journal of Biomechanics, 1981. **14**(12): p. 857-872.
124. Sanderson, D.J. and A. Black, *The effect of prolonged cycling on pedal forces*. Journal of Sports Sciences, 2003. **21**(3): p. 191-199.
125. Richards, J.G., *The measurement of human motion: A comparison of commercially available systems*. Human Movement Science, 1999. **18**(5): p. 589-602.
126. Hirokawa, S., *3-Dimensional mathematical-model analysis of the patellofemoral joint*. Journal of Biomechanics, 1991. **24**(8): p. 659-671.
127. Hug, F., et al., *Is interindividual variability of EMG patterns in trained cyclists related to different muscle synergies?* Journal of Applied Physiology, 2010. **108**(6): p. 1727-1736.
128. Kyle, C.R., *Selecting Cycling Equipment*, in *High-Tech Cycling*, E.D. Burke, Editor. 2003, Human Kinetics: Champaign, IL. p. 1-48.
129. Heil, D.P., *Body mass scaling of frontal area in competitive cyclists not using aero-handlebars*. European Journal of Applied Physiology, 2002. **87**(6): p. 520-528.
130. Defraeye, T., et al., *Aerodynamic study of different cyclist positions: CFD analysis and full-scale wind-tunnel tests*. Journal of Biomechanics, 2010. **43**(7): p. 1262-1268.
131. Ironman.com. *Ironman World Championship 2009 Results*. 2009 [cited 2011 March 20]; Available from: <http://ironman.com/assets/files/results/worldchampionship/2009.pdf>.
132. Bonacci, J., et al., *Altered movement patterns but not muscle recruitment in moderately trained triathletes during running after cycling*. Journal of Sports Sciences, 2010. **28**(13): p. 1477-1487.

Vita

Hanaki-Martin,Saori

EDUCATION

<u>Illinois State University, Normal, IL</u>	
M.S. in Kinesiology and Recreation - Biomechanics	2005
Thesis: "Kinematic differences between one- and two-leg drop landings"	
<u>University of Montana, Missoula, Montana</u>	
B.S. Honors in Health and Human Performance	2000
Area of Concentration: Athletic Training	

PROFESSIONAL EXPERIENCES

<u>University of Louisville, Louisville, KY</u>	
Instructor	2010
Present	
<u>University of Kentucky, Lexington, KY</u>	
Part-Time Instructor	2009 - 2010
Laboratory Manager & Research Assistant	2005 – 2010
<u>Drayer Physical Therapy Institute, Lexington, KY</u>	
Research Coordinator	2006 – 2008
Conference Co-coordinator: ACL Retreat	2006
<u>Illinois State University, Normal, IL</u>	
Par -Time Instructor	2004 - 2005
Research Assistant	2003 – 2004
Clinical Instructor	2001 - 2004

PROFESSIONAL SERVICE & DEVELOPMENT

<u>Honors and Scholastics Committee, University of Louisville, Louisville, KY</u>	
Committee Member	2011
<u>Idea to Action (Quality Enhancement Plan) Ad Hoc Committee,</u>	
<u>CEHD, University of Louisville</u>	
Committee Member	2010 – 2011
<u>Marshall Center, Department of Athletics, University of Louisville</u>	

Statistical Consultant	2011
<u>International Society of Biomechanics in Sports Annual Meeting</u>	
<u>Pre-Conference, Marquette, MI</u>	
Session Chair	2010
<u>Journal of Sports Rehabilitation</u>	
Reviewer	2009 - 2010

HONORS AND AWARDS

Visiting Faculty Coach, University of Louisville	2010
Graduate Student Travel Grants, University of Kentucky	2009 & 2010
Jorndt Research Award, Illinois State University	2005
Student-Mentor Award, Illinois Association for Health, Physical Education, Recreation and Dance	2003 & 2004
Athletic Training Fellowship – New Hampshire Musculoskeletal Institute	2000 – 2001
Dean's List, University of Montana - Missoula	1998 – 2000
Academic Scholarship, University of Montana - Missoula	1999

PUBLICATIONS AND ABSTRACTS

Davis, I., Ireland, M.L., **Hanaki, S.** (2007). ACL Injury – Gender Bias. *Journal of Orthopaedic & Sports Physical Therapy*. 37 (2) A2-A7.

Hanaki, S. & McCaw, S.T. (2005). A Comparison of Lower Extremity Kinematics of One- and Two-Leg Landings. *Medicine, Science in Sports and Exercise*. 37(5) S66. Abstract

McCaw, S.T. & **Hanaki, S.** (2005). Joint Contributions to Energy Absorption Differ between Drop Landings onto One or Two Legs. *Medicine, Science in Sports and Exercise*. 37(5) S66-S67. Abstract

Adolph, J.T., McCaw, S.T., Hopkins, J.T., **Hanaki, S.** (2004). Lower extremity joint kinematics differ between high school and college female athletes during drop landings. *Journal of Athletic Training*. 39 (2) S69. Abstract

PRESENTATIONS

Webb, J., Hunt, K., **Hanaki-Martin, S.**, Doyle, B., Curry, J., MacDonald, A. (2011). Building Performance-Based Assignments Using the Paul-Elder Critical Thinking Model. *3rd Annual i2a Institute*, University of Louisville.

Hanaki-Martin, S., Mullinaux, D.R., Jeon, K., Shapiro, R. (2010). Forward Seat Position Effects on Cycling Kinematics. *International Society of Biomechanics in Sports Annual Meeting*.

Hanaki-Martin, S. (2010). General Cycling Mechanics & Factors Associated with Injury. *Kentucky Athletic Trainers' Society Annual Meeting*.

Hanaki-Martin S., Mullineaux, D.R. & Underwood, S.M. (2009). Effects of Independent Crank Arms and Slope on Pedaling Mechanics. *International Society of Biomechanics in Sports Annual Meeting*.

Mullineaux, D.R., **Hanaki-Martin, S.**, Jeon, K., Cunningham, T.J., Shapiro, R., Noehren, B.W., Sugimoto, D. (2010). Kinematics to estimate three-dimensional joint kinetics during walking. *World Congress on Biomechanics*.

Hanaki, S. & McCaw, S.T. (2005). A Comparison of Lower Extremity Kinematics of One- and Two-Leg Landings.

American College of Sports Medicine Annual Meeting.

Hanaki, S. & McCaw, S.T. (2005). Quantification of Energy Absorbed by the Lower Extremity Depends on Endpoint of the Impact Phase. *International Society of Biomechanics Congress*.

Hanaki, S. (2004). A Comparison of Lower Extremity Kinematics Between One- and Two-Leg Drop Landings. *Illinois Association for Health, Physical Education, Recreation and Dance (IAHPERD)*.

Hanaki, S. (2003). Current Concepts in Low Back Exercise. *Illinois Association for Health, Physical Education, Recreation and Dance (IAHPERD)*.

UNPUBLISHED RESEARCH/TECHNICAL REPORT

Hanaki-Martin, S., Shapiro, R., Uhl, T., Seeley, M., Johnson, D. (2008). Biomechanical and Cognitive Effects of Unloading Knee Brace in Individuals with Medial Knee Osteoarthritis. *Project sponsored by Don Joy Ortho*.